

**Dissertation zur Erlangung des Doktorgrades
der Fakultät für Chemie und Pharmazie
der Ludwig-Maximilians-Universität München**



Challenges and Chances of the Combination of Hyperthermia
with Mesenchymal Stem Cell-Mediated Sodium Iodide
Symporter Gene Therapy

Mariella Stephanie Tutter

aus

München, Deutschland

2020

Erklärung

Diese Dissertation wurde im Sinne von § 7 der Promotionsordnung vom 28. November 2011 von Frau Professor Dr. Christine Spitzweg betreut und von Herrn Professor Dr. Ernst Wagner von der Fakultät für Chemie und Pharmazie vertreten.

Eidesstattliche Versicherung

Diese Dissertation wurde eigenständig und ohne unerlaubte Hilfe erarbeitet.

München, 10.03.2020

Mariella Tutter

Dissertation eingereicht am 10.03.2020

1.Gutachter: Prof. Dr. Ernst Wagner

2.Gutachterin: Prof. Dr. Christine Spitzweg

Mündliche Prüfung am 30.04.2020

Für tutti Tuttis

Table of Contents

1. Introduction.....	1
1.1 Biology of Cancer.....	1
1.2 The Tumor Microenvironment.....	2
1.3 Strategies for Cancer Therapy.....	3
1.4 Gene Therapy.....	4
1.5 The Sodium Iodide Symporter (NIS).....	5
1.5.1 Characteristics.....	5
1.5.2 Theranostic function of NIS.....	6
1.5.3 NIS Gene Therapy.....	8
1.6 Mesenchymal Stem Cells (MSCs).....	11
1.6.1 Characteristics of MSCs.....	11
1.6.2 MSCs as Gene Transfer Vehicles.....	11
1.6.3 MSC-mediated NIS Gene Therapy.....	12
1.6.4 How to Improve MSC Efficacy.....	13
1.7 Hyperthermia.....	14
2. Aims of the Thesis.....	15
3. MSC-mediated NIS Gene Therapy.....	16
3.1 Abstract.....	17
3.2 Introduction.....	18
3.3 Material and Methods.....	20
3.4 Results.....	23
3.5 Discussion.....	31
3.6 Conclusion.....	33
3.7 Key points.....	33
3.8 Acknowledgements.....	34
3.9 Supplementary Table 1.....	35
4. Hyperthermia-inducible MSC-mediated NIS Gene Therapy.....	36

4.1	Abstract	37
4.2	Graphical abstract	38
4.3	Introduction.....	39
4.4	Material and Methods	41
4.5	Results.....	47
4.6	Discussion	57
4.7	Abbreviations.....	61
4.8	Acknowledgements	61
4.9	Competing Interests	61
4.10	Supplement	62
5.	Summary	63
6.	Publications	66
6.1	Original Papers.....	66
6.2	Oral Presentations.....	67
6.3	Poster Presentations	68
6.4	Awards.....	69
6.5	Grants.....	69
7.	References	71
8.	Acknowledgements.....	85

1. Introduction

1.1 Biology of Cancer

Cancer is defined as abnormal, independent cell growth which can invade or spread to other parts of the body, with defects in the regulatory circuits that govern normal cell proliferation and homeostasis. This can affect virtually every cell of the body and therefore more than 100 forms of the disease exist. Cancer is expected to become the main cause of death worldwide in the 21st century, as its prevalence and the associated mortality are rapidly growing. One in five men and one in six women will suffer from one kind of cancer in their life, and one in eight men and one in eleven women will die of the disease [1]. This increase is attributed to a growing and aging population and lifestyle issues that have led to a higher prevalence of main risk factors [2], such as smoking, heavy alcohol consumption, obesity, and type 2 diabetes [1].

The transition of normal cells to a neoplastic state and development of a malignant tumor state is a multistep process [3]. In the course of tumor development, malignant cells can develop the capacity of autonomously maintaining cell growth signaling [4]. They can acquire, among others, the ability to synthesize stimulatory mitogenic factors or induce neighboring cells to do so for them, or they can alter the expression profile and structure of growth signal receptors [3]. Another step in carcinogenesis is the impairment of anti-proliferative signaling circuits, whereby the cells gain the ability to not be excluded from the proliferative cell cycle such that they are not nudged into a quiescent (G0) or post-mitotic state. In addition, neoplastic cells find a way to make themselves resistant to cell death by apoptosis, necrosis or autophagy [3]. Almost all types of cancer cells are assumed to have mutations, such as loss of pro-apoptotic regulators due to p53 tumor suppressor gene modifications or overexpression of anti-apoptotic regulators such as the bcl-2 oncogene, allowing them to evade apoptosis. These mutations generally lead to autonomous cell growth [3-5]. In mammals, however, healthy cells also possess an intrinsic multiplication restriction mechanism in the shape of the telomeres which cap the ends of chromosomes. Their erosion during each cell cycle is thought to ultimately provoke cell death. For this reason, the maintenance of the telomeres is also a crucial prerequisite for tumorigenesis [3]. In addition, a tumor needs to ensure sufficient nutrient and oxygen supply and disposal of cell waste by developing the competence to initiate neovascularization through triggering an “angiogenic switch” in endothelial cells, a property which cells only present during organogenesis under normal circumstances [5]. In order to escape from the primary tumor mass and move to a new, nutrient-rich environment, cancer cells must also develop the skills of tissue invasion and metastasis [3]. Two emerging characteristics that a tumor needs for its growth are firstly the ability to modify its energy metabolism in a way to adapt to enhanced cell growth and secondly to escape elimination by

the ever-alert immune system [3-5]. It has been found that cancer cells can increase their glucose uptake and switch their glucose metabolism to glycolysis even under aerobic conditions and working mitochondria (Warburg Effect), which is even emphasized under hypoxic conditions often seen in a tumor [6].

1.2 The Tumor Microenvironment

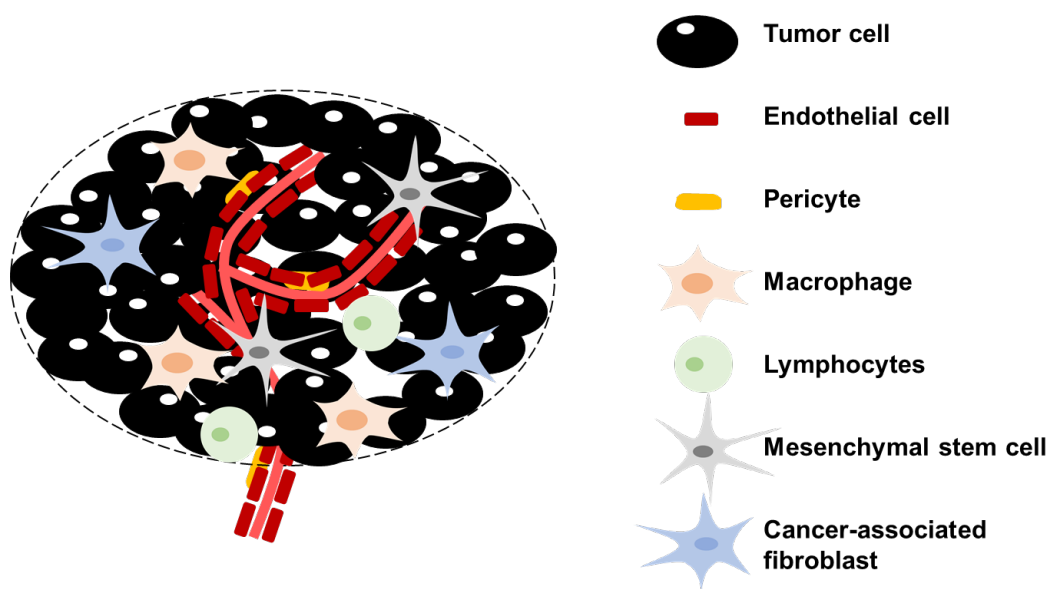


Figure 1 Illustration of the tumor microenvironment adapted from Balkwill et al. 2012 and Hanahan et al. 2000.

A tumor mass does not only consist of the malignant tumor cells, but also of the surrounding cells, the extracellular matrix (ECM) and signaling molecules, altogether forming the “tumor microenvironment” (**Figure 1**) [5]. Endothelial cells, which form the tumor-associated blood vessels, are found in the tumor stroma, structurally supported by pericytes or pericyte-like fibroblasts. The tumor stroma is also infiltrated by cells of the immune system, which have both tumor antagonizing and promoting properties. Inflammatory cells can release signaling molecules, such as growth, survival, and proangiogenic factors, and thus support tumor angiogenesis, stimulate proliferation and help metastatic dissemination [7]. The predominant cell type in the tumor stroma are fibroblasts, which create the structural foundation of a tumor by secreting ECM components and enzymes. Fibroblasts within the tumor environment secrete diverse mitogenic growth factors and are referred to as cancer-associated fibroblasts (CAFs). The tumor stromal cells can derive from pre-existing tissues or they can originate from adjacent normal tissue progenitor cells or from bone marrow stem cells [5, 7]. Within the tumor, a close collaborative network evolves between cancer cells and their supporting stroma. For a successful anti-cancer treatment the tumor as a whole has to be taken into account, including its distinct differentiated cells and especially including its microenvironment [3].

1.3 Strategies for Cancer Therapy

The search for new anticancer drugs and other treatment strategies is a constantly evolving field and every year new treatment approaches are being developed. At this point, surgery is still the most effective treatment for localized, solid tumors. Almost half of all tumors are also treated with radiotherapy (RT), often in a combined therapy concept, which provides highly effective treatment also for non-resectable local cancers or metastases [8]. In 1946, a new era started with the introduction of the first chemotherapeutic drug into modern oncology, mechlorethamine, an alkylating agent. In the following years, various new cytotoxic drugs were developed, such as antimetabolites (methotrexate, 5-fluorouracil), antimitotics (vinblastine, etoposide, or paclitaxel), or cytotoxic antibiotics (doxorubicin, actinomycin D). In the 1960s, new combined treatment protocols were implemented, resulting in greater efficacy without reaching the maximum tolerated dose of a single drug. A new age of anticancer therapy began in the '80s and '90s, when "targeted cancer therapy" became possible through advances in molecular and cell biology, allowing the targeting of specific tumor molecules such as growth factors and their receptors, signal transducers, or cytoplasmic proteins. The first clinical trial of a monoclonal antibody in 1997, trastuzumab, directed against the mutated HER2/neu receptor of breast cancer, paved the way for development of up to 30 different monoclonal antibodies approved by the European Medicines Agency (EMA) and/or the U.S. Food and Drug Administration (FDA) by 2017. An additional emerging approach is the selective targeting of the signaling pathways activated in tumors using small molecules. To date, two categories have been developed, selective tyrosine kinase inhibitors such as imatinib (BCR-ABL fusion protein, ABL, c-Kit, platelet-derived growth factor [PDGF] receptor), lapatinib (HER2 and epidermal growth factor [EGF] receptors), or sunitinib (vascular endothelial growth factor [VEGF] receptor, PDGF receptor, c-Kit) and intracytoplasmic serine/threonine kinase inhibitors such as rapamycin (mTOR), vemurafenib (BRAF), or trametinib (MEK). Most recently, a new specific anticancer strategy was developed in the form of immune checkpoint inhibitors. This involves the use of monoclonal antibodies directed against surface proteins expressed by tumors (anti-programmed cell death protein 1 [anti-PD1]) or T-cell protein receptors (anti-cytotoxic T-lymphocyte-associated antigen 4 [anti-CTLA4]), which downregulate the native immune response against the tumor [9].

Another novel and very promising approach in the field of anti-tumoral research is cancer gene therapy.

1.4 Gene Therapy

Gene therapy involves the therapeutic transfer of genetic material to the cells of a patient as a potential curative or preventive approach for a variety of diseases, such as those for which no other sufficient treatment option is available at present. Recently, there has been great progress in the area of gene therapy in a large variety of disorders, particularly genetic diseases such as primary immunodeficiencies, hemoglobin and coagulation disorders, neurological malfunctions, retinal disorders and a variety of cancer types [10]. This has resulted in the groundbreaking first EMA approval of the gene therapy products Glybera[®] (uniQure) for treatment of lipoprotein lipase deficiency in 2012 and Strimvelis[®] (GlaxoSmithKline) for adenosine deaminase deficiency (ADA-SCID) in 2016. This was followed in 2018, by the first CAR-T cell therapy products Kymriah[®] (Novartis) and Yescarta[®] (Gilead) for leukemia and lymphoma respectively [11], Luxturna[®] (Spark Therapeutics) for the treatment of patients enduring a loss of vision due to inherited retinal dystrophy, and most recently, in 2019, by Zynteglo[®] for the treatment of beta thalassemia (bluebird bio).

The field of gene therapy has made considerable strides in the last decade in large part due to the development of new vector platforms and an increasing repertoire of therapeutic genes. Still, in most of the almost 2600 clinical trials conducted in the field of gene therapy worldwide by 2018, one of the biggest obstacles has been the limited amount of genetically modified material reaching the site of action resulting in an insufficient therapeutic effect. Therefore, a wide range of different gene transfer vehicles are under intensive clinical investigation, ranging from different kinds of viruses (adeno-, retro-, or lentivirus) to non-viral vehicles, such as lipofection, naked DNA or different kinds of modified cells, such as macrophages, T-cells, or stem cells [11, 12]. In addition, a critical element in the design of clinical gene therapy trials is the search for opportunities for non-invasive monitoring of the *in vivo* distribution of viral and non-viral vectors, as well as monitoring of the biodistribution, level and duration of transgene expression. The sodium iodide symporter (NIS) has emerged as one of the most promising reporter and therapy genes available today, combining a diagnostic with a cytotoxic function (theranostic gene) by its ability to transport diagnostic and therapeutic radionuclides.

1.5 The Sodium Iodide Symporter (NIS)

1.5.1 Characteristics

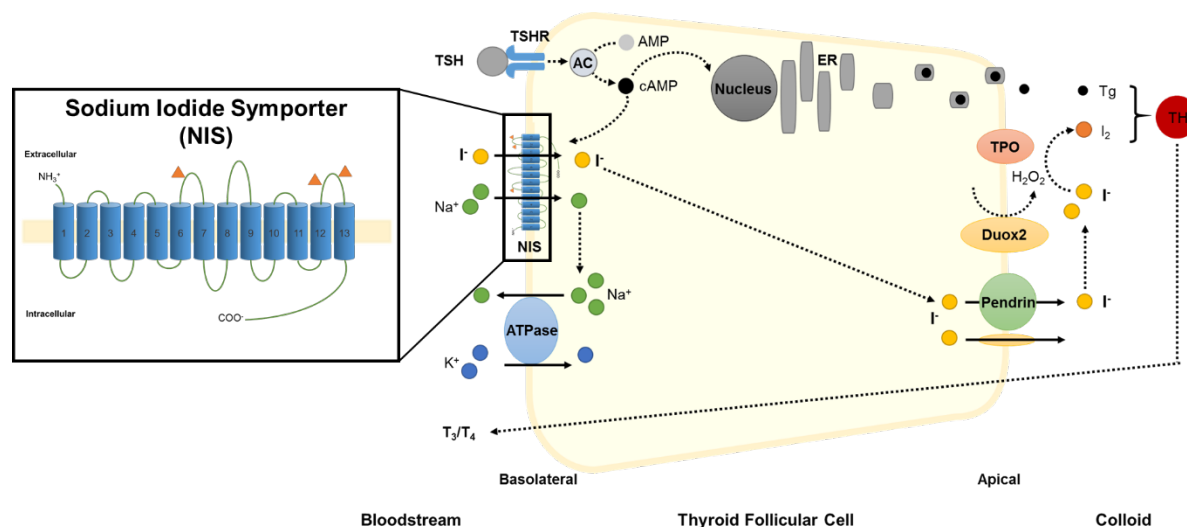


Figure 2 Schematic illustration of the protein structure of the sodium iodide symporter (NIS) (left) and the role of NIS in thyroid hormone synthesis (right) adapted from Spitzweg et al. 2001, Hingorani et al. 2010, and Ravera et al. 2017.

The sodium iodide symporter (NIS; *SLC5A5*) is an intrinsic transmembrane glycoprotein that consists of 643 amino acids in humans arranged in 13 putative transmembrane segments (**Figure 2 left**). NIS belongs to the solute carrier family 5 (SLC5) that transports negatively charged solutes into the cytoplasm. The symporter actively co-transport two sodium (Na^+) and one iodide ion (I^-) across the basolateral membrane into thyroid follicular cells (**Figure 2 right**). The transfer is electrogenic, driven by the electrochemical sodium gradient provided by the ouabain-sensitive Na^+/K^+ -ATPase. The efflux of I^- into the follicular lumen is not yet fully understood, but thought to be in part dependent upon the chloride/iodide transporter pendrin, chloride channels, and/or the sodium-monocarboxylate transporter [13]. I^- transport across the basolateral membrane is the first and crucial step of thyroid hormone synthesis, in which later I^- is oxidized to iodine (I_2) catalyzed by the thyroperoxidase (TPO). This is followed by the covalent incorporation of I_2 into the backbone of the protein thyroglobulin (TG) in a process called iodide organification. The last step, the coupling of iodotyrosine residues, results in the thyroid hormones (TH) tri-iodothyronine (T_3) and thyroxine (T_4). The thyroid hormones are stored in the colloid and released into the bloodstream triggered by thyroid-stimulating hormone (TSH). In addition, TSH, acting through the cAMP signal transduction pathway, is the key regulator of I^- transport and NIS expression in the thyroid at transcriptional and post-transcriptional levels [13, 14]. Physiologically, thyroid hormones are important for the maturation, growth and metabolism of various organs, especially for the development of the nervous system and the brain. This illustrates the great significance and clinical impact of NIS.

In addition to the thyroid gland, NIS is also endogenously expressed at lower levels in other tissues including the salivary glands, the gastric mucosa, the choroid plexus, the ciliary body of the eye, and the mammary glands during lactation. However, the expression of non-thyroidal NIS is not TSH-regulated and only the thyroid is equipped with an efficient iodide organification system [15, 16].

NIS is also able to transport various other anions, such as thiocyanate (SCN^-), nitrate (NO_3^-), chlorate (ClO_3^-), or tetrafluoroborate (TFB [BF_4^-]) [17, 18]. However, not all of them are transported with the same stoichiometry as I^- (1:2), the transport of Na^+ and ClO_4^- for example, was found to be electroneutral (1:1) [19]. Recently, it was shown that the very low intrinsic affinity of NIS for I^- increases tenfold, when NIS has bound two Na^+ ions. For this reason, approximately 79% of NIS molecules have bound two Na^+ , thereby allowing a sufficient I^- uptake, despite the submicromolar I^- serum concentration [20].

1.5.2 Theranostic function of NIS

The variety of potential substrates of NIS has opened the prospect of using specific radioisotopes for imaging techniques or therapy modalities, which constitutes the “theranostic” (therapy + diagnostic) function of NIS. The commercially available radioisotopes ^{123}I , ^{131}I and $^{99\text{m}}\text{Tc}$ can be used for whole body scintigraphy using a gamma camera to visualize thyroid cancer and metastases. In addition to scintigraphy, single photon emission computed tomography (SPECT) and positron emission tomography (PET) are routinely performed in the clinic using radioisotopes such as ^{125}I , ^{131}I , $^{99\text{m}}\text{Tc}$, and ^{188}Re (SPECT) or ^{124}I and ^{18}F -TFB (PET), that provide a higher resolution and 3D images [20]. After the diagnostic evaluation of a thyroid tumor by imaging, an exact personalized dosimetric calculation can be performed for a therapeutic application of radionuclides. Based on their β -particle emitting properties, the radionuclides ^{131}I , ^{188}Re , and ^{211}At are feasible for therapeutic purposes [15, 20, 21].

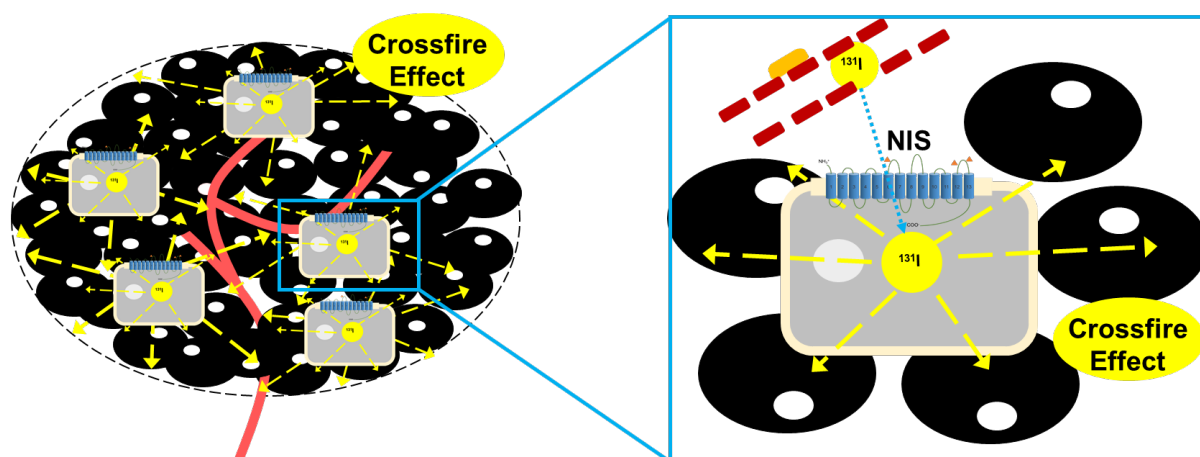


Figure 3 Schematic representation of the bystander effect of NIS in a tumor cell based on the crossfire effect of a β -emitting particle, adapted from Spitzweg and Morris 2002.

Radiation causes ionization or excitation of cellular components, which leads to the breaking of chemical bonds and the formation of free radicals, causing damage to proteins, especially the induction of double-strand breaks of the DNA. Cells hit by ionizing radiation mostly undergo apoptosis [22]. The crossfire effect of the β -particle with a path length of 2.4 mm in tissue as is seen with ^{131}I reaches cancer cells neighboring the ^{131}I incorporating cells, thereby causing a so-called bystander effect (**Figure 3**). ^{131}I has been used in the clinic since 1946 with great success as first line treatment for differentiated thyroid cancer after thyroidectomy with a well-known safety profile [13]. The effectivity of this method makes thyroid cancer one of the best manageable types of cancer with an overall survival of over 90% [23].

The described dual function of NIS allows non-invasive diagnostic imaging of functional NIS gene expression before proceeding with a highly effective therapeutic application of ^{131}I for thyroid cancer. Excitingly, the transfer of the NIS gene to non-thyroidal tumors opens the prospect of radioiodide imaging and therapy of other cancer types besides thyroid cancer.

1.5.3 NIS Gene Therapy

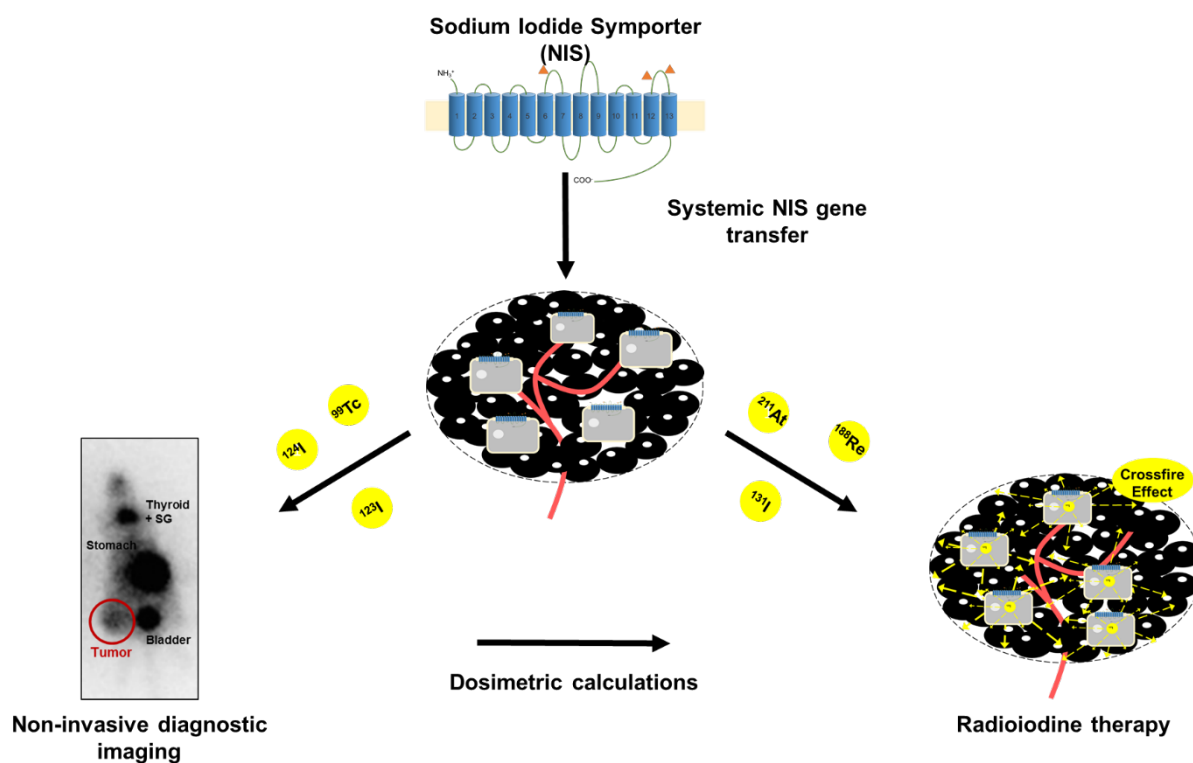


Figure 4 Concept of theranostic NIS gene therapy adapted from Spitzweg and Morris 2002.

NIS represents in many ways an ideal reporter and therapy protein. As it is a normal human gene and protein, it is non-immunogenic. It shows a high degree of specificity as native expression in tissues other than the thyroid is low. The over 70 years of experience with ¹³¹I therapy has shown a well-characterized safety profile in patients [22]. The potential damage to the salivary glands causes mostly minor side effects such as xerostomia or dry mouth, which are well manageable especially when compared to the benefit of good tumor growth control. Patients can be pre-treated with L-T₄ in order to downregulate NIS expression and thereby reduce ¹³¹I uptake of the normal thyroid to reduce the harm to the thyroid. Overall, the high degree of individual, personalized therapy options by using different radionuclides for a broad range of imaging modalities and the high efficacy of radioiodide therapy make *NIS* an outstanding theranostic gene for a cytoreductive gene therapy approach (**Figure 4**).

Following the cloning of the *NIS* gene in 1996 [24], initial experiments of *ex vivo* *NIS* gene transfer [25] and local *NIS* gene delivery by intratumoral injections were conducted [26]. Subsequently, a series of diverse approaches have been evaluated for the systemic *in vivo* gene transfer into non-thyroidal tumors using viruses, nanoparticles or mesenchymal stem cells (MSCs) as carriers.

The concept of exogenous administration of NIS has been investigated in various *in vitro* and *in vivo* tumor models including multiple myeloma [27], neuroblastoma [28], anaplastic thyroid cancer [29], glioma [30], cancer of the liver [31], the colon [32, 33], the breast [34], the pancreas [35-37], and the prostate [26, 38-41]. These very promising proof-of-principle studies have led to the use of NIS as imaging and/or therapy gene in phase I/II clinical trials in various non-thyroidal cancer entities (NCT01503177, NCT01846091, NCT02364713, NCT02700230, NCT02919449, NCT02962167, NCT03120624, NCT03171493, NCT03647163), including prostate cancer (NCT00788307), and multiple myeloma (NCT00450814, NCT02192775, NCT03017820).

A variety of modified viruses represent the most common shuttle vectors for gene therapy and were used in around two thirds of all gene therapy clinical trials conducted in 2017 [11]. This also applies to the majority of the preclinical and clinical NIS gene therapy trials underway. Early studies by Prof. Dr. Christine Spitzweg and her group using human NIS linked to the cytomegalovirus (CMV) or to the mouse alpha-fetoprotein (AFP) promoter were able to demonstrate an efficient tumor-selective NIS gene transfer to prostate cancer or hepatocellular carcinoma (HCC), respectively, after local infection [26, 42]. A replication-selective oncolytic adenovirus using the same AFP promoter construct for transcriptional targeting of NIS expression was developed to increase transduction and therapeutic efficacy by an additional oncolytic effect. This approach showed a markedly improved survival as compared to virotherapy alone [43]. However, in the case of systemic application, a significant concentration of virus was found in the liver. In addition, the induction of immune and inflammatory responses, and the elimination of the viral vectors by neutralizing antibodies represent common limitations of adenovirus-mediated gene therapy. To help address this issue, Dr. Geoffrey Grünwald in the Spitzweg laboratory evaluated the efficacy of adenoviral vectors that had been coated with poly(amidoamine) dendrimers (PAMAM). He was able to demonstrate significantly reduced hepatic transgene expression levels after systemic injection and an enhanced tumor targeting [44]. The use of tumor-specific ligands such as GE11 for the epidermal growth factor receptor (EGFR), which is upregulated in a large number of tumors, has also been used to improve tumor selectivity and, subsequently, the safety of virus-mediated gene therapy. Combining an EGFR-targeting with a dendrimer-coated adenovirus for NIS gene delivery was found to result in reduced liver toxicity and a strongly enhanced therapeutic effect, as seen by significantly reduced tumor growth and improved survival [45].

The use of viral vectors generally include the risk of infecting tissues other than tumors. In addition, their genetic loading capacity is limited and they may provoke an unwanted immune response. Therefore, synthetic, non-viral vectors that mimic viral behavior have emerged as a new research area, in particular as systems that can be formulated in a purposeful way with multifunctional domains that address the challenges of improved safety, exact targeting, and easy upscaling [46].

In collaboration with Prof. Dr. Ernst Wagner and his laboratory at the Department of Pharmacy, LMU Munich, Dr. Kathrin Klutz in the Spitzweg laboratory conducted the first studies of synthetic polymers for *NIS* gene therapy using oligoethylenimine (OEI)-grafted polypropylenimine dendrimers (G2-HD-OEI) [28]. In subcutaneous (s.c.) syngeneic neuroblastoma tumors and HCC xenografts, the G2-HD-OEI-polymers complexed with *NIS* DNA (polyplex) yielded a high tumoral accumulation of polyplexes leading to functional *NIS* expression in the tumor [28, 47]. In the next developmental step novel linear polyethylenimine (LPEI) based polymers, shielded by polyethylenglycol (PEG) to reduce toxicity and prolong blood circulation time, were combined with an incorporated peptide GE11 as EGFR-specific ligand. These agents were shown to improve tumor specific targeting and enhance internalization rates [48]. For successful translation of this polymer-based approach to clinical trials in humans, the feasibility of the established vectors was tested in advanced tumor models, such as disseminated colon cancer metastases [49] and pancreatic ductal adenocarcinoma (PDAC) [36]. In order to exploit the potential of polymers to employ a broad platform of ligands, in a subsequent study, Dr. Sarah Urnauer investigated the peptide sequence CGHKAKGPRK (B6) as a second potential tumor-selective peptide, which was originally obtained from a phage display screen for TfR-binding, but for which the cellular receptor remains unknown. B6 when used as a targeting ligand for systemic *NIS* gene delivery showed high tumoral levels of *NIS* protein expression leading to a strong therapeutic effect after radioiodide application [50]. In order to further enhance efficacy, as well as to minimize response failure due to tumor heterogeneity, a bifunctional polymer was subsequently developed that simultaneously targets two potential tumor-expressed receptors (EGFR and cMET/HGFR) for *NIS* gene therapy. The therapeutic efficacy of the dual-targeting concept resulted in significantly reduced tumor growth and perfusion, which was associated with prolonged animal survival [51]. As a next step towards a future clinical application, additional polymers were developed in the laboratory of Prof. Dr. Ernst Wagner designed to further improve systemic application of *NIS* with advanced safety, biocompatibility, and transduction efficacy. A novel sequence-defined polymer containing polyethylene glycol (PEG) and cationic (oligoethanoamino) amide cores coupled with a cMET-binding peptide (cMBP2) was found to allow a well-optimized transfection efficiency resulting in a significant therapeutic response, while dramatically reducing toxicity [52].

An additional novel non-viral method for systemic gene transfer currently under study is the use of adoptively applied genetically modified mesenchymal stem cells (MSCs) as gene delivery vehicles, based on their innate tumor tropism of MSCs and ease of isolation and genetic modification.

1.6 Mesenchymal Stem Cells (MSCs)

1.6.1 Characteristics of MSCs

MSCs are defined as multipotent progenitor cells that are found in many tissues including the bone marrow and that are capable of differentiating into multiple cell types including osteocytes, chondrocytes, smooth muscle cells, stromal cells, and fibroblasts [53, 54]. They are characterized by a fibroblast-like morphology, a phenotypically specific cell surface marker profile [55, 56], adherence to cell culture plastic, and a high *in vitro* expansion potential [55, 57, 58]. *In vivo*, MSCs have the unique property of active migration from a tissue niche to the peripheral circulation and eventually to sites of tissue damage or ischemia [54]. Many different groups have demonstrated the systemic delivery of MSCs to sites of tissue damage, such as the myocardium after myocardial infarction [59, 60], brain injuries after cerebral ischemia [61] or the lungs in a model of pulmonary fibrosis [62]. In addition, MSCs have low immunogenicity and potentially avoid immune rejection.

1.6.2 MSCs as Gene Transfer Vehicles

MSCs possess the innate ability to traffic to sites of inflammation and tissue injuries, including those present in cancer [63], as tumor stroma formation is thought to resemble a chronic wound [64, 65]. The homing of MSCs depends mainly on the combined effects of various inflammatory cytokines, chemokines, and growth factors secreted by the tumor and the tumor microenvironment [66-68]. The active recruitment of adoptively applied MSCs to various types of cancer, such as breast cancer [69], glioma [30, 70], colon cancer metastases [32], and hepatocellular carcinoma (HCC) [71, 72] has been demonstrated. These and other features make MSCs attractive candidates as therapy vehicles for the targeted delivery of therapeutic agents into the microenvironments of growing tumors [67].

One approach that has shown efficacy in this regard was the engineering of MSCs to constitutively secrete immunomodulatory anticancer proteins such as IFN- β , IL-2, or IL-12 [73, 74]. A second general approach that has been subsequently shown to have strong anti-tumor effects was to modify MSCs to produce the tumor necrosis factor-related apoptosis inducing ligand (TRAIL) in order to directly induce apoptosis [75].

Another strategy consists of loading MSCs with therapeutic drugs such as doxorubicin [69] or paclitaxel [76] for the direct transport of these agents to the tumor stroma. MSCs have also been used for the delivery of oncolytic viruses such as a conditionally replicative adenovirus or measles virus [77] (reviewed recently in [78, 79]) to growing tumors. A different general approach has used engineered versions of MSCs to deliver a therapeutic suicide gene, such as the herpes simplex virus type 1 thymidine kinase (HSV-TK), to selectively target tumors of the breast, pancreas, brain, and liver [80-83]. The subsequent therapeutic administration of ganciclovir, which is exclusively phosphorylated by HSV-TK, results in the formation of toxic metabolites and thereby reduced primary tumor growth and the incidence of metastases *in vivo* [84]. The safety and tolerability of this approach in patients with advanced gastrointestinal adenocarcinoma has been subsequently confirmed in a phase I/II clinical trial [85].

The sodium iodide symporter (*NIS*) described above, represents an important and promising theranostic gene for future clinical development of MSC-mediated gene therapy.

1.6.3 MSC-mediated NIS Gene Therapy

Due to their excellent tumor-homing properties, MSCs engineered to express NIS have been shown to efficiently migrate to solid tumors as evidenced by the tracking of NIS signal. In addition, NIS allows the characterization of whole body biodistribution of the engineered cells prior to NIS-mediated radioiodide therapy. Using this approach, successful MSC-mediated transfer of the *NIS*-transgene has been seen in various cancer entities, such as HCC [31, 72], glioma [30], breast cancer [34], prostate cancer [26, 40, 41], colon cancer metastases [32], multiple myeloma [27], and pancreatic ductal adenocarcinoma [35, 37]. In each of these cases, the subsequent therapeutic administration of ¹³¹I led to a significantly decreased tumor growth with a prolonged survival of animals *in vivo* [31, 82, 86, 87].

The first proof-of-principle experiments with NIS-MSC were performed in Prof. Spitzweg's laboratory in close collaboration with Prof. Dr. Peter Nelson, Medizinische Klinik IV, LMU Munich, using MSCs stably expressing NIS under control of the constitutively active CMV promoter (CMV-NIS-MSCs). The experiments confirmed a tumor-selective MSC-mediated *NIS* gene transfer to s.c. HCC xenograft tumors [86]. The administration of ¹³¹I resulted in a significant delay in tumor growth as compared to controls. The selective expression of transgenes such as NIS within the tumor environment was thought to be crucial to limiting potential off target side effects. A degree of selective control of transgene expression can be achieved by the use of gene promoters linked to signal or differentiation pathways that occur mostly or sometimes only within the tumor microenvironment.

In a more refined approach, more tumor stroma specific gene promoters were evaluated: Dr. Kerstin Knoop successfully investigated MSCs expressing NIS under the control of the tumor stroma-inflammatory RANTES/CCL5 promoter [72] and Dr. Andrea Müller developed MSCs driven by an hypoxia responsive synthetic promoter activated by tumor hypoxia [31]. In addition, by building on the role of transforming growth factor B1 (TGFB1) and the SMAD downstream target proteins in the context of tumor and tumor stroma biology, Dr. Christina Schug developed MSCs which express a synthetic SMAD-responsive promoter [87]. Most recently, Dr. Kathrin Schmohl used a vascular endothelial growth factor (VEGF)-NIS construct to target tumor angiogenesis [88].

In these settings, the biodistribution of the genetically engineered MSCs was analyzed by ^{123}I -scintigraphy or ^{124}I - and ^{18}F -TFB PET-imaging using *NIS* as reporter gene in s.c. and orthotopic HCC xenografts and colon cancer metastases *in vivo* tumor models. The efficient recruitment of MSCs after systemic application and with administration of ^{131}I , a significant reduction of tumor growth and prolonged survival of the animals was seen, further demonstrating the potential of *NIS* as a theranostic gene.

1.6.4 How to Improve MSC Efficacy

Effective homing of MSCs to the tumor stroma is crucial for a successful MSC-mediated therapeutic approach; therefore, an improvement in active engraftment of MSCs at the tumor site is of great interest. Priming MSCs in culture with chemokines, such as tumor necrosis factor (TNF)- α [89], or keeping them under hypoxic conditions [90], can result in an increased migratory behavior of MSCs *in vitro* and *in vivo*. The upregulation of chemokine receptors, such as CXCR4, is also able to boost tumor homing, as the CXCR4-SDF-1 axis was found to be a key regulator of MSC recruitment [91] (reviewed in [66]).

Another promising approach is to combine existing anticancer strategies such as chemotherapy or radiotherapy with *NIS* gene therapy. External beam radiation therapy (EBRT) has been shown to upregulate the chemokines and cytokines needed for MSC recruitment [92, 93]. Dr. Christina Schug in the group of Prof. Spitzweg recently demonstrated a significantly enhanced selective migration of MSCs after pre-treatment of tumors with EBRT in HCC xenograft tumors [94]. Combining the concept of EBRT with TGFB1-mediated *NIS* induction (SMAD-*NIS*-MSCs) yielded a dramatically improved therapeutic efficacy with tumor remission in a subset of animals [95].

Similarly, regional hyperthermia, another established antitumoral therapy modality, has been proposed to upregulate the inflammatory machinery of the body as well as to condition the tumor for an enhanced therapy response.

1.7 Hyperthermia

Hyperthermia is characterized by the elevation of body or tissue temperature in response to exogenous heat stimulation, reaching temperatures from 39 °C to 42.5 °C in a clinical setting. In contrast to fever, the temperature rise occurs without the presence of a pyrogenic agent [96, 97]. Hyperthermia is under intense investigation in the clinic as an adjuvant in multimodal cancer treatment approaches, especially for superficial tumors such as sarcoma, melanoma, breast, or colon cancer [98], as heat shows great chemo- and radiosensitizing qualities. A sub-lethal damage to a cancer cell caused by chemo- or radiotherapy can be enhanced to a lethal dose by the administration of heat. Non-invasive monitoring and precise adjustment of heat is essential. As of late, this is achieved in the clinic by using hybrid magnetic resonance-guided high-intensity focused ultrasound that allows simultaneous real-time temperature mapping of the heated region and energy deposition [99].

Mild hyperthermia, at temperatures in the range of 39 to 44 °C, is able to disturb the *de novo* synthesis of DNA by denaturation of synthetases and polymerases which leads to an arrest of the cell cycle. It can also induce apoptosis or necrosis and interfere with a number of DNA repair mechanisms [100]. In addition, changes of the fluidity and stability of cell membranes, resulting in modifications of the cytoskeleton are reported in response to hyperthermia. Recently, hyperthermia has gained interest in the context of oncological immunotherapy, especially concerning the therapy of metastases, as it can activate immune cells, initiate the release of exosomes and HSPs that present tumor antigens, and enhance surface molecule expression on heated tumor cells. Thus, the immunogenicity of tumor cells is increased. Lately, a phenomenon called the abscopal effect, which was first described for local radiotherapy, was also detected for hyperthermia. It describes the finding that local tumor treatment at one site is able to affect the growth of distant tumors and metastases. This effect is presumably mediated by activation of the immune system [101-104]. Furthermore, regional hyperthermia has been proposed to activate cells of the innate immune system [105]. It has been reported that, for example, natural killer cells or neutrophils show enhanced recruitment in response to heat application [106]. In addition, the enhanced trafficking of lymphocytes from draining tissues to secondary lymphatics triggered by heat treatment was shown to be potentially provoked by an increased expression of chemokines linked to lymphoid migration [101, 107].

Though the exact underlying molecular mechanisms of MSC migration are not yet fully understood, they are thought to resemble the processes underlying the recruitment of leukocytes to inflammatory tissues [66] which is mediated by high local concentrations of chemokines. This opens the exciting prospect of employing hyperthermia-induced amplification of chemokine secretion to augment MSC migration.

2. Aims of the Thesis

The previous work of Prof. Dr. Christine Spitzweg and her laboratory in collaboration with Prof. Dr. Peter Nelson and Prof. Ernst Wagner clearly demonstrated the enormous potential of genetically engineered mesenchymal stem cells (MSCs) for the tumor-selective delivery of the *NIS* gene. *NIS* as a well-characterized theranostic gene allows for the detailed non-invasive *in vivo* tracking of MSCs by ^{123}I -scintigraphy and ^{124}I -PET imaging, as well as effective therapeutic application of radionuclides (^{131}I , ^{188}Re). As a logical consequence of the successful proof-of-principle studies, and as a next step towards clinical application, the primary goal of this thesis was evaluation of the potential enhancement of the effectiveness, and tumor selectivity, of MSC-mediated *NIS* gene therapy through the combination with regional hyperthermia protocols.

The first aim of this thesis was the investigation of the stimulatory effect of regional hyperthermia with regards to the selective recruitment of MSCs to the tumor stroma *in vitro* and *in vivo* through heat-induced stimulation of cytokine secretion.

The second aim was the establishment of MSCs stably expressing *NIS* under the control of a heat-inducible HSP70B promoter. The application of heat-inducible promoters could in theory allow a spatial and temporal control of high level transgene expression by regional hyperthermia applied after MSC administration, thereby inducing strong promoter activation independent of their differentiation pathway (as compared to the previous use of TGFB1 or RANTES promoter).

3. MSC-mediated NIS Gene Therapy

This chapter has been adapted from:

Mariella Tutter¹, Christina Schug¹, Kathrin A. Schmohl¹, Sarah Urnauer¹, Carolin Kitzberger¹, Nathalie Schwenk¹, Matteo Petrini², Christian Zach³, Sibylle Ziegler³, Peter Bartenstein³, Wolfgang Weber⁴, Gabriele Multhoff⁵, Ernst Wagner⁶, Lars H. Lindner², Peter J. Nelson¹ and Christine Spitzweg^{1*}

Regional hyperthermia enhances mesenchymal stem cell recruitment to tumor stroma: Implications for mesenchymal stem cell-based tumor therapy

[Submitted manuscript]

¹Department of Internal Medicine IV, University Hospital of Munich, LMU Munich, Munich, Germany, ²Department of Internal Medicine III, University Hospital of Munich, LMU Munich, Munich, Germany, ³Department of Nuclear Medicine, University Hospital of Munich, LMU Munich, Munich, Germany, ⁴Department of Nuclear Medicine, Klinikum rechts der Isar der Technischen Universität München, Munich, Germany, ⁵Center for Translational Cancer Research (TranslaTUM), Radiation Immuno-Oncology group, Klinikum rechts der Isar der Technischen Universität München, Munich, Germany, ⁶Department of Pharmacy, Center of Drug Research, Pharmaceutical Biotechnology, LMU Munich, Munich, Germany

3.1 Abstract

The tropism of mesenchymal stem cells (MSCs) for growing tumor forms the basis for their use as gene delivery vehicles for the tumor-specific transport of therapeutic agents, such as the sodium iodide symporter (NIS). The *NIS* gene encodes a theranostic protein that allows non-invasive monitoring of the *in vivo* biodistribution of functional NIS expression by radioiodine imaging as well as the therapeutic application of ^{131}I . Regional hyperthermia is currently used as an adjuvant for various tumor therapies and is reported to enhance the secretion of immunomodulatory chemokines, cytokines and growth factors, well-known attractants of MSCs.

Methods: Following hyperthermia (41 °C for 1h) of experimental human hepatocellular carcinoma cells (HuH7) the chemokine secretion profile was analyzed by RT-PCR and chemotaxis of MSCs was tested in a 3D live cell tracking migration assay. An *in vivo* subcutaneous HuH7 mouse xenograft tumor model was used, where a single systemic injection of CMV-NIS-MSCs was applied 6h, 24h, 48h after or 24h, 48h before hyperthermia treatment and tumoral ^{123}I accumulation was assessed by ^{123}I -scintigraphy. The optimal imaging regime was then used for a ^{131}I therapy study

Results: Chemokine mRNA analysis indicated a substantial increase in expression levels after heat exposure. Enhanced chemotaxis of MSCs was found in relation to a gradient of supernatants from untreated to heat-treated cells. The optimal *in vivo* regime showed significantly increased ^{123}I -uptake in tumors of heat-treated animals (41 °C) when thermostimulated 24h after CMV-NIS-MSC injection compared to control animals (37 °C). *Ex vivo* affirmed by NIS-specific immunohistochemistry and RT-PCR, thereby confirming tumor-selective, temperature-dependent MSC migration. Therapeutic efficacy was demonstrated following CMV-NIS-MSC-mediated ^{131}I therapy combined with regional hyperthermia that resulted in stimulation of tumor growth reduction associated with prolongation of survival in the regional heat-treated animals as compared to normothermic mice or to the saline control group.

Conclusion: In the present report, we described the enhanced recruitment of adoptively applied MSCs engineered to express the theranostic *NIS* gene to tumors in response to regional hyperthermia.

3.2 Introduction

Thermal therapy (hyperthermia) is an emerging therapeutic modality for the treatment of cancer that makes use of the diverse biological effects that occur following regionally induced heating. Hyperthermia, in contrast to fever, is defined as addition of excess heat resulting in a rise of tissue or core temperature without a regulated change in the hypothalamic set point, and in absence of pyrogenic agents [96]. While the intrinsic biologic effects of elevated temperature in cancer tissues is still not well understood, it has been well-demonstrated that increasing the temperature of the tumor (39 °C to 42.5 °C) acts as an adjuvant in multimodal cancer treatment schemes in clinical practice [96, 108]. Hyperthermia is able to induce irreversible cellular DNA damage, to interfere in the DNA repair response cascades, to alter the fluidity and stability of cell membranes, and concomitantly modify the cytoskeleton in treated cells. These physiological changes effectively sensitize tumor cells to chemo- or radiotherapy and can thus enhance the beneficial effects of therapeutic strategies that target DNA stability [109]. In addition, studies are currently underway using thermally labile liposomes to enhance the targeting of chemotherapy agents during regional hyperthermia [110].

Regional hyperthermia has also been proposed to induce tumor immunogenicity and can result in enhanced systemic tumor control by stimulating immune control of both primary tumor and metastases [105], especially cells of the innate immune system can be activated by heat. The best studied phenomenon in this regard involves the enhanced trafficking of lymphocytes from draining tissues to secondary lymphatics in response to hyperthermia, primarily by the enhanced expression of chemokines, integrins and the chemokine receptors linked to lymphoid migration (CCL21, ICAM and CCR7) [recently summarized in [101, 107]]. Mesenchymal stem cells (MSCs) also show a pronounced capacity for recruitment to growing tumors, the exact molecular mechanisms at work are not fully understood, but are thought to parallel the processes underlying the recruitment of leukocytes from the peripheral circulation to inflamed tissues [66].

MSCs are defined as multipotent progenitor cells that are capable of differentiating into multiple cell types including osteocytes, chondrocytes, smooth muscle cells, stromal cells, and fibroblasts [53]. *In vivo*, MSCs have the unique property of migration from the bone marrow or other tissue niches to the peripheral circulation followed by their active recruitment to sites of tissue damage and ischemia, as generally present in solid tumors [54]. The recruitment of adoptively applied MSCs to various cancer types, such as breast cancer [69], glioma [30, 70], multiple myeloma [111], ovarian cancer [63], colon cancer metastases [32], hepatocellular carcinoma (HCC) [71, 86], as well as pancreatic cancer [35-37] has been demonstrated by various groups including ours.

This general feature has made engineered versions of MSCs attractive candidates for the use as shuttle vectors to efficiently deliver a therapeutic gene or agent deep into microenvironments of growing tumors [67]. The homing of MSCs is thought to depend on the combined effects of various inflammatory cytokines, chemokines, and growth factors secreted within the tumor microenvironment [112]. Hyperthermia has been shown to enhance the release of these inflammatory chemokines and cytokines shown to attract MSCs [105, 107, 113]. We hypothesized that mild regional hyperthermia could act as a means of enhancing the selective recruitment of MSC to the tumor stroma and thus open the exciting prospect of enhancing tumor selectivity as well as the therapeutic efficacy of MSC-mediated cancer gene therapy.

In the present report, we characterized the stimulatory effect of regional hyperthermia on recruitment of adoptively applied MSCs, engineered to express the theranostic sodium iodide symporter (*NIS*) gene, to experimental hepatocellular tumors. When used as a reporter gene, *NIS* allows non-invasive monitoring of the *in vivo* biodistribution, level and duration of functional *NIS* expression by ^{123}I -scintigraphy, ^{124}I -PET, or $^{99\text{m}}\text{TcO}_4$ -SPECT imaging [31, 32, 37, 72, 86, 87, 94, 95, 114, 115]. The biology of *NIS* as a therapy gene has been widely applied in patients for over 70 years allowing a highly effective therapeutic application of ^{131}I , or alternative radionuclides such as ^{211}At or ^{188}Re [13, 16].

3.3 Material and Methods

Cell culture

SV40 large T antigen-immortalized human bone marrow-derived MSCs were stably transfected with *NIS* driven by the CMV promoter (CMV-NIS-MSCs) and cells were cultured as described previously [86]. For heat-treatment cell culture dishes were sealed with parafilm and submerged in a circulating water bath for 30 to 120 minutes at 40 to 42 °C followed by a recovery time in an incubator at 37 °C (5% CO₂, 95% humidity) for 0-7 days.

¹²⁵I uptake assay and cell viability assay

Functional NIS expression was determined *in vitro* using a ¹²⁵I uptake assay and cell viability was determined using a commercially available thiazolyl blue tetrazolium blue (MTT) reagent, as described previously [116]. Results were normalized to cell survival and expressed as counts per minute (cpm) / A620.

HuH7 supernatants

1 x 10⁶ HuH7 cells were seeded in a 100 mm³ cell culture dish and 12 hours before thermostimulation full growth medium was replaced by serum-free DMEM. Supernatants from heat-treated and non-treated cells were collected 0 to 48 hours after heat treatment and immediately stored at -80 °C.

Quantitative real-time PCR and ELISA

HuH7 RNA und supernatants for ELISA were isolated 0 - 48 hours after hyperthermia of heat-treated and control cells as described previously [95]. Quantitative real-time (RT)-PCR was run in a Mastercycler ep gradient S PCR cyler (Eppendorf, Hamburg, Germany) or a Lightcycler 96 System (Roche, Basel, Switzerland) using the primers listed in **Supplementary Table 1**.

3D migration assay

Chemotaxis of CMV-NIS-MSCs, seeded in collagen I (0.3 x 10⁶ cells/ml), in relation to a gradient of unheated and heat-treated HuH7 supernatants was tested in a live cell tracking migration assay using the μ -slide Chemotaxis^{3D} system (ibidi, Planegg, Germany) and

monitored by time-lapse microscopy (Leica Microsystems, Wetzlar, Germany) for 24 hours as described previously [94].

***In vivo* regional hyperthermia**

Establishment of subcutaneous HuH7 xenograft mouse model in female CD1 nu/nu mice (Charles River Laboratories, Wilmington, Massachusetts, USA) was performed as described previously [86]. All animal experiments were approved by the regional governmental commission for animals (Regierung von Oberbayern, Munich, Germany). For regional hyperthermic treatment, mice were anesthetized by inhalation of isoflurane/oxygen anesthesia and placed on top of a water bath at 41 °C or, as control, at 37 °C for 1 hour. The water bath was covered with a plastic plate specifically designed to allow only the tumor bearing leg to be submerged into the water, through small holes in the plastic cover. Body temperature was monitored using a rectal thermometer (Homeothermic Blanket Systems with Flexible Probe; Harvard Apparatus, Massachusetts, USA).

¹²³I-scintigraphy after NIS gene transfer

When the tumors reached a volume of 500-800 mm³, a single systemic injection of 0.5 x 10⁶ CMV-NIS-MSCs into the tail vein was applied to HuH7 tumor-bearing mice and hyperthermia was locally applied either 48 hours, 24 hours or, 6 hours before, or 24 hours or 48 hours after MSC injection. 72 hours after MSC administration, mice received 18.5 MBq of ¹²³I (GE Healthcare Buchler GmbH & Co. KG, Braunschweig, Germany) intraperitoneally (i.p.) and iodide biodistribution was measured by serial scanning on a gamma camera (e.cam, Siemens, Munich, Germany) using a low-energy, high resolution collimator. As control of NIS-specific iodide accumulation, perchlorate (Merck KGaA, Darmstadt, Germany) was injected 30 min prior to ¹²³I injection. Regions of interest (ROIs) were analyzed by HERMES GOLD (Hermes Medical Solutions, Stockholm, Sweden) software and tumoral iodide accumulation was expressed as % of the injected dose (ID) per gram tumor (% ID/g). Dosimetric calculations were performed using the Medical Internal Radiation Dose (MIRD) technique with a RADAR dose factor (www.doseinfo-radar.com).

***Ex vivo* analysis**

Immunohistochemical staining of paraffin-embedded tumor sections and control organs was performed using a NIS-specific antibody (Merck Millipore; dilution 1:500) as described

previously [117]. Tumor samples taken 8 hours, 24 hours, and 48 hours after heat treatment (including 8 hours ^{123}I -scintigraphy) were analyzed by RT-PCR. $\Delta\Delta\text{-Ct}$ values were normalized to the internal control (the average of β -actin, UBC and r18s).

^{131}I -therapy study

When tumors had reached a size of 5mm in diameter, the drinking water was supplemented with 5 mg/ml L-T4 (Sigma Aldrich) and the mice received a low iodine diet (ssniff Spezialdiäten GmbH, Soest, Germany) to reduce thyroidal iodide uptake and thereby potentially enhance tumoral iodide accumulation. At a tumor volume of around 100 mm^3 , the mice received a single systemic injection of CMV-NIS-MSCs via the tail vein, followed by hyperthermic treatment ($41\text{ }^\circ\text{C}$ or $37\text{ }^\circ\text{C}$ for 1 hour) 24 hours later. 2 days after hyperthermia $55.5\text{ MBq }^{131}\text{I}$ was applied intraperitoneally (CMV-NIS-MSCs + $41\text{ }^\circ\text{C}$ + ^{131}I , $n = 8$; CMV-NIS-MSCs + $37\text{ }^\circ\text{C}$ + ^{131}I , $n = 7$). As control group, MSCs and ^{131}I was replaced by saline and mice were treated with $37\text{ }^\circ\text{C}$ (NaCl + $37\text{ }^\circ\text{C}$ + NaCl, $n = 5$). Mice were sacrificed based on tumor growth (tumor volume exceeded 1500 mm^3) and animal care protocols.

Statistical analysis

All *in vitro* experiments were performed at least three times and values are expressed as mean \pm SEM. Statistical significance was tested by two-tailed Student's t-test or by ANOVA with post-hoc Tukey (honestly significant difference) test for multiple comparisons. Survival was plotted by Kaplan-Meier survival plots and analyzed by log rank test. p -values < 0.05 were considered significant (* $p < 0.05$; ** $p < 0.01$; *** $p < 0.001$).

3.4 Results

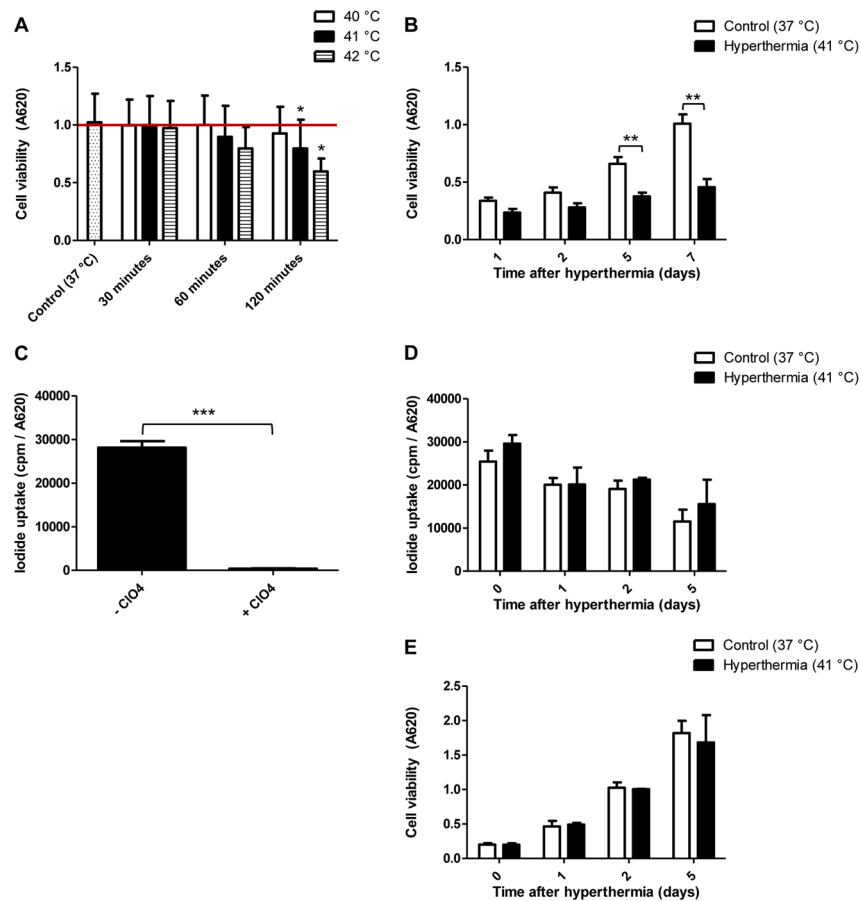


Figure 5 Hyperthermia effects in vitro. The effect of hyperthermia on HuH7 cells in vitro was analyzed by MTT assay 24 hours after heat treatment. Red line represents the cell viability of the 37 °C controls (A; dotted graph). Following hyperthermia at 41 °C for 60 minutes, long-term cell viability was evaluated (B). In vitro iodine uptake of CMV-NIS-MSCs was determined by a ¹²⁵I uptake assay (C). In addition, the effects of hyperthermia on the iodine accumulation by CMV-NIS-MSCs (D) and their viability (E) was evaluated.

Effects of hyperthermia on cell survival

Hyperthermic treatment led to acute cell killing only when the heat treatment was applied for an extended period of time (120 minutes) or at higher temperatures (42 °C) (Figure 5 A). In a long-term cell survival evaluation, following moderate hyperthermia (60 minutes at 41 °C), growth of heat-treated HuH7 cells was significantly reduced as compared to controls as seen 5 and 7 days after heat exposure (Figure 5 B).

Functional NIS expression in vitro

CMV-NIS-MSCs showed high functional NIS expression (28.114 ± 1516 cpm / A620) in vitro as seen in a ¹²⁵I uptake assay (Figure 5 C), which was sensitive to the NIS-specific inhibitor perchlorate (378 ± 60 cpm / A620). Thermostimulation caused no significant difference in ¹²⁵I

accumulation between heated (41 °C) and non-heated cells (37 °C) (**Figure 5 D**). In addition, cell viability, demonstrated no significant alteration in response to mild heat treatment (**Figure 5 E**).

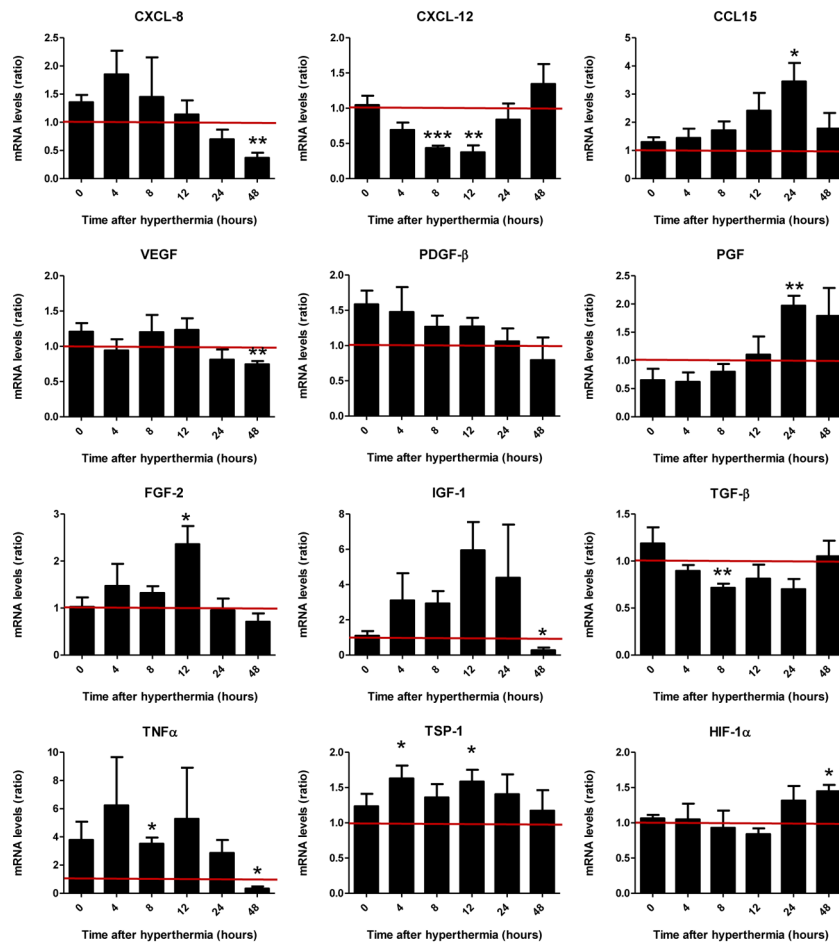


Figure 6 Chemokine and cytokine gene expression profile of HuH7 in vitro. RT-PCR analysis of mRNA extracted from heat-treated HuH7 cells 0 to 48 hours after hyperthermia compared to non-heated HuH7 using primers listed in **Supplementary table 1**.

Chemokine secretion profile of HCC tumor cells

mRNA analysis indicated a substantial increase in the expression of growth factors and chemokines after heat exposure of HuH7 cells as compared to controls (37 °C) (**Figure 6**). While the chemokine CXCL8, platelet-derived growth factor-β (PDGF-β), vascular endothelial growth factor (VEGF), tumor necrosis factor-α (TNF-α), and thrombospondin-1 (TSP-1) levels were found to be increased immediately (0-4 hours) following hyperthermia, the chemokine CCL15, placental growth factor (PGF), basic fibroblast growth factor (FGF-2), and insulin-like growth factor-1 (IGF-1) were increased later (12-24 hours). 48 hours after thermostimulation the enhanced expression of all factors tested had returned to untreated control levels. Transforming growth factor-β (TGF-β), interleukin-1-beta (IL-1β) and hypoxia-inducible factor-1-α (HIF-1α), in contrast, were not found to be influenced by thermostimulation, while CXCL12

mRNA levels were significantly reduced. No mRNA for hepatocyte growth factor (HGF), epidermal growth factor (EGF), CCL2, CCL5 and interleukin 6 (IL-6) was detected (data not shown).

ELISA then confirmed effects seen on the mRNA level on protein level in supernatants of HuH7 cells, affirming the heat-induced secretion (**Figure 7**).

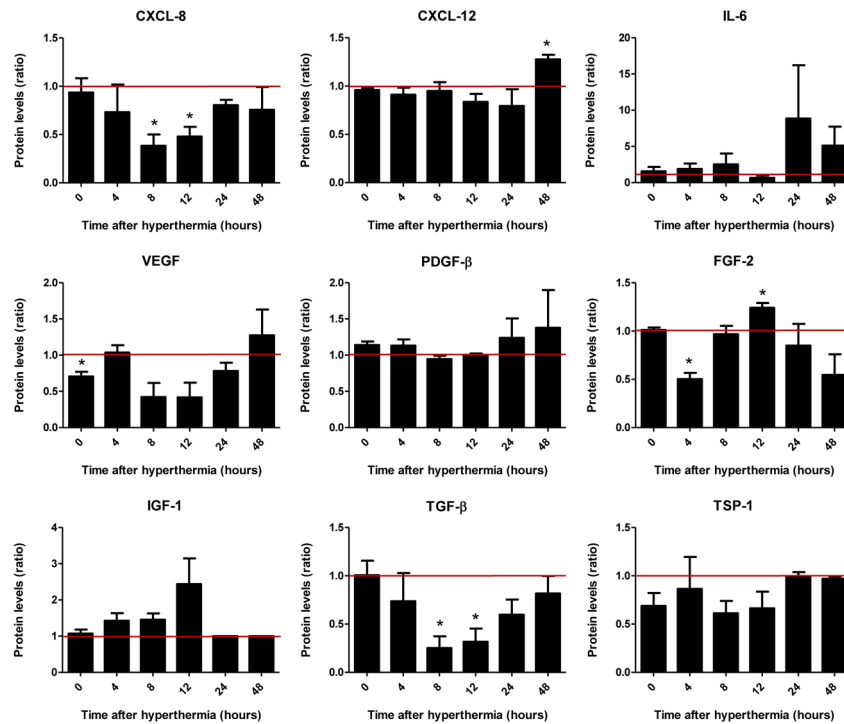


Figure 7 Protein expression analysis of HuH7 in vitro. Protein levels in culture supernatants derived from heat-treated HuH7 cells 0-48 hours after hyperthermia were analyzed by ELISA.

MSC-migration

CMV-NIS-MSCs showed no directed chemotaxis when subjected to supernatants derived from untreated HuH7 cells in both chambers (**Figure 8 A**). However, MSCs under the influence of a gradient between supernatants derived from untreated and heat-treated HuH7 cells showed directed chemotaxis to supernatants collected 24 hours after thermostimulation (**Figure 8 D**). This effect was even stronger with supernatants collected 48 hours after hyperthermia (**Figure 8 E**), whereas only random chemokinesis was seen with supernatants which were collected at earlier time points, i.e. 0 hours (**Figure 8 B**) and 12 hours (**Figure 8 C**) after heat treatment. Quantification of chemotactic parameters revealed a strong increase in γ FMI (**Figure 8 F**) and mean directness (**Figure 8 I**), a slightly increased velocity (**Figure 8 G**), and a significant rise in the mean CoM (red dots) (**Figure 8 H**) of MSCs towards supernatants from heat-treated HuH7 cells, demonstrating enhanced MSC migration.

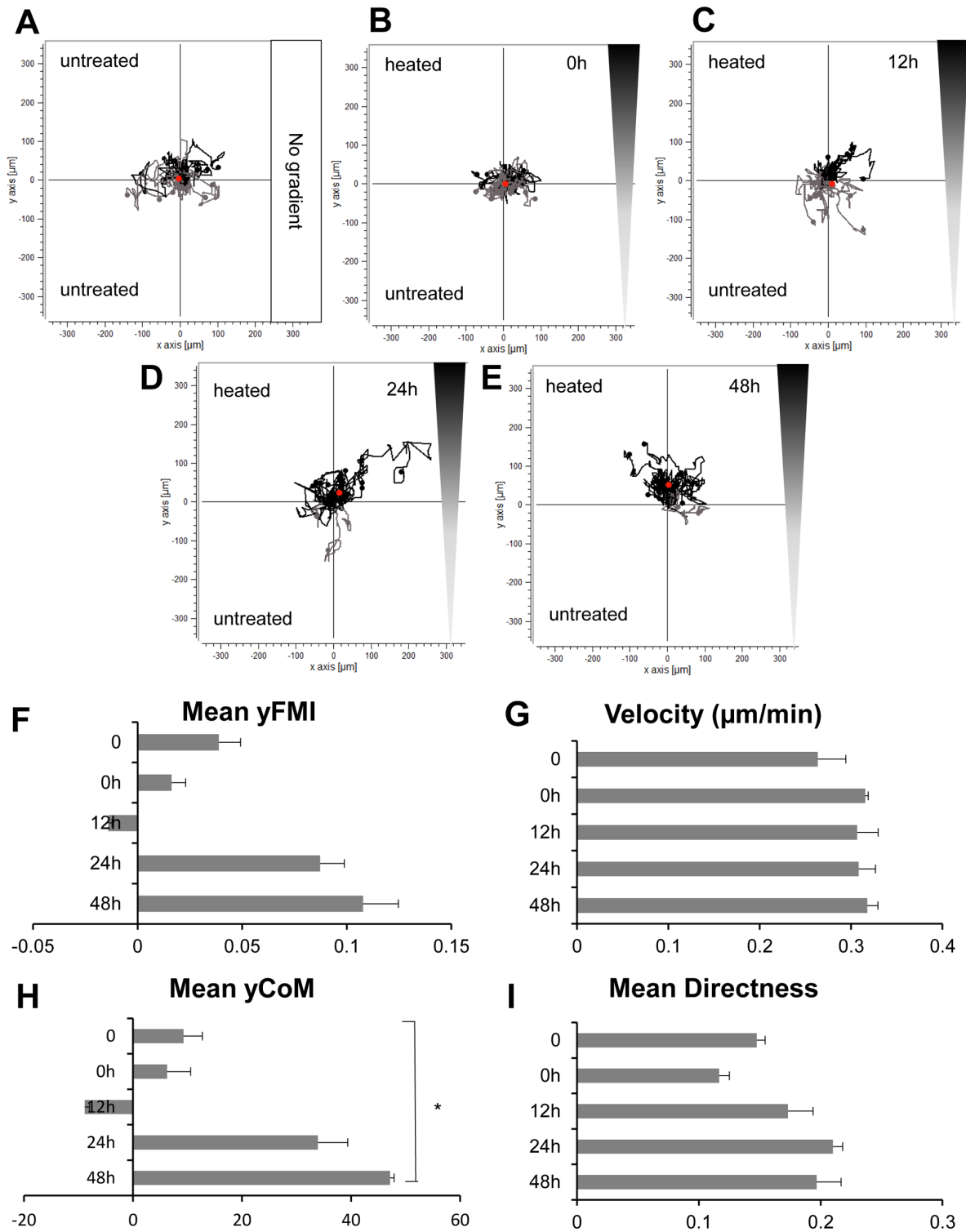


Figure 8 CMV-NIS-MSCs migration assay. MSCs subjected to supernatants derived from untreated HuH7 cells in both chambers (A). Cells under the influence of a gradient between supernatants from untreated (top chamber) and thermo-stimulated HuH7 cells derived 0 to 48 h after hyperthermia (bottom chamber) (B-E). Quantification of chemotaxis parameters as mean forward migration index (yFMI) (F), velocity (G), the mean center of mass (yCoM; red dots) (H), and mean directness (I) of MSCs.

¹²³I-scintigraphy

Quantitative analysis of tumoral radioiodine accumulation after CMV-NIS-MSC application (**Figure 9 A**) revealed significantly increased uptake of ¹²³I in heat-treated as compared to non-heated tumors (tumoral iodine accumulation 1 hour post ¹²³I injection of 37 °C-controls: $5.4 \pm 0.5\%$ ID/g; $n = 6$), with the strongest effect found in group D ($8.9 \pm 1.1\%$ ID/g; $n = 6$), where the MSCs were injected 24 hours prior to the thermostimulation, followed by group E ($8.0 \pm 1.5\%$ ID/g; $n = 6$) and group C ($6.5 \pm 2.0\%$ ID/g; $n = 7$), where MSCs were administered 48 hours before, or 6 hours after, hyperthermic treatment. In contrast, when heat was applied 24 hours prior to MSC injection, only a slight rise of tumoral iodine accumulation was seen in group B ($6.0 \pm 0.7\%$ ID/g; $n = 6$) as compared to controls, and essentially control levels were seen in group A ($5.9 \pm 1.4\%$ ID/g; $n = 6$), where regional hyperthermia was administered 48 hours before the MSCs. The NIS-specific iodide uptake could be blocked by administration of perchlorate (**Figure 9 B**).

Ex vivo analysis

Analysis of *ex vivo* steady state mRNA levels for the *NIS* gene demonstrated significantly increased NIS mRNA expression in tumors heated to 41 °C, as compared to controls at 37 °C (**Figure 9 C**). Strong NIS-specific immunoreactivity (red) was visible in the tumor stroma of heat-treated tumors whereas controls exhibited weaker signals. No immunoreactivity was detected in non-target organs (**Figure 9 D**). The *ex vivo* chemokine and cytokine mRNA expression profile (**Figure 10**) showed a time and temperature dependent mRNA expression that largely paralleled those seen in the *in vitro* study (**Figure 6**).

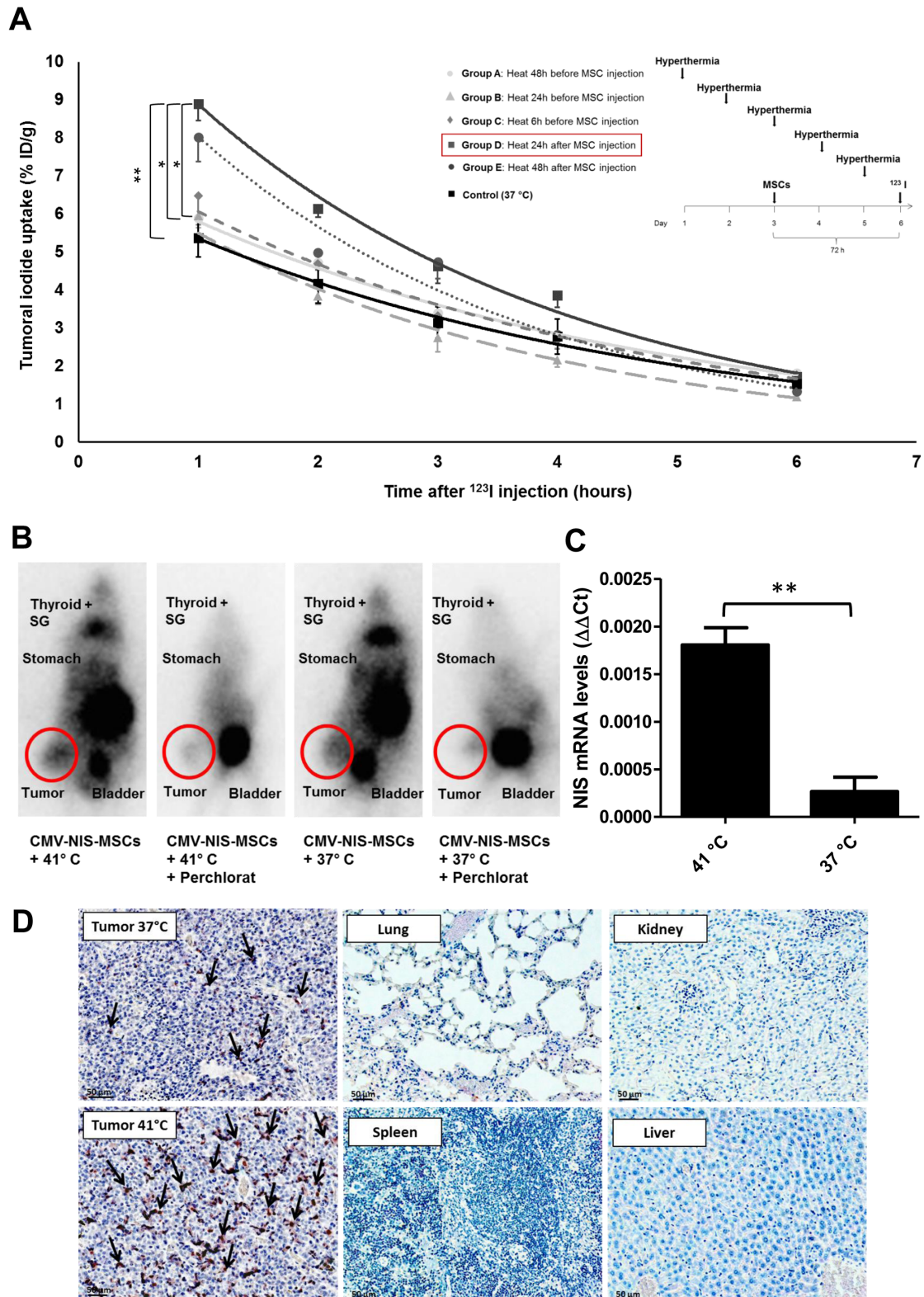


Figure 9 ¹²³I-scintigraphy following CMV-NIS-MSC administration. S.c. HuH7 tumor bearing mice were injected with CMV-NIS-MSCs and subjected to hyperthermic treatment (1 hour at 41 °C or 37 °C, as controls) at different time points (A). One representative image for the best performing hyperthermia treatment group and the control group (B). mRNA isolated from frozen tumor sections was analyzed for NIS by RT-PCR (C). NIS-specific immunohistochemistry (red) was performed of tumors of 37 °C-control animals and heat-treated tumors of mice (group D) and control organs (D).

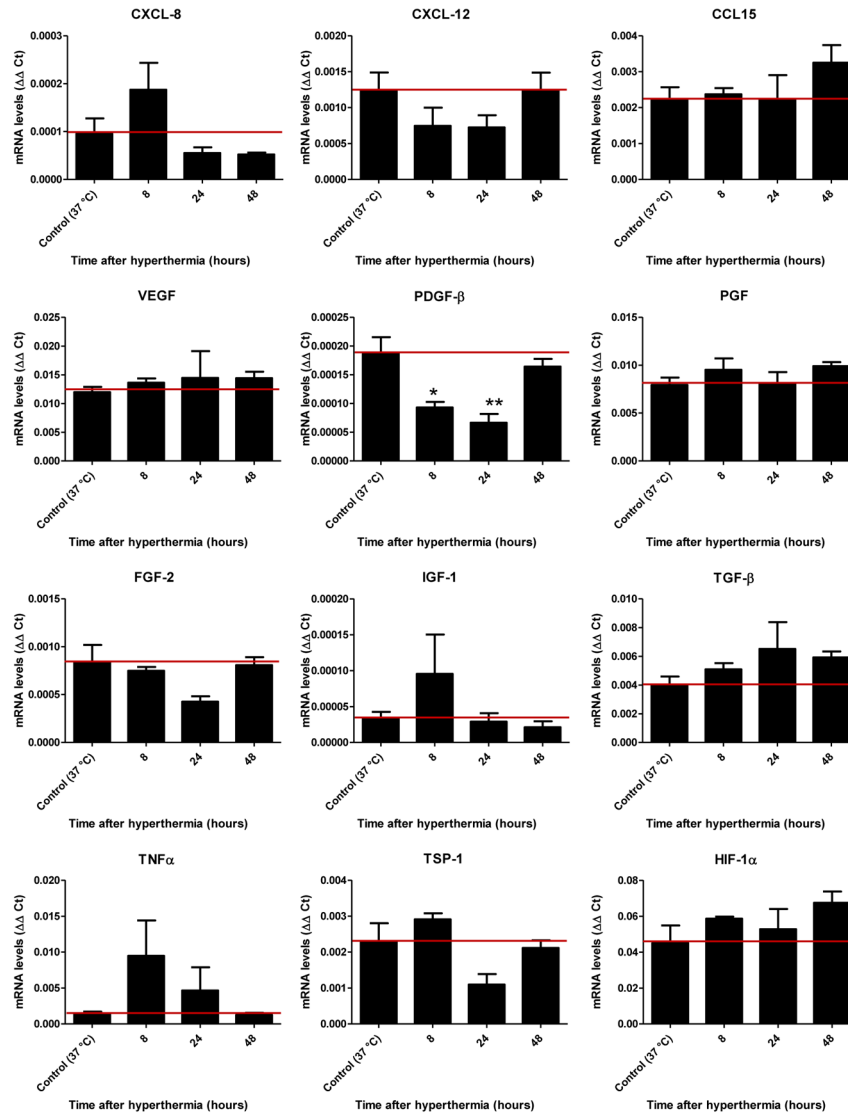


Figure 10 Chemokine and cytokine secretion profile of HuH7 in vivo. mRNA was isolated from frozen tumor sections from heat-treated tumors 8 hours, 24 hours and 48 hours later and expression levels of different chemokines and cytokines were evaluated by RT-PCR.

In vivo radioiodide therapy study

Combination treatment with tumoral hyperthermia at 41 °C resulted in a stimulation of tumor growth inhibition as compared to 37 °C-controls and to the saline only control group (**Figure 11 A**), with a partial tumor remission seen in one mouse. Hyperthermia co-treatment also resulted in a prolonged survival (**Figure 11 B**) (CMV-NIS-MSCs + 41 °C + ¹³¹I) as compared to the control groups (CMV-NIS-MSCs + 37 °C + ¹³¹I and saline only). On day 26 after therapy start, all animals of the saline control had to be sacrificed due to tumor volume reaching the allowed limit of 1500 mm³, whereas 85.7% of MSC + ¹³¹I therapy groups were still alive, demonstrating a significantly prolonged overall survival. All mice from the 37 °C controls reached endpoint criteria by day 32, at this time point 50% of the hyperthermia group was still

vital. The survival of the hyperthermic therapy group was plotted until day 140 and the surveillance of two mice was still ongoing at the time of this report. 4 out of 8 heat-treated mice showed a similar survival as the normothermic therapy group (around 30 days), whereas 2/8 lived more than 1 week, and 2/8 even 100 days longer than the controls with a partial remission seen in one mouse.

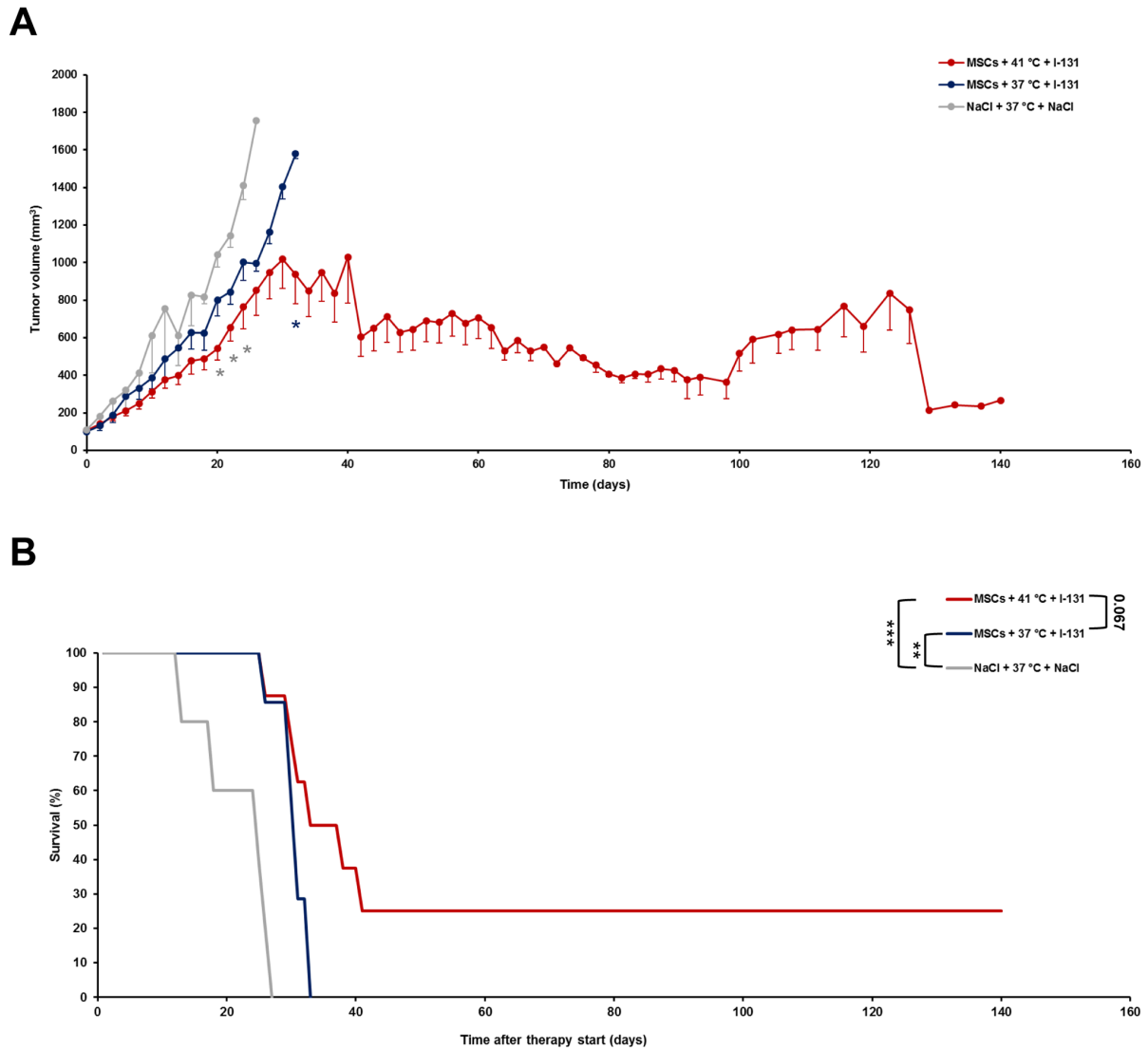


Figure 11 In vivo ¹³¹I therapy study. In a s.c. Huh7 xenograft mouse model, the best treatment scheme identified in the imaging study was adapted for a therapy study using ¹³¹I. Tumor growth (A) and survival (B) were monitored for the treatment with CMV-NIS-MSCs, regional hyperthermia, and ¹³¹I (red line), compared to the normothermic control group (blue line) and the saline only group (grey line).

3.5 Discussion

The response of cancer cells to hyperthermia is of great clinical interest. Its use as an adjuvant in multimodal treatment approaches enhances therapeutic effectiveness without increasing general toxicity. The benefit of hyperthermia in combination with radio-, chemo-, or radio-chemotherapy has been well-established in various randomized clinical trials [reviewed in [118]]. Hyperthermia is able to induce changes within the tumor microenvironment thought to help to trigger an anti-tumor immune response [100, 119]. In addition, hyperthermia is capable of increasing the amount of neutrophils, natural killer cells, and lymphocytes in the tumor microenvironment [107]. Leukocyte trafficking is a highly regulated process that may be influenced by hyperthermia at multiple stages. Hyperthermia can augment lymphocyte diapedesis across the endothelial layer, improve their adhesive properties to the endothelium, and thereby facilitate their infiltration [106].

The well-characterized innate ability of MSCs to traffic to solid tumors [63] is thought to derive from the observation that tumor stroma formation resembles a chronic, non-healing wound and MSC are recruited to “help repair” the damaged tissue [64, 65]. This general process has been adapted by many groups, including our own, as a "Trojan Horse"-like tumor therapy approach by using engineered versions of MSCs as vehicles for the delivery of agents deep into the tumor environment [63, 67, 120]. This approach has now advanced to clinical trials [[85], NCT02530047, NCT03298763].

In the present study, we characterized the effects of regional hyperthermia on the direct recruitment of MSCs, and specifically, on events that occur within hours or days following treatment. We could show that *in vitro*, hyperthermia (41 °C for 1 hour) led to enhanced transient production of cytokines and chemokine linked to MSC migration. Cells respond metabolically when subjected to a heat challenge. They upregulate heat shock proteins (HSPs) and other cell protective proteins, while reducing the steady state levels of genes not involved in the heat response [98]. Subsequent mRNA analysis of heat-treated tumor sections *ex vivo* presented a similar cytokine secretion profile as seen *in vitro*, thereby confirming the upregulation of immunomodulatory factors potentially enhancing MSC migration *ex vivo*. These effects were further validated in a 3D migration model that showed enhanced migration towards conditioned media taken from heat-treated HuH7 cells, thereby demonstrating for the first time the potential of hyperthermia to attract MSCs to heat-treated tumor cells *in vitro*.

In a further step towards *in vivo* application, we investigated the effects of the heat-treatment protocol (41 °C for 1 hour) on the cell viability *in vitro* and observed only a significant reduction of cell viability of the cancer (HuH7) cells and not on the MSCs. This confirms the previous observation that normal tissues are not damaged during hyperthermia, while tumors, in contrast, are more sensitive to hyperthermia [108].

The enhanced recruitment effects seen in the *in vitro* experiments were further validated *in vivo*. A promising candidate therapy gene for the next generation of clinical applications of MSC-mediated cancer gene therapy is the *NIS* transgene. *NIS* as a well-characterized theranostic gene allows detailed non-invasive *in vivo* tracking of MSCs by ^{123}I -scintigraphy or ^{124}I -PET imaging, as well as the highly effective therapeutic application of radionuclides (^{131}I , ^{188}Re) [13, 17]. We and others have demonstrated MSC-mediated transfer of therapeutic transgenes to diverse cancer entities, including; hepatocellular carcinoma [31, 72], glioma [30], breast cancer [34], prostate cancer [26, 40, 41], colon cancer metastases [32], multiple myeloma [27], and pancreatic ductal adenocarcinoma [35, 37]. In our studies using the *NIS* theranostic gene, we have found that MSC injections followed by the therapeutic administration of ^{131}I demonstrated a significantly reduced tumor growth with a prolonged survival of animals [31, 82, 86, 94].

In the present study, a single systemic injection of CMV-*NIS*-MSCs combined with thermostimulation at 41 °C showed that hyperthermia can enhance the selective MSC migration towards the tumor stroma in a s.c. HCC (HuH7) xenograft mouse model. Testing the application of heat at different time points before and after MSC injection, we observed the highest tumoral iodine uptake when injecting MSCs 24 hours prior to hyperthermia (group D). After intravenous injection, MSCs are initially trapped in the microcapillaries of the lungs [121] and start to migrate from the lungs to other organs, such as the liver, spleen, or kidneys or, if present, to a tumor only after 24 hours [122]. This effect helps explain our observation of the highest recruitment seen when applying heat 24 hours post MSC injection, which allowed optimized timing of the transiently enhanced tumoral chemokine and cytokine secretion following hyperthermia and the egress of the adoptively transferred cells from the lungs.

The optimal regional hyperthermia recruitment protocol identified by non-invasive imaging using ^{123}I -scintigraphy was then further tested and validated in the context of *NIS* gene-based ^{131}I -therapy. Animals treated with MSC, hyperthermia, and ^{131}I showed significantly reduced tumor growth and prolonged survival compared to the normothermic group and to the saline control group, demonstrating a significantly improved efficacy of MSC-mediated *NIS* gene therapy. The tumoral therapy response showed signs of a late divergence in tumor growth and survival curves, a phenomenon that has been described in immune therapy trials [123] as well in a phase III trial of neoadjuvant chemotherapy plus regional hyperthermia [124]. In our *in vivo* study, overall, we observed a heterogeneous response to hyperthermia therapy, with 4 out of 8 hyperthermia-treated mice showing a clear therapeutic effect from significant reduction of tumor growth to partial remission. Heterogeneous response rates have also been seen in clinical hyperthermia trials, such as in the recent EORTC 62961-ESHO 95 phase III trial on neoadjuvant chemotherapy alone or with regional hyperthermia for localized high-risk soft-tissue sarcoma [124, 125]. We believe that a main reason for the heterogeneous response

may be our experimental setup for hyperthermia application using a conventional water bath with its limitations in establishing and monitoring stable and homogenous intratumoral temperatures. Several trials have demonstrated a strong correlation between intratumoral temperatures and response to treatment [126]. Recent technical improvements in the sources used to apply and measure heat have expanded the clinical use of hyperthermia. In this regard, a hybrid magnetic resonance-guided high-intensity focused ultrasound has been adapted for tumor hyperthermia therapy that allows a highly focused heating of the region with real-time temperature mapping and energy deposition [99].

3.6 Conclusion

In our imaging-guided preclinical study, we were able to demonstrate significant stimulation of selective tumoral recruitment of genetically engineered MSCs by local hyperthermia application. Using *NIS* in its function as reporter gene, we were able to determine the optimal timing of hyperthermia treatment in the course of MSC application by non-invasive imaging that ultimately resulted in a significant therapeutic effect of CMV-NIS-MSC-based ^{131}I therapy in liver cancer xenografts. These data open the promising prospect of using hyperthermia to enhance the effectiveness of MSC-mediated cancer gene therapy for future clinical application and of potential implementation of this strategy in other MSC-based therapy contexts such as regenerative medicine.

3.7 Key points

QUESTION: How is the recruitment of adoptively applied MSCs, engineered to express the theranostic *NIS* gene, to tumors altered in response to regional hyperthermia?

PERTINENT FINDINGS: Regional heat-treatment of subcutaneous hepatocellular carcinoma (HuH7) xenograft tumors resulted in a significant stimulation of tumor-selective recruitment of genetically engineered MSCs analyzed by ^{123}I -scintigraphy. Therapeutic ^{131}I -application led to prolonged survival with reduced tumor growth.

IMPLICATIONS FOR PATIENTS CARE: This translational study opens the prospect of combining the effects of regional hyperthermia with focused *NIS* gene therapy.

3.8 Acknowledgements

We are grateful to Dr. Barbara von Ungern-Sternberg, Rosel Oos, and Dr. Markus Strigl (Department of Nuclear Medicine, University Hospital of Munich, LMU Munich, Munich, Germany), and Jakob Allmann (Department of Nuclear Medicine, Klinikum rechts der Isar der technischen Universität München, Munich, Germany) for their support with imaging and therapy studies. The authors thank Prof. Doris Mayr (Department of Pathology, University Hospital of Munich, LMU Munich, Munich, Germany) for preparation of paraffin-embedded slides. The authors owe special thanks to Prof. Julia Mayerle, Dr. Ujjwal Mahajan and Dr. Ivonne Regel (Department of Internal Medicine II, University Hospital of Munich, LMU Munich, Munich, Germany) for their generous assistance with “know-how” and equipment.

This work was supported by the following sources: grant from the Wilhelm Sander-Stiftung to C. Spitzweg (2014.129.1) and a grant from the Deutsche Forschungsgemeinschaft within the Collaborative Research Center SFB 824 to C. Spitzweg (project C8) as well as a within the Priority Program SPP1629 to C. Spitzweg and P.J. Nelson.

This work was performed as partial fulfillment of the doctoral thesis of M. Tutter at the Faculty for Chemistry and Pharmacy of the LMU Munich.

3.9 Supplementary Table 1

Gene	Forward primer (5' -> 3')	Reverse primer (5' -> 3')
CXCL8	TCTGCAGCTCTGTGTGAAGG	TTCTCCACAACCCTCTGCAC
CXCL12	AGAGCCAACGTCAAGCATCT	TAGCACAGCCTGGATAGCAA
CCL15	CTGCTGCACCTCCTACATCT	CATGCAATCCTGAACTCCCG
FGF-2	GGAGAAGAGCGACCCTCAC	AGCCAGGTAACGGTTAGCAC
PDGF-β	TTGGCTCGTGGAAGAAGG	CGTTGGTGCGGTCTATGA
PGF	CATCCTGTGTCTCCCTGCTG	GTCTCCTCCTTTCCGGCTTC
TGF-β	CAGCACGTGGAGCTGTACC	AAGATAACCACTCTGGCGAGTC
VEGF	CTACCTCCACCATGCCAAGT	ATGATTCTGCCCTCCTCCTT
IGF-1	GCTGGTGGATGCTCTTCAGT	TTGAGGGGTGCGCAATACAT
TNFα	CAGAGGGCCTGTACCTCATC	GGAAGACCCCTCCAGATAG
TSP-1	TTGTCTTTGGAACCACACCA	CTGGACAGCTCATCACAGGA
HIF-1α	GCTTTAACTTTGCTGGCCCC	TTCAGCGGTGGGTAATGGAG
NIS	TGCTAAGTGGCTTCTGGGTTGT	ATGCTGGTGGATGCTGTGCTGA
SV40	TTGCTGTGCTTACTGAGGATG	CCAATTATGTCACACCACAGA
β-actin	AGAAAATCTGGCACCACACC	TAGCACAGCCTGGATAGCAA
r18s	CAGCCACCCGAGATTGAGCA	TAGTAGCGACGGGCGGTGTG

4. Hyperthermia-inducible MSC-mediated NIS Gene Therapy

This chapter has been adapted from:

Mariella Tutter¹, Christina Schug¹, Kathrin A. Schmohl¹, Sarah Urnauer¹, Nathalie Schwenk¹, Matteo Petrini², Wouter J. Lokense², Christian Zach³, Sibylle Ziegler³, Peter Bartenstein³, Wolfgang Weber⁴, Ernst Wagner⁵, Lars H. Lindner², Peter J. Nelson¹ and Christine Spitzweg¹.

Effective control of tumor growth through spatial and temporal control of theranostic sodium iodide symporter (NIS) gene expression using a heat-inducible gene promoter in engineered mesenchymal stem cells.

[This manuscript has been accepted for publication in *Theranostics* and assigned the DOI doi:10.7150/thno.41489]

¹*Department of Internal Medicine IV, University Hospital of Munich, LMU Munich, Munich, Germany,* ²*Department of Internal Medicine III, University Hospital of Munich, LMU Munich, Munich, Germany,* ³*Department of Nuclear Medicine, University Hospital of Munich, LMU Munich, Munich, Germany,* ⁴*Department of Nuclear Medicine, Klinikum rechts der Isar der Technischen Universität München, Munich, Germany,* ⁵*Department of Pharmacy, Center of Drug Research, Pharmaceutical Biotechnology, LMU Munich, Munich, Germany*

4.1 Abstract

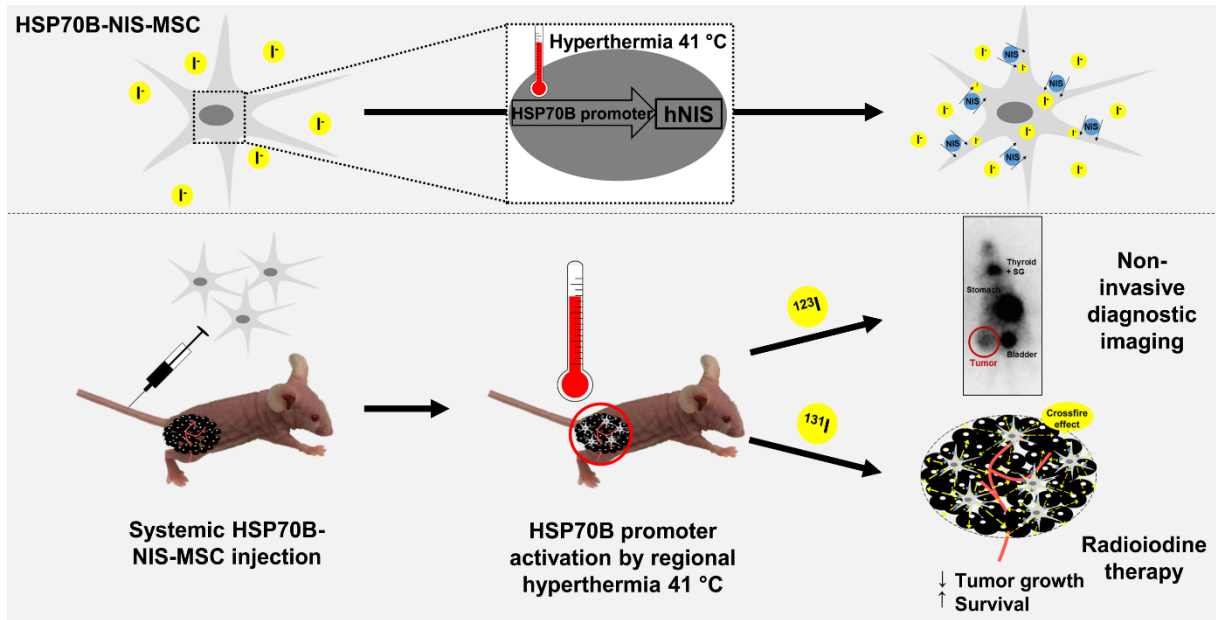
Purpose: The tumor homing characteristics of mesenchymal stem cells (MSCs) make them attractive vehicles for the tumor-specific delivery of therapeutic agents, such as the sodium iodide symporter (NIS). NIS is a theranostic protein that allows non-invasive monitoring of the *in vivo* biodistribution of functional NIS expression by radioiodine imaging as well as the therapeutic application of ^{131}I . To gain local and temporal control of transgene expression, and thereby improve tumor selectivity, we engineered MSCs to express the *NIS* gene under control of a heat-inducible HSP70B promoter.

Experimental Design: NIS induction in heat-treated HSP70B-NIS-MSCs was verified by ^{125}I uptake assay, RT-PCR, Western blot and immunofluorescence staining. HSP70B-NIS-MSCs were then injected i.v. into mice carrying subcutaneous hepatocellular carcinoma HuH7 xenografts, and hyperthermia (1 hour at 41 °C) was locally applied to the tumor. 0 – 72 hours later radioiodine uptake was assessed by ^{123}I -scintigraphy. The most effective uptake regime was then selected for ^{131}I therapy.

Results: The HSP70B promoter showed low basal activity *in vitro* and was significantly induced in response to heat. *In vivo*, the highest tumoral iodine accumulation was seen 12 hours after application of hyperthermia. HSP70B-NIS-MSC-mediated ^{131}I therapy combined with hyperthermia resulted in a significantly reduced tumor growth with prolonged survival as compared to control groups.

Conclusions: The heat-inducible HSP70B promoter allows hyperthermia-induced spatial and temporal control of MSC-mediated theranostic *NIS* gene radiotherapy with efficient tumor-selective and temperature-dependent accumulation of radioiodine in heat-treated tumors.

4.2 Graphical abstract



4.3 Introduction

The sodium iodide symporter (NIS) is a transmembrane glycoprotein that actively co-transport two sodium and one iodide ion across the plasma membrane into the cytoplasm of thyroid follicular cells (reviewed in [16]). The ability to accumulate and store iodide is a characteristic of thyroid tissue and a prerequisite for thyroid hormone synthesis. This feature allows the efficient treatment/curing of thyroid cancer through the systemic administration of radioiodide [13]. NIS-expressing target cells absorb β -emitting radioisotopes, such as ^{131}I or ^{188}Re , and drive cell death via β -particulate radiation of the expressing cell and the neighboring tissues through bystander effects as the decaying particles have a path length of up to 2.4 mm in tissue.

Genetically targeting NIS to non-thyroidal tumor tissues has opened the prospect of transferring standard clinical protocols for radioiodine imaging and therapy to a wide range of extra-thyroidal tumor entities [127]. Following cloning of the *NIS* gene in 1996 [24], initial experiments of *ex vivo* *NIS* gene transfer [25] and local *NIS* gene delivery by intratumoral injections have been described [26]. Subsequently, a series of diverse approaches have been evaluated for the systemic *in vivo* gene transfer into non-thyroidal tumors using viruses, nanoparticles or mesenchymal stem cells (MSCs) as carriers [27, 28, 30, 33-35, 39-41, 43-45, 47-52, 128-131]. To this end, adoptively applied MSCs have been demonstrated to exhibit an innate tumor tropism and have been extensively studied as potential tumor-selective gene transfer vehicles including progressing to clinical studies [31, 32, 37, 54, 57, 72, 83, 85-87, 94, 95, 120, 132-134]. Our group initially demonstrated the efficient transfer of functional *NIS* expression with accompanying therapeutic effects using MSCs transfected with *NIS* under the control of the constitutively active CMV-promoter [86]. As a next step, to reduce potential non-tumor side effects by enhancing tumor-selective NIS expression, we studied the potential use of the tumor stroma-induced CCL5 (RANTES) gene promoter, which allowed a robust tumoral iodine accumulation in experimental tumors in mice leading to significantly reduced tumor growth and prolonged survival of the experimental animals after ^{131}I and ^{188}Re treatment [72].

To expand our strategies to include local as well as temporal control of *NIS* transgene induction and enhanced tumor selectivity of MSC-mediated *NIS* gene therapy, we engineered MSCs to express the *NIS* gene under control of a heat-inducible HSP70B promoter (HSP70B-NIS-MSCs).

Heat shock proteins (HSPs) are a heterogeneous group of molecular chaperones that includes the well-characterized 70-kDa HSP70 protein. The members of this family exhibit various cellular housekeeping and stress-related functions, such as the prevention of misaggregation, degradation, disaggregation and refolding of misfolded denatured proteins [135]. Their synthesis can be induced within minutes in response to stress, such as heat, through the

trimerization of heat shock factor-1 monomers that translocate to the nucleus where they bind to heat shock elements in target gene promoters, thereby activating a paused RNA polymerase II and allowing transcription to proceed (reviewed in [136]).

Among the different heat-responsive promoters tested for gene therapy, the human HSP70B promoter was found to have a relatively low background activity and allow a rapid high level of heat-induced transgene expression *in vitro* and *in vivo* (reviewed in [137]). It was evaluated here as a candidate gene promoter for MSC-mediated NIS gene therapy. In the current study, we established and evaluated the use of a stable MSC line engineered with a heat-inducible HSP70B-NIS construct for enhanced control of tumor-specific NIS gene therapy.

4.4 Material and Methods

Plasmid constructs and stable transfection of MSCs

The plasmid construct pcDNA6.2ITRNEO-HSP70B-NIS, containing the full-length *NIS* gene (cDNA kindly provided by SM Jhiang, Ohio State University, Columbus, Ohio, USA) driven by the human HSP70B promoter, two sleeping beauty transposition sites and a geneticin resistance gene, was established as described previously [87] using the MultiSite Gateway Pro Plus Kit (Thermo Fisher Scientific, Waltham, Massachusetts, USA).

Simian virus 40 large T antigen-immortalized human bone marrow-derived MSCs were used for the experiments as the immortalized MSCs have been previously shown to retain the multilineage differentiation capacity, morphology and surface antigen pattern of primary MSCs but show greater expansion potential as aging and senescence are switched off [138]. Transfection of MSCs was performed using the Neon Transfection System (Thermo Fisher Scientific) according to the manufacturer's instructions. Wild type MSCs (5×10^5 cells) were electroporated with a total of 3 μ g plasmid (pcDNA6.2ITRNEO-HSP70B-NIS plus pCMV(CAT)T7-SB100X, containing a sleeping beauty transposon system [provided by Z Ivics, Max Delbrück Center for Molecular Medicine, Berlin, Germany]) with a pulse voltage of 1300 Volt, a pulse width of 30 ms and a pulse number of 1. After 24 h incubation at 37 °C in a humidified CO₂ incubator, selection medium was added containing 1% geneticin (G-418; Invitrogen, Carlsbad, California, USA). The clone showing the highest accumulation of radioiodide in an *in vitro* iodide uptake assay (see below), reflecting functional NIS expression, was used for further experiments (HSP70B-NIS-MSC).

Cell Culture

Cells were cultured in an incubator at 37 °C, with 5% (v/v) CO₂ atmosphere and 95% relative humidity. The human hepatocellular carcinoma (HCC) cell line HuH7 (JCRB0403; Japanese Collection of Research Bioresources Cell Bank, Osaka, Japan) was grown in Dulbecco's Modified Eagle Medium (1 g/l glucose; Sigma Aldrich, St. Louis, Missouri, USA) supplemented with 10% (v/v) fetal bovine serum (FBS; FBS Superior, Biochrom GmbH, Berlin, Germany) and 100 U/ml penicillin and 100 μ g/ml streptomycin (P/S; Sigma-Aldrich). The human MSC line (HSP70B-NIS-MSC) was cultured in Roswell Park Memorial Institute (RPMI)-1640 culture medium (Sigma-Aldrich) enriched with 10% FBS, P/S and G-418.

***In vitro* heat treatment**

For the *in vitro* hyperthermia experiments, the cell culture dishes were sealed and the cells were exposed to heat at different temperatures ranging from 39 to 42 °C in a water bath for 30 to 60 min and then maintained in an incubator at 37 °C for 4 to 48 h.

¹²⁵I uptake assay

NIS-mediated uptake of ¹²⁵I in HSP70B-NIS-MSCs was measured as described previously [116, 139]. Briefly, cells were seeded on 12-well plates and iodide uptake studies were performed at different time points (0 – 24 h) after heat treatment. Cells were incubated in Hanks' Balanced Salt solution (Gibco/Life Technologies, Carlsbad, California, USA), complemented with 10 µM NaI, 100 000 counts per minute (cpm) of Na¹²⁵I/ml (PerkinElmer, Waltham, Massachusetts, USA) and 10 mM 4-(2-hydroxyethyl)-1-piperazineethanesulfonic acid (HEPES; Sigma) (pH 7.3) for 45 min. The NIS-specific inhibitor KClO₄ (100 mM; Merck Millipore, Burlington, Massachusetts, USA) was added to control wells to verify NIS specificity of uptake. After washing, cells were lysed in 1 N NaOH (Carl Roth GmbH + Co KG, Karlsruhe, Germany) for 15 min and trapped ¹²⁵I was analyzed by γ-counting (Beckman Coulter GmbH, Krefeld, Germany). Results were normalized to cell survival (see below) and expressed as cpm / A620.

Cell viability assay

The commercially available MTT (3-(4,5-dimethylthiazol-2-yl)-2,5-diphenyltetrazolium bromide) assay (Sigma Aldrich) was performed following the manufacturer's instructions. The absorbance of the resulting formazan product was measured on a Sunrise microplate absorbance reader (Tecan, Männedorf, Switzerland) at a wavelength of 620 nm using the software Magellan (Tecan).

Quantitative real-time PCR

Total RNA of the heat treated and control HSP70B-NIS-MSCs was isolated 0 – 48 h after thermo-stimulation using the RNeasy Mini Kit with QIAshredder (Qiagen, Venlo, Netherlands) according to the manufacturer's recommendations. Single stranded cDNA was generated using Superscript III reverse transcriptase (Invitrogen). Quantitative real-time PCR (RT-PCR) was performed using the SYBR green PCR master mix (Qiagen) in a Mastercycler ep gradient S PCR cycler (Eppendorf, Hamburg, Germany). The following primers were used: *SLC5A5*

(hNIS) (5'-TGCGGGACTTTGCAGTACATT-3') and (5'-TGCAGATAATTCCGGTGGACA-3'), *HSPA1A* (5'-GATCAACGACGGAGACAAGC-3') and (5'-GCTGCGAGTCGTTGAAGTAG-3'), *HSPA7* (5'-TTCCATGAAGTGGTTCACGA-3') and (5'-TTGACGCTGGTGTCTTTGAG-3'), and *ACTB* (β -actin) (5'-AGAAAATCTGGCACCCACACC-3') and (5'-TAGCACAGCCTGGATAGCAA-3'). Levels of cDNA were normalized to the internal control β -actin. Relative expression levels were calculated using comparative $\Delta\Delta$ -Ct values.

Membrane preparation and Western blot

Membrane proteins from heat-treated and control cells were extracted as described previously [116] and protein concentration measured by Bradford assay (BioRad Laboratories Inc., Hercules, California, USA). Western blot analysis was conducted as reported previously [116], using a mouse monoclonal NIS-specific antibody (Merck Millipore; dilution 1:1700) overnight at 4 °C and a horse-radish peroxidase-labeled goat anti-mouse antibody (Jackson ImmunoResearch Europe Ltd., Ely, UK; dilution 1:2000) for 1 h at room temperature. After 1 min incubation with enhanced chemiluminescence Western blotting detection reagent (WESTAR ETA C 2.0; Cyanagen Srl, Bologna, Italy), images were taken with an ECL ChemoCam Imager (INTAS, Göttingen, Germany). As control for protein loading, the membrane was stripped (Restore Western Blot Stripping Buffer, Thermo Fisher Scientific) and re-probed with a monoclonal anti- β -actin antibody produced in mouse (Sigma Aldrich; dilution 1:1500). The intensity of the bands was measured by densitometry using ImageJ software (NIH, Bethesda, Maryland, USA) and normalized to the β -actin loading control, expressed as the relative amount of NIS protein.

Immunofluorescence staining

HSP70B-NIS-MSCs were seeded directly on FBS-coated microscope slides and grown until 60% confluent. 6 h after hyperthermia, the slides were air-dried overnight at room temperature and monolayers fixed with 80% methanol (Carl Roth) for 5 min at 4 °C, followed by 100% acetone (Carl Roth) for 2 min at -20 °C. Following blocking with 12% bovine serum albumin (Sigma-Aldrich) in phosphate-buffered saline (PBS; Sigma Aldrich) for 30 min, cells were then incubated with a primary mouse monoclonal NIS-specific antibody (Merck Millipore; dilution 1:500) for 90 min. A secondary Cy3 AffiniPure donkey anti-rabbit IgG antibody (Jackson ImmunoResearch; dilution 1:400) and bisbenzimidazole (Hoechst; Sigma Aldrich; dilution 1:2000) to counterstain nuclei were added for 30 min. Pictures were taken using an Axiovert 135 TV fluorescence microscope in combination with an AxioCam MRm CCD camera and the AxioVision Rel. 4.8 software (Carl Zeiss Microscopy GmbH, Jena, Germany).

Establishment of subcutaneous HuH7 xenografts

5 – 6 week old female CD1 nu/nu mice were bought from Charles River (Sulzfeld, Germany) and kept under specific pathogen-free conditions with *ad libitum* access to water and mouse chow. The regional governmental commission for animals (Regierung von Oberbayern, Munich, Germany) authorized all experimental protocols.

Subcutaneous (s.c.) tumors were established by s.c. injection of 5×10^6 HuH7 cells re-suspended in 100 μ l PBS into the right flank region of the animals. Tumor volumes were determined using a caliper and calculated by the equation height x length x width x 0.52. When the tumor reached a volume $> 1500 \text{ mm}^3$ or showed signs of necrosis, mice were sacrificed.

In vivo regional hyperthermia

For regional hyperthermia treatment *in vivo*, mice were anesthetized with inhalation isoflurane narcosis and placed on a water bath covered with a plastic plate that was specifically designed to allow only the tumor bearing leg to be submerged into the water through holes in the plastic cover. A rectal thermometer (Homeothermic Blanket Systems with Flexible Probe; Harvard Apparatus, Massachusetts, USA) monitored body temperature.

Non-invasive monitoring of *in vivo* NIS biodistribution

As soon as tumors reached a volume of approximately 500 mm^3 , 5×10^5 HSP70B-NIS-MSCs were injected systemically via the tail vein every second day for a total of three times. 3 days later, regional hyperthermia was applied (41°C or, as control, 37°C for 1 h). The mice received 18.5 MBq (0.5 mCi) of ^{123}I (GE Healthcare Buchler GmbH & Co. KG, Braunschweig, Germany) intraperitoneally (i.p.) after 0, 6, 12, 18, 24, 36, 48, and 72 h and gamma camera imaging (e.cam, Siemens, Munich, Germany) was performed using a low-energy, high-resolution collimator. Intrinsic thyroïdal iodide uptake was reduced by the addition of 5 mg/ml L-thyroxine (L-T4; Sigma Aldrich) to the drinking water ten days before ^{123}I administration. Using the HERMES GOLD (Hermes Medical Solutions, Stockholm, Sweden) software, regions of interest were evaluated and tumoral iodide uptake was calculated and expressed as percentage of injected dose (ID) per tumor (% ID/tumor). Using the Medical Internal Radiation Dose (MIRD) concept, dosimetry was calculated with a RADAR dose factor (www.doseinfo-radar.com).

Ex vivo immunohistochemical NIS protein staining

Paraffin-embedded tumor sections and a series of control organs from the mice used for ¹²³I-scintigraphy were immunohistochemically stained as described previously [117]. Staining was performed using a primary mouse monoclonal NIS-specific antibody (Merck Millipore; dilution 1:500) for 90 min followed by a biotin-SP-conjugated goat anti-mouse IgG antibody (Jackson ImmunoResearch; dilution 1:200) for 20 min and then peroxidase-conjugated streptavidin (Jackson ImmunoResearch; dilution 1:300) for an additional 20 min. Immunohistochemically stained tumor sections were scanned using the Panoramic MIDI digital slide scanner and pictures taken with Caseviewer software (3DHISTECH Ltd., Budapest, Hungary) and control organs were imaged on an Olympus BX41 microscope equipped with an Olympus XC30 CCD camera (Olympus, Shimjukum Tokio, Japan).

Ex vivo mRNA expression analysis

Frozen tumor sections of the ¹²³I-scintigraphy were shredded using 20G and 25G syringes and RNA was isolated using the RNeasy Mini Kit with QIAshredder (see above). RT-PCR was run on a Lightcycler 96 System (Roche, Basel, Switzerland) and levels of cDNA were normalized to the mean of the internal controls β -actin, r18s and UBC. In addition to *NIS*, the primers r18s (5'-CAGCCACCCGAGATTGAGCA-3') and (5'-TAGTAGCGACGGGCGGTGTG-3') and UBC (5'-ATTTGGGTCGCGGTTCTTG-3') and (5'-TGCCTTGACATTCTCGATGGT-3') were used.

¹³¹I-therapy study

Therapy trials were started when tumors had an average size of 5 x 5 mm. Ten days before radioiodide injection, drinking water of mice was supplemented with L-T4 and standard mouse chow was switched to a low iodine diet (ssniff Spezialdiäten GmbH, Soest, Germany) to reduce radioiodine uptake by the thyroid gland and enhance potential tumoral iodine accumulation. Animals were randomly assigned to four treatment groups. HSP70B-NIS-MSCs were injected intravenously (i.v.) three times on every second day, followed by hyperthermia application 72 h later. 12 – 18 h after the heat treatment, 55.5 MBq (1.5 mCi) ¹³¹I (GE Healthcare) were injected i.p. This cycle was repeated 24 h after ¹³¹I administration, for a total of three times, with the second and third cycle consisting of only one MSC injection to reduce therapy duration (therapy group: HSP70B-NIS-MSCs + 41 °C + ¹³¹I; *n* = 9). To investigate the potential direct effects of hyperthermia on MSCs, we used saline instead of ¹³¹I (NaCl; Fresenius Kabi, Bad Homburg, Germany; HSP70B-NIS-MSCs + 41 °C + NaCl; *n* = 7). In an additional control group, MSCs and radioiodide were replaced by saline (NaCl + 41 °C + NaCl; *n* = 10) to investigate

the potential effects of hyperthermia alone. As controls, the therapy schemes as described above were also conducted with 37 °C instead of 41 °C (HSP70B-NIS-MSCs + 37 °C + ¹³¹I; $n = 10$, HSP70B-NIS-MSCs + 37 °C + NaCl; $n = 8$, and NaCl + 37 °C + NaCl; $n = 9$). The tumor volume of the mice was estimated as described above and mice were sacrificed when the tumor volume exceeded 1500 mm³.

Ex vivo immunofluorescence assay

Immunofluorescence staining on dissected frozen tissue samples of HuH7 tumors and quantitative analysis of cellular proliferation (Ki67; Abcam, Cambridge, UK; dilution 1:200) and blood vessel density (CD31; BD Pharmingen, Heidelberg, Germany; dilution 1:100) were performed according to the protocol described previously [51]. Pictures were taken using a Leica DMI6000B microscope equipped with a Leica DFC365 FX camera and Leica MM AF software (Leica Microsystems GmbH, Wetzlar, Germany). Quantification of six visual fields per tumor section was performed using ImageJ software.

Statistical analysis

All *in vitro* experiments were performed at least in triplicate and results are reported as mean \pm standard error of the mean (SEM), mean fold change \pm SEM or in percent. Statistical significance was tested by two-tailed Student's t-test, one-way analysis of variance (ANOVA) followed by post-hoc Tukey (honestly significant difference) test for comparison of more than two groups, two-way ANOVA followed by post-hoc Tukey test for the repeated measurements in the imaging study, or by log-rank for Kaplan-Meier survival plots. p values < 0.05 were considered significant (* $p < 0.05$; ** $p < 0.01$; *** $p < 0.001$).

4.5 Results

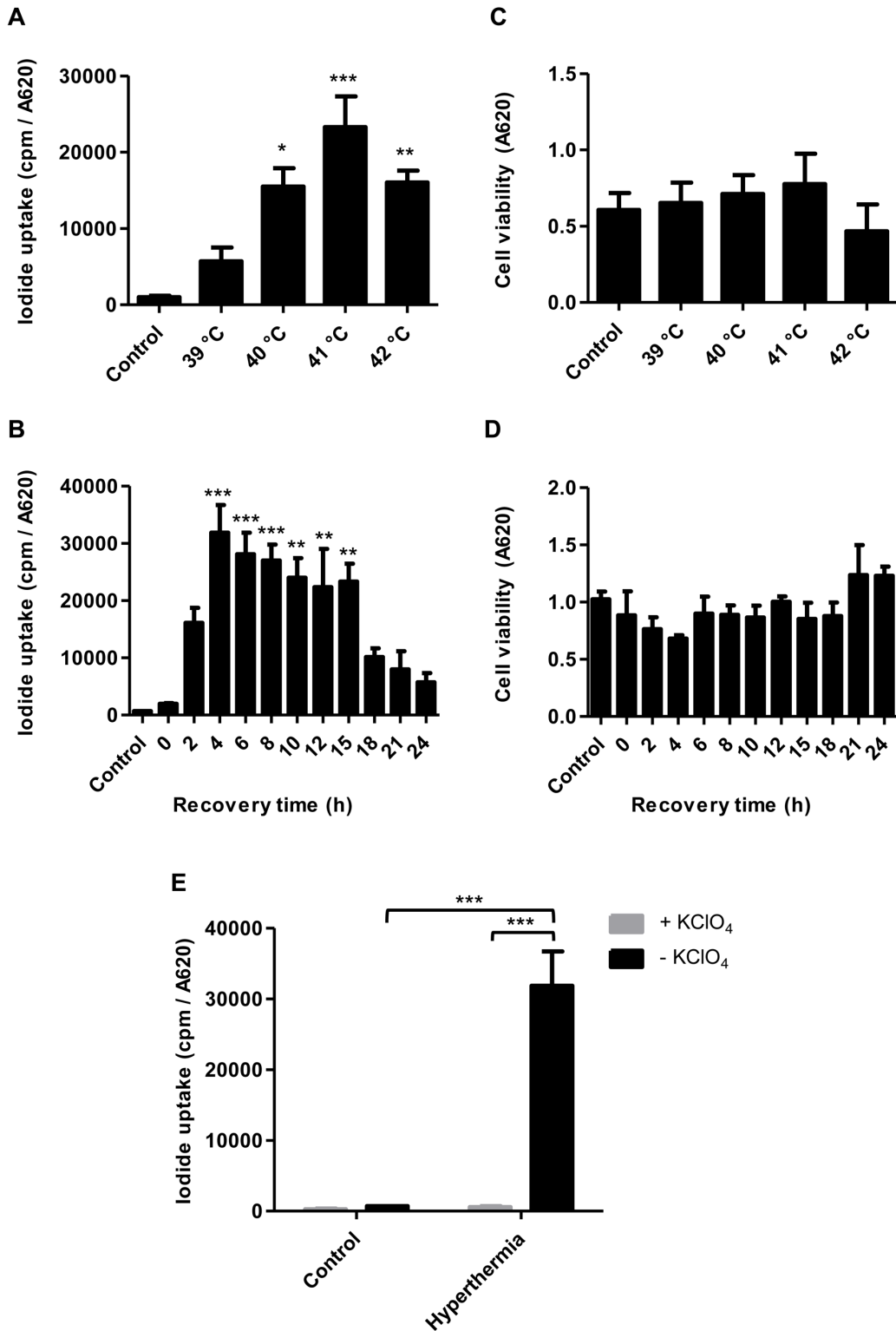


Figure 12 *In vitro* radioiodide uptake studies of HSP70B-NIS-MSCs. HSP70B-NIS-MSCs were heat-treated in a water bath at temperatures ranging from 39 to 42 °C for 60 min, or as control at 37 °C, and functional NIS expression was analyzed by an *in vitro* iodide uptake assay (A). ¹²⁵I uptake assay was performed at different time points (0 – 24 h) after promoter activation by heating the cells at 41 °C for 60 min (B). Cell viability after thermo-stimulation was analyzed by MTT assay (C + D). The NIS-specific inhibitor perchlorate was added to control the NIS dependency, analyzed 4 h after hyperthermia treatment and compared to unheated HSP70B-NIS-MSC control cells (E). Data are represented as mean ± SEM (n = 3; one way ANOVA analysis; *p < 0.05; **p < 0.01; ***p < 0.001).

***In vitro* radioiodide uptake studies of HSP70B-NIS-MSCs**

Radioiodide uptake assays were performed to verify functional NIS expression by HSP70B-NIS-MSCs. The HSP70B promoter showed a low basal activity (no ^{125}I uptake above background levels of unheated HSP70B-NIS-MSCs control cells) *in vitro* but showed a significantly induced expression in response to heat. Testing a temperature range from 39 to 42 °C, we observed the strongest radioiodine accumulation at 41 °C (**Figure 12 A**). HSP70B-NIS-MSCs tolerated temperatures up to 41 °C well, but showed reduced viability yielding 71% viable cells at 42 °C (**Figure 12 C**). In addition to temperature-dependence of NIS induction, we also characterized the time dependence of functional iodide uptake. The induction of ^{125}I accumulation was found to occur rapidly after heat exposure with a maximum level reached as early as 4 h after hyperthermia application showing a 46-fold induction of iodide uptake as compared to unheated HSP70B-NIS-MSC-control cells (**Figure 12 B**). The increase in iodide accumulation activity displayed a plateau with high uptake levels remaining for up to 15 h after heat-induced promoter activation. No significant change in cell viability was observed in response to heat in this time frame (**Figure 12 D**). As a control, the iodide uptake was shown to be sensitive to the NIS-specific inhibitor perchlorate, demonstrating NIS dependency (**Figure 12 E**).

***In vitro* NIS mRNA and protein levels of HSP70B-NIS-MSCs**

Parallel analysis of NIS mRNA levels by RT-PCR (**Figure 13 A**) confirmed heat-induced and time-dependent *NIS* expression with the highest mRNA levels measured 4 h after heat treatment. Induction of mRNA expression of endogenous HSPs HSP70 (HSPA1A) (**Figure 13 B**) and HSP70B (HSPA7) (**Figure 13 C**) occurred in the same time frame as that seen for the *NIS* transgene. Western blot analysis showed a similar pattern of NIS protein expression with maximum protein levels seen 8 h after thermo-stimulation (**Figure 13 D**). In addition, validation using immunofluorescence staining showed significant NIS-specific immunofluorescence in HSP70B-NIS-MSCs after hyperthermic treatment whereas only weak immunoreactivity was observed in non-heated, control HSP70B-NIS-MSCs, and no expression was seen in wild type MSCs (**Figure 13 E**).

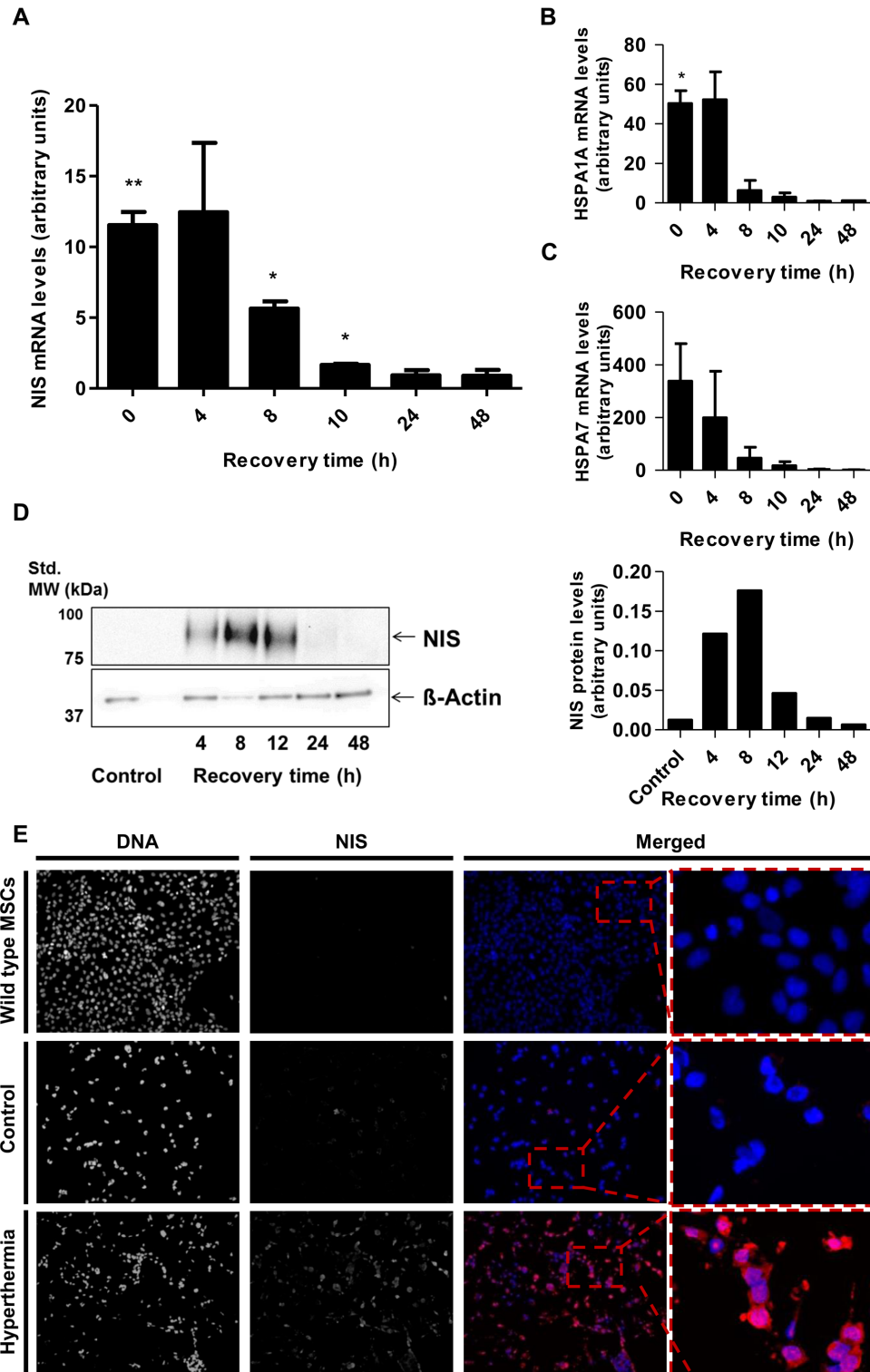


Figure 13 *In vitro* NIS mRNA and protein levels of HSP70B-NIS-MSCs. RT-PCR analysis of mRNA extracted from heat-treated (60 min at 41 °C) and unheated HSP70B-NIS-MSCs after 0 – 48 h, using primers for NIS (SLC5A5) (A), the endogenous HSP70 (HSPA1A) (B) and HSP70B (HSPA7) (C). Results were normalized to β -actin (ACTB), heat-treated compared to unheated MSCs for each time point and expressed as the mean \pm SEM ($n = 3$; two-tailed Student's t test; * $p < 0.05$; ** $p < 0.01$). NIS protein levels were assessed by Western blot (D), extracted by membrane isolation at 4 – 48 h after thermo-stimulation or, as controls, of unheated HSP70B-NIS-MSCs. The intensity of the bands was measured by densitometry and normalized to the β -actin loading control. NIS-specific immunofluorescence staining (red) of heat-treated HSP70B-NIS-MSCs (bottom row), unheated HSP70B-NIS-MSCs (middle row), and unheated wild-type MSCs (top row) seeded and fixated on coverslips (E).

Radioiodide biodistribution *in vivo* after MSC-mediated NIS gene transfer

By placing a thermo probe intratumorally, we confirmed rapid, stable and sufficient tumoral temperature (41.0 ± 0.1 °C or, as control, 37.0 ± 0.1 °C respectively) delivery, while the body temperature of the mice stayed within physiological levels [data not shown]. Following these studies, subsequent analyses were conducted without the invasive tumoral probe, which could distort results as the wound caused by the probe could potentially influence MSC recruitment.

After three HSP70B-NIS-MSCs injections, tumor-bearing mice were heat-treated regionally for 1 h at 41 °C, to activate the heat-inducible HSP70B promoter, or as control at 37 °C. 0 to 72 h later, 18.5 MBq ^{123}I were administrated and functional NIS expression was analyzed by gamma camera imaging. The images of the ^{123}I -scintigraphy revealed the strongest tumoral iodine accumulation, mediated by functional NIS, in animals with a latency of 12 h (**Figure 14 C**) between hyperthermia and radioiodine injection, whereas mice in the 37 °C control group (**Figure 14 F**) exhibited the weakest signal. Quantitative analysis of serial scanning (**Figure 14 G**) showed no difference to 37 °C control levels (maximum of tumoral iodide uptake 1 h post ^{123}I injection [**Figure 14 H**]: 37 °C control $6.83 \pm 1.99\%$ ID/tumor) when radioiodine was injected directly after thermo-stimulation (**Figure 14 B, G-H**; 0 h $7.78 \pm 1.30\%$ ID/tumor). However, a slight increase of tumoral iodine accumulation was observed (**Figure 14 G-H**; $8.58 \pm 1.86\%$ ID/tumor) when there was a period of 6 h between hyperthermia and ^{123}I injection. Significantly increased and maximal radioiodine levels were reached at the 12 h interval between promoter activation by heat treatment and radioiodide administration (**Figure 14 C,G-H**; $9.77 \pm 2.33\%$ ID/tumor) with a plateau up to 18 h (**Figure 14 G-H**; $9.41 \pm 0.86\%$ ID/tumor). All other groups, with a gap of 24 h (**Figure 14 D,G-H**; $7.78 \pm 0.85\%$ ID/tumor), 36 h (**Figure 14 G-H**; $7.99 \pm 2.22\%$ ID/tumor), 48 h (**Figure 14 G-H**; $6.79 \pm 0.79\%$ ID/tumor) and 72 h (**Figure 14 E,G-H**; $6.96 \pm 1.18\%$ ID/tumor) between HSP70B stimulation and imaging exhibited a similar iodine uptake as the control group. Physiological radioiodide accumulation in the thyroid and salivary glands (SG), stomach and, due to renal elimination of ^{123}I , in the urinary bladder, was visible in all animals (**Figure 14 B-F**). Dosimetric calculations revealed a higher tumor-absorbed dose of 70 ± 28 mGy/MBq/g tumor and an effective half-life of 3.6 h for ^{131}I in heat-treated animals with the 12 h interval, as compared to the unheated control group with 44 ± 15 mGy/MBq/g tumor-absorbed dose and a calculated effective half-life of 3.2 h for ^{131}I .

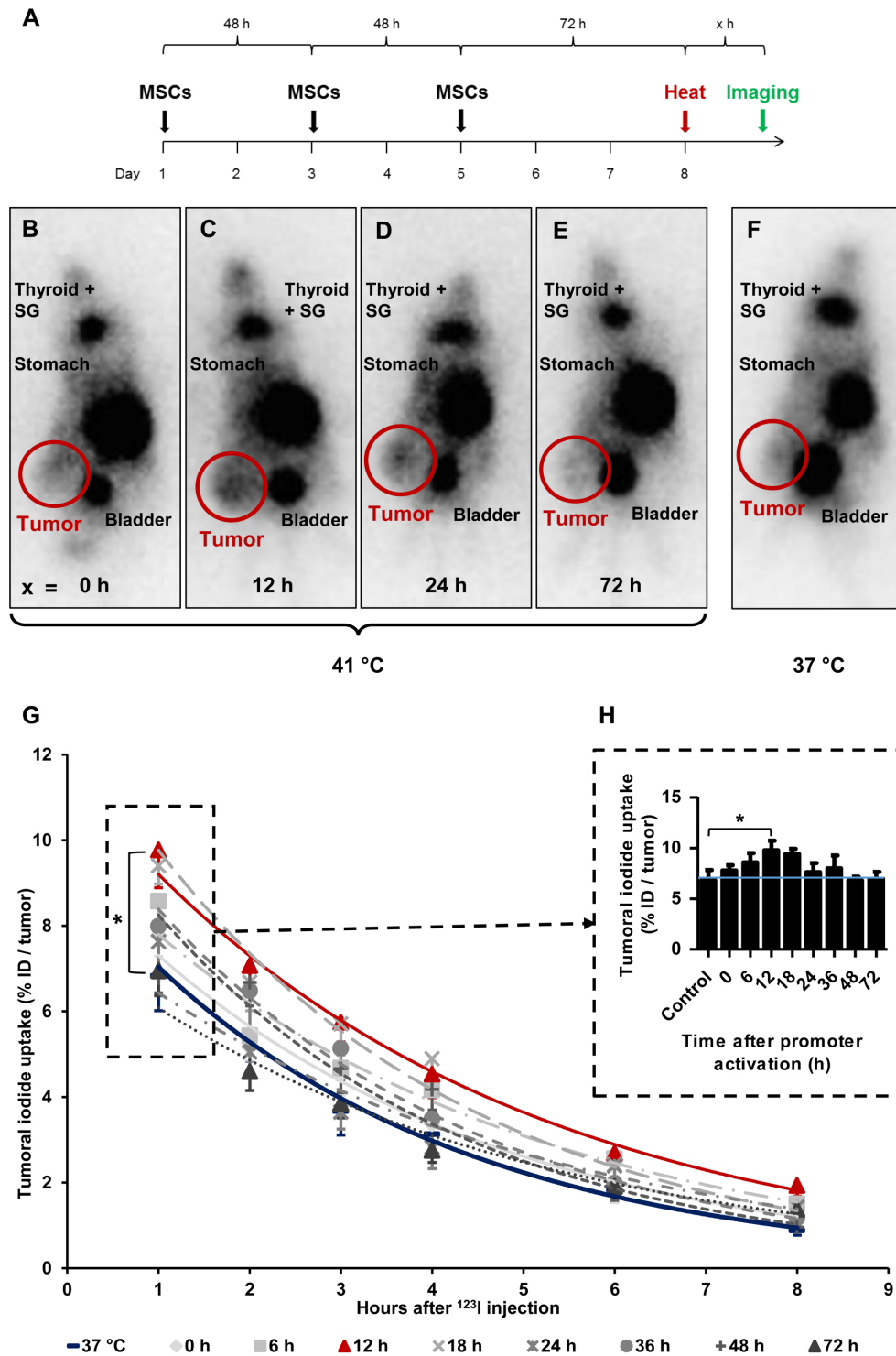


Figure 14 Radioiodide biodistribution in vivo after MSC-mediated NIS gene transfer. In vivo, using the hepatocellular carcinoma (HuH7) xenograft mouse model, HSP70B-NIS-MSCs were injected into the tail vein of mice, followed by hyperthermia, or as controls normothermia at 37 °C, 3 days later. 0–72 h after promoter activation by thermo-stimulation, 18.5 MBq ¹²³I were injected and serial gamma camera imaging started (A). Images of gamma camera imaging taken 2 h after radioiodide of animals with 0 h (B; n = 7), 6 h (n = 5), 12 h (C; n = 7), 18 h (H; n = 4), 24 h (D; n = 6), 36 h (n = 4), 48 h (n = 5) and 72 h (E; n = 4) between promoter activation by hyperthermia and radioiodine injection and control animals, treated at 37 °C (F; n = 5) (one representative image for each treatment group). Quantification of serial ¹²³I-scintigraphy (G) representing the efflux of the injected ¹²³I and comparison of the tumoral ¹²³I accumulation 1 h post injection (H) (the blue line represents the controls at 37 °C). Results are expressed as mean ± SEM; two-way ANOVA with post-hoc Tukey test *p < 0.05.

Ex vivo analysis of NIS expression

Paraffin-embedded tissue sections derived from HuH7 xenografts after ^{123}I -scintigraphy were stained immunohistochemically using a monoclonal NIS antibody. Tumor sections from control animals (37 °C; **Figure 15 A**) showed much less perivascular human NIS-specific immunoreaction (red) as did the group of thermo-stimulated animals (41 °C, 12 h gap; **Figure 15 B**). Control organs (liver, lungs, spleen and kidney) of heat-treated (**Figure 15 C**) and control animals (**Figure 15 D**) did not show NIS-specific immunoreactivity. Frozen tumor sections were processed for mRNA isolation. RT-PCR showed an upregulation of NIS (**Figure 15 E**), as well as the endogenous HSPs, HSP70 (**Figure 15 F**) and HSP70B (**Figure 15 G**) in a temperature- and time-dependent fashion as an additional confirmation of the functional NIS expression as well as the efficient heat transfer to the tumors.

MSC-mediated NIS gene therapy *in vivo*

Following validation of functional NIS expression by non-invasive radioiodine imaging, a therapy trial with ^{131}I was initiated based on the approach that showed optimal tumoral iodine accumulation as seen by the ^{123}I -scintigraphy. After three MSC administrations, radioiodine was injected 12 to 18 h after hyperthermic treatment to be within the plateau phase as seen *in vitro* and by gamma camera imaging. This cycle was repeated for a total of three times, but cycle two and three consisted of only one MSC application to reduce the overall length of the treatment scheme (**Figure 16 A**). Mice injected with saline only with (41 °C) (NaCl + 41 °C + NaCl) or without hyperthermia (37 °C) (NaCl + 37 °C + NaCl), and mice receiving saline instead of ^{131}I with (41 °C)(HSP70B-NIS-MSCs + 41 °C + NaCl) and without hyperthermia (37 °C) (HSP70B-NIS-MSCs + 37 °C + NaCl), served as controls and exhibited an uninterrupted and exponential tumor growth (**Figure 16 B** and **Supplementary Figure 1**). Mice treated with HSP70B-NIS-MSCS and ^{131}I following hyperthermia at 41 °C (HSP70B-NIS-MSCs + 41 °C + ^{131}I) exhibited a significantly reduced tumor growth as compared to all control groups, which was associated with prolonged survival of the mice (**Figure 16 C**). In one mouse, an impressive partial remission was observed with tumor shrinkage from 410 mm³ to 28 mm³ until day 78. As compared to the saline control groups, survival analysis also revealed a significantly prolonged survival of mice treated with HSP70B-NIS-MSCs of up to 78 days after therapy start in the hyperthermia group (HSP70B-NIS-MSCs + 41 °C + ^{131}I) and up to 40 days (HSP70B-NIS-MSCs + 37 °C + ^{131}I) in the normothermic group. At day 22 after the start of therapy, all animals within the NaCl + 41 °C + NaCl group had to be sacrificed based on tumor growth, whereas 100% of the HSP70B-NIS-MSCS + 41 °C + ^{131}I and 70% of the HSP70B-NIS-MSCS + 37 °C + ^{131}I groups were still alive. By day 26, all animals in the saline control groups had reached the endpoint criteria.

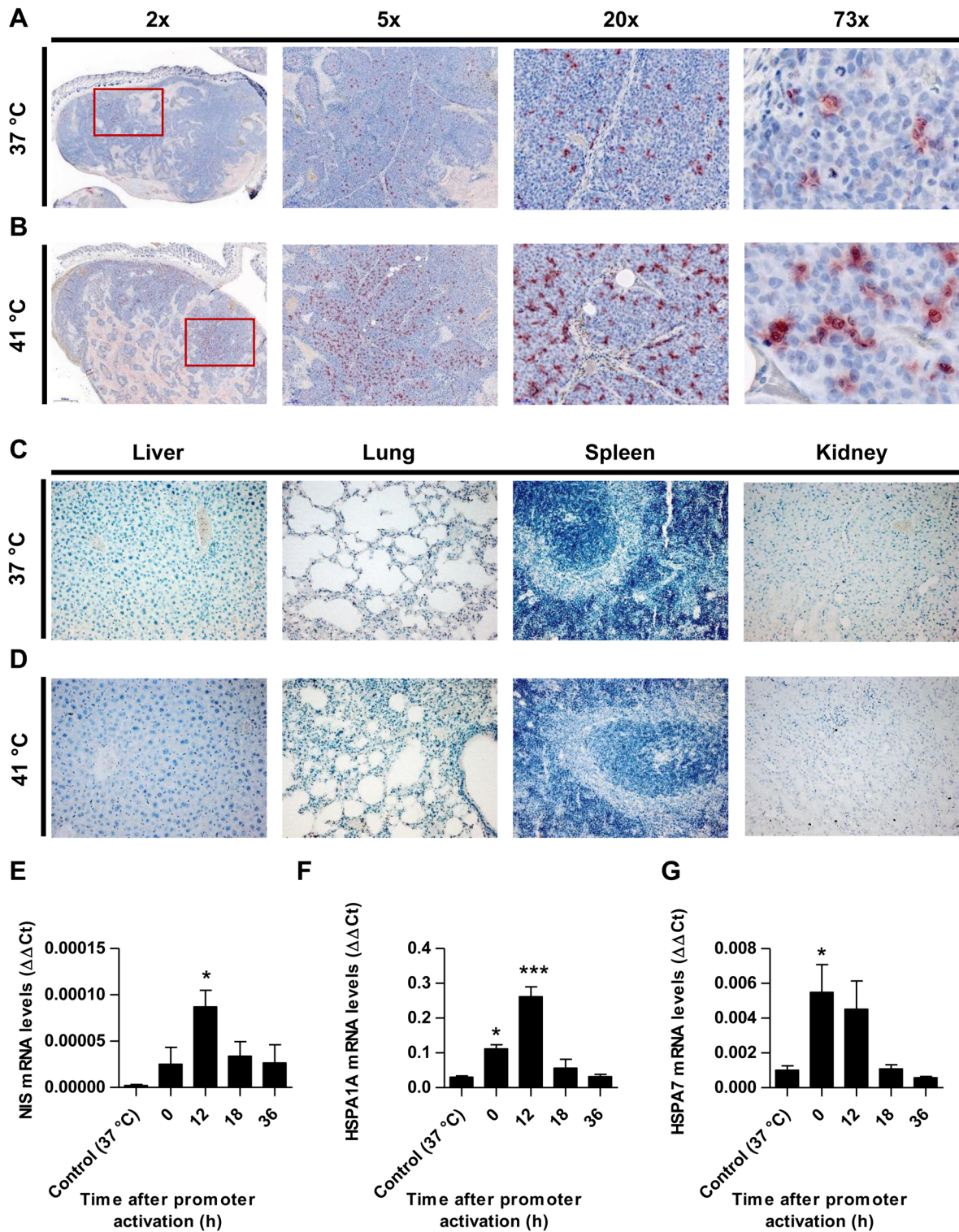


Figure 15 Ex vivo analysis of NIS expression. NIS-specific immunohistochemistry (red) was performed on paraffin-embedded HuH7 tumor sections. Tumors of mice of 37 °C controls (A) compared to mice which were heat-treated with a 12 h latency between promoter activation and ¹²⁵I administration (B). Control organs (liver, lung, spleen and kidney) of mice receiving 37 °C (C) or 41 °C (D) treatment. One representative image is shown each at 2x – 73x magnification for tumor sections and 20x for control organs. mRNA was isolated from frozen tumors sections of heat treated mice (groups in which 0, 12, 18, and 36 h were in between promoter activation and start of ¹²⁵I-scintigraphy) and controls (37 °C) at the end of the serial gamma camera imaging and analyzed for NIS (E), endogenous HSPA1A (F) and HSPA7 (G) by RT-PCR (n = 4; one-way ANOVA; *p < 0.05, ***p < 0.001).

Hyperthermia-inducible MSC-mediated NIS Gene Therapy

The median survival after therapy start for the therapy group HSP70B-NIS-MSC + 41 °C + ¹³¹I was 31 days, for the HSP70B-NIS-MSCS + 37 °C + ¹³¹I 25 days, for NaCl + 41 °C + NaCl treated animals 13 days, and for the NaCl + 37 °C + NaCl group 17 days. The treated mice showed no major adverse effects of radionuclide treatment and were sacrificed due to tumor load, only one mouse due to respiratory problems on day 78 after therapy start.

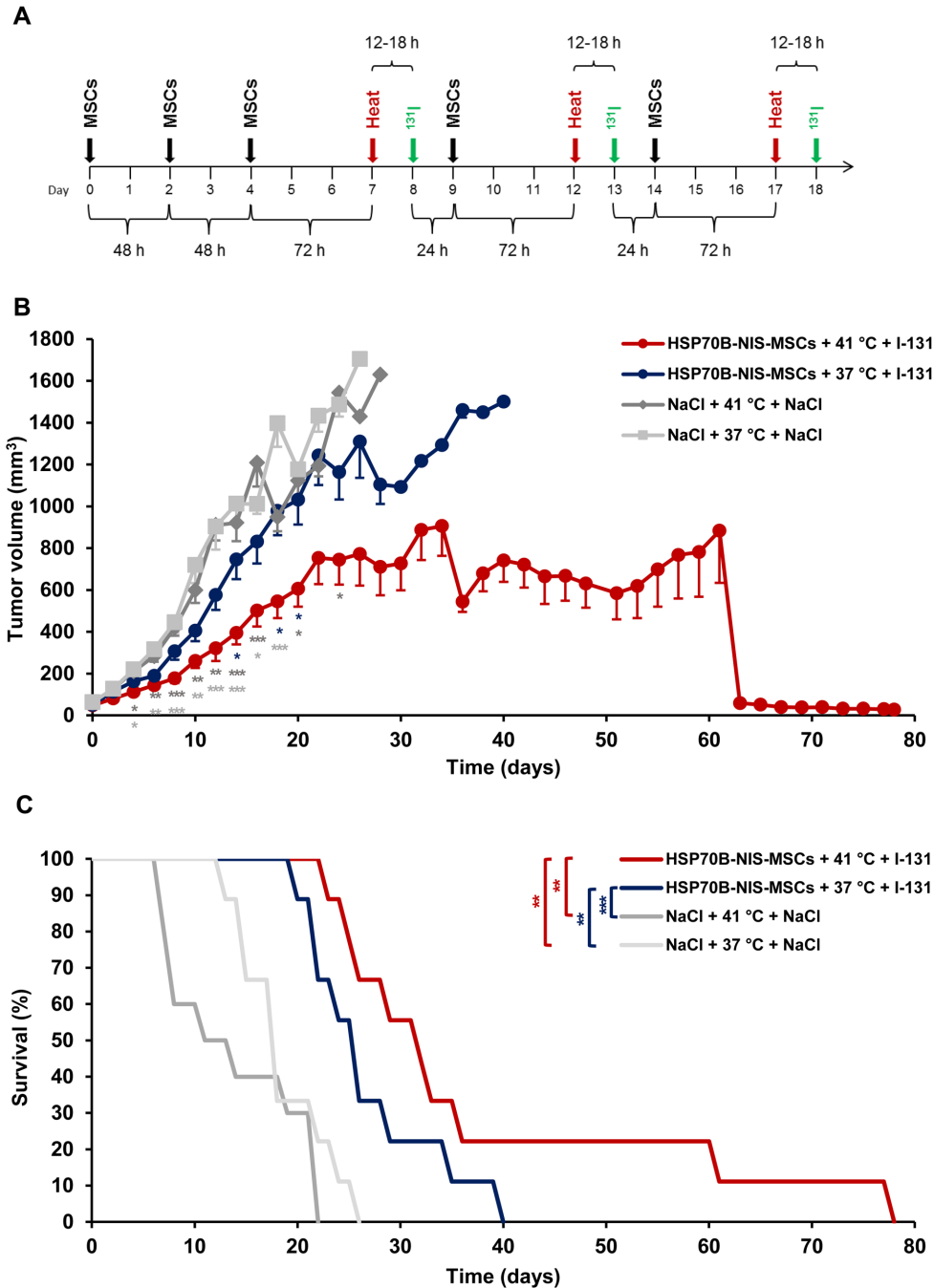


Figure 16 Heat-induced MSC-mediated NIS gene therapy in vivo. Three days after systemic injections of HSP70B-NIS-MSCs (black arrows), hyperthermia (red arrows) was administered to mice harboring HuH7 xenograft tumors. 12 to 18 h later, 55.5 MBq of therapeutic ¹³¹I (green arrows) was applied. This treatment cycle was repeated for a total of three times (A). Tumor growth (B) and overall survival (C) were evaluated for the treatment with HSP70B-NIS-MSCs, hyperthermia and ¹³¹I (HSP-NIS-MSCs + 41 °C + ¹³¹I; n = 9), compared to control groups, receiving hyperthermia and saline (NaCl + 41 °C + NaCl; n = 10) and to normothermic groups (HSP70B-NIS-MSCs + 37 °C + ¹³¹I; n = 9 and NaCl + 37 °C + NaCl; n = 10). Results are expressed as mean ± SEM (one-way ANOVA for tumor growth and log-rank test for log-rank for Kaplan-Meier survival plots; *p < 0.05; **p < 0.01; ***p < 0.001).

***Ex vivo* proliferation and blood vessel density analysis**

At the end of the observation period, the tumors were dissected and frozen tumor sections were stained using an antibody to identify blood vessels (CD31; red) and a Ki67-specific antibody to display general cell proliferation (green) (**Figure 17 A-D**). Tumors treated with HSP70B-NIS-MSCs, radioiodide and hyperthermia (HSP70B-NIS-MSCs + 41 °C + ¹³¹I) (**Figure 17 A**) showed a significantly lower proliferation index as did the saline control groups (**Figure 17 E**), as well as a significantly lower blood vessel density compared to all three control groups (**Figure 17 F**), thereby demonstrating an antiangiogenic effect and thus further validating successful HSP70B-NIS-MSC-mediated ¹³¹I therapy.

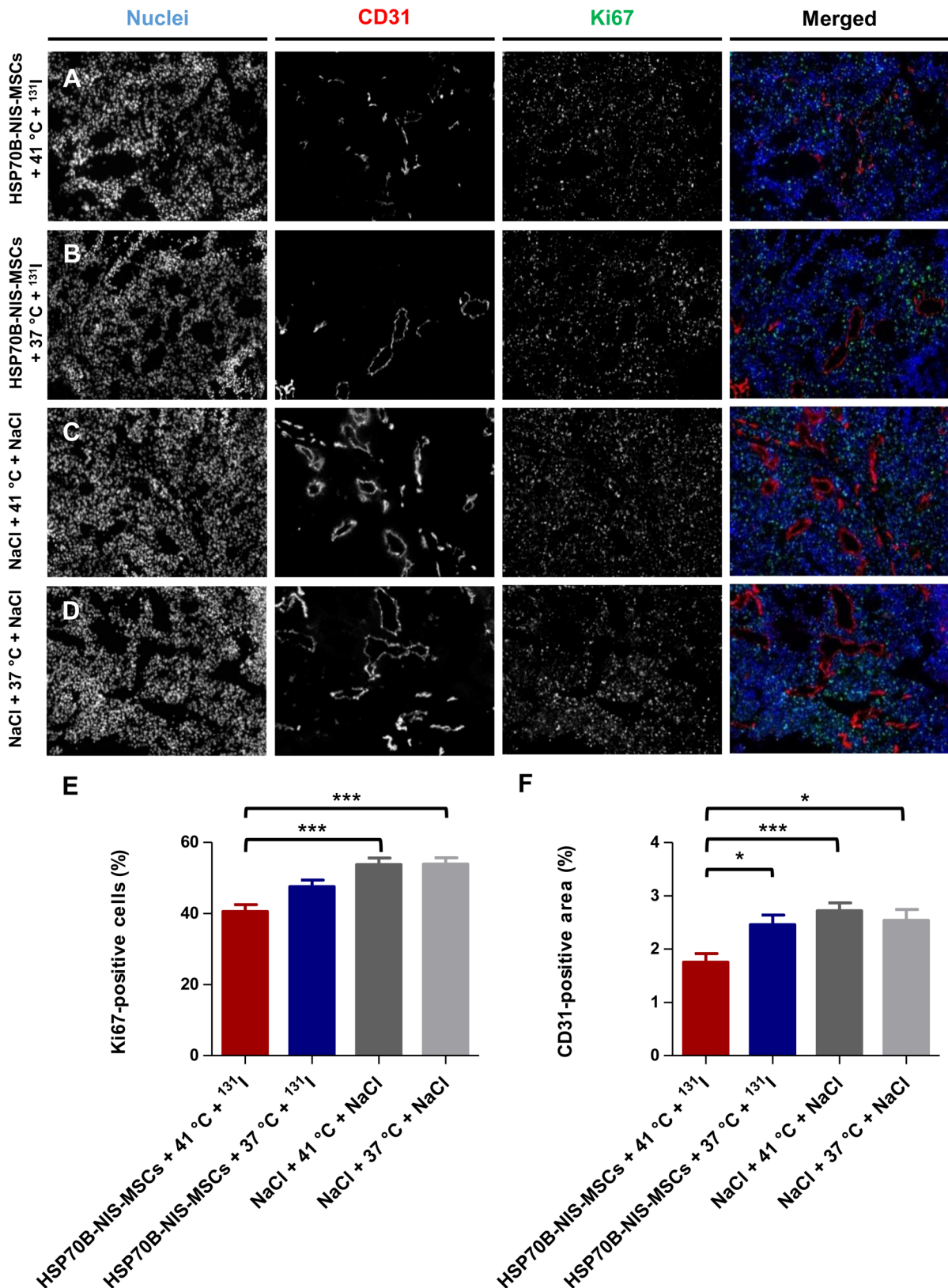


Figure 17 Reduced ex vivo proliferation and blood vessel density as result of heat-induced MSC-mediated NIS gene therapy. Ki67 [(E); green; proliferation index] and CD31 [(F); red; labeling blood vessels] immunofluorescence staining of frozen tumor sections was performed on tumors derived from mice receiving HSP70B-NIS-MSCs at the end of the ¹³¹I therapy (A; n = 9), unheated controls (B; n = 9) and mice receiving saline with (C; n = 10) or without (D; n = 9) heat treatment instead of MSCs. Nuclei were counterstained with Hoechst (blue). One representative image is shown each at 10x magnification. Results are expressed as mean ± SEM (one-way ANOVA; *p < 0.05; ***p < 0.001).

4.6 Discussion

When used as a theranostic gene, the symporter *NIS* acts as an effective molecular reporter gene with robust therapeutic options, thus enabling the visualization and treatment of tumors through the application of appropriate radionuclides. *NIS* efficiently transports various radionuclides, allowing the application of easily available and extensively studied radionuclides such as ^{123}I , ^{124}I , ^{18}F -tetrafluoroborate or $^{99\text{m}}\text{Tc}$ for *in vivo* imaging of functional *NIS* expression, and ^{131}I , ^{188}Re , or ^{211}At for the delivery of therapeutic applications (summarized in [15, 20, 140]). The treatment of thyroid cancer with ^{131}I has been performed in the clinic with great success since 1946 with a well-understood safety profile and is still the most preferred treatment modality, after thyroidectomy, for differentiated thyroid cancer [13]. The potential use of exogenously applied *NIS* to induce radioiodine accumulation in non-thyroidal tumors has been investigated in a variety of *in vitro* and *in vivo* tumor models, such as anaplastic thyroid cancer [29], glioma [30], acute myeloid leukemia [131], multiple myeloma [27], cancer of the prostate [26, 38-41], the liver [31], the colon [32, 33], the breast [34], and the pancreas [35-37] by several groups including our own. These very promising proof-of-principle studies have led to phase I/II clinical studies with *NIS* as a reporter gene and / or therapy gene using virus-mediated *NIS* gene delivery for locally recurrent prostate cancer (NCT00788307), multiple myeloma (NCT00450814, NCT02192775, NCT03017820) and for various other non-thyroidal cancer types (NCT01503177, NCT01846091, NCT02364713, NCT02700230, NCT02919449, NCT02962167, NCT03120624, NCT03171493, NCT03647163) [141-144].

The ultimate goal of tumor gene therapy is the efficient delivery of a transgene by the use of systemically applied vectors. To this end, engineered versions of MSCs represent attractive candidates as gene delivery vehicles [120]. MSCs are actively recruited to sites of tissue injuries or chronic inflammation and contribute to tissue remodeling [145]. The body sees “tumors as wounds that do not heal” [64, 65] and for this reason it drives the mobilization of MSCs from various tissue stores and their subsequent migration to developing tumor stroma [80, 146]. MSCs exhibited selective incorporation into growing tumor stroma [63, 67] driven by high local concentrations of inflammatory chemokines and cytokines secreted by the tumor and the tumor stroma [112, 147]. This tumor tropism of MSCs has been used as a “Trojan Horse”-like therapy approach in which genetically engineered MSCs deliver a therapeutic agent, in our case the *NIS* gene, deeply into growing tumors [31, 32, 37, 72, 78, 79, 86-88, 94, 95, 148]. The adaption of engineered MSCs as a therapeutic approach to treat solid cancers using *NIS* has proceeded towards clinical application with the initiation of a first series of phase I/II trials using measles virus (MV)-*NIS* transfected MSCs in recurrent ovarian cancer (NCT02068794). In addition, a clinical trial using MSCs as gene delivery vehicles based on our previous work was completed using MSCs modified with CCL5-driven HSV-TK for the treatment of gastrointestinal cancer [85]. In additional clinical trials, researchers are evaluating

IFN- β expressing MSCs in ovarian cancer (NCT02530047) at MD Anderson Cancer Center, and the safety and anti-tumor capacity of TRAIL-modified MSCs in metastatic non-small cell lung cancer (NCT03298763) at University College London Hospital.

While MSCs show significant tumor tropism, a portion of the adoptively applied MSCs potentially also home to normal tissues, such as the spleen or the lung [72]. Therefore, selective control of the expression of the transgene provides a means of limiting potential damage to non-tumor tissues. Our group has demonstrated that this can be achieved by using specific gene promoters linked to signals or differentiation pathways that occur mostly or only within the tumor setting. We have previously shown that MSCs expressing *NIS* under control of the tumor stroma-specific RANTES/CCL5 promoter [72], a HIF-1 α -driven synthetic promoter activated by tumor hypoxia [31], or using a synthetic promoter responsive to transforming growth factor B1 (TGFB1) present in the tumor setting [87] can lead to a robust and efficient *NIS* expression within tumors. In these settings, the biodistribution of our genetically engineered MSCs was analyzed by ^{123}I -scintigraphy or ^{124}I - and ^{18}F -TFB PET-imaging, using *NIS* as reporter gene. The subsequent systemic application of ^{131}I was shown for each approach to result in a significant reduction in tumor growth and a prolonged survival of the animals, thus demonstrating both the great potential of *NIS* as a theranostic gene and the potential benefit of engineered MSCs as therapy vehicles. External beam radiation was recently found to efficiently enhance MSC recruitment to treated tumors as well as to strongly increase tumor levels of TGFB1 [94]. Using a TGFB1-inducible SMAD-responsive promoter for MSC-mediated *NIS* gene therapy in combination with external beam radiation dramatically increased the therapeutic efficacy of *NIS* gene therapy with complete tumor remission seen in a subset of mice [95].

The present study builds on these results to evaluate a potentially more precise means of controlling theranostic transgene expression through the use of the heat-inducible HSP70B promoter that was shown here to confer local and temporal control of strong and robust induction of transgene expression. The HSP70B (*HSPA7*) gene was discovered in 1985 [149], is encoded near the highly homologous HSP70B' (*HSPA6*) on chromosome 1 [150], and, although mRNA is expressed after thermo-stimulation, it does not appear to encode a functional protein [151].

The heat-inducible HSP70B promoter was selected for use in our MSC-mediated *NIS* gene transfer approach. *In vitro* characterization of HSP70B-NIS-MSCs demonstrated a time- and temperature-dependent *NIS*-mediated iodine accumulation. The HSP70B promoter showed only background expression before heat was applied, but was significantly induced allowing a more than 45-fold functional *NIS* response to 60 min of heat treatment at 41 °C. *NIS* expression reached a maximum by 6 to 8 h after thermo-stimulation that was confirmed at mRNA and

protein levels by RT-PCR, Western blot and NIS-specific immunofluorescence, respectively. These results are in line with previous studies that used the HSP70B promoter, where a similar pattern of temperature- and time-dependent promoter activity was observed *in vitro* [152-155].

We could validate these findings in an *in vivo* HCC xenograft mouse model using ¹²³I-scintigraphy imaging studies that revealed a pattern of time-dependent tumoral iodine uptake, mediated by NIS, *in vivo* that closely matched our *in vitro* results. The strongest iodine uptake *in vivo* was found 12 h after hyperthermia treatment that was only slightly later than that seen in the cell culture studies (6 – 8 h after promoter activation). As seen with other HSP proteins that are often increased in tumor settings without thermo-stimulation due to the proteotoxic stressful conditions that cancer cells face, including nutrient deprivation, the presence of free reactive oxygen species, hypoxia, acidosis and high levels of mutant proteins [156, 157], the HSP70B promoter (HSP70B-NIS-MS) showed increased basal activity within the tumor microenvironment *in vivo* as evidenced by gamma camera images in the 37 °C control group. This parallels the observation that HSP70 is typically found to be increased in tumors [158] and is currently evaluated as tumor-specific diagnostic and therapeutic target [159]. Importantly, the HSP70B-NIS-MSs were not found to be activated in non-target organs (**Figure 15 C + D**).

Therapy using hyperthermia and ¹³¹I led to a strongly reduced tumor growth, prolonged survival with reduced blood vessel density and proliferation index, demonstrating the long-term antiangiogenic therapeutic efficacy of ¹³¹I. At normothermic conditions (37 °C), treatment with HSP70B-NIS-MSs followed by ¹³¹I application resulted in slightly reduced tumor growth (22% showed a response to the therapy). HSP70B-NIS-MSs, ¹³¹I and hyperthermia (41 °C) treatment resulted in a robust and significant therapeutic effect with reduced tumor growth in 67% of the animals, and a partial tumor remission in one animal. Hyperthermia and MSs alone (HSP70B-NIS-MSs + 41 °C + NaCl) showed no difference in survival or tumor growth (**Supplementary Figure 1 A + B**) compared to unheated controls (HSP70B-NIS-MSs + 37 °C + NaCl). Damage to the thyroid as well as the salivary glands is a potential and well-documented side effect of radioiodide therapy. In the present study, we used protocols similar to those used for patients that downregulate NIS expression in the thyroid gland (which is TSH regulated) by L-T4 pretreatment that helps to limit the damage to the thyroid and increases the circulating levels of radioiodide. Most of the iodide uptake in the cervical region seen on the images in Figure 3 is caused by iodide uptake in the salivary glands (that is not TSH regulated) which is anatomically close to the thyroid gland in mice and much bigger in comparison to the thyroid gland in humans [160]. Xerostomia is a recognized side effect of radioiodine treatment in some patients, but importantly, it is clinically manageable and has to be weighed against the benefit of effective tumor growth control.

One of the limitations of the present study is the somewhat heterogeneous tumoral response to hyperthermia. The therapy worked well in most of the animals, but in 33% of the animals the effect was reduced. This is believed to be due in part to the general model system applied here that used a water-based regional heat transfer method that has limitations for homogenous heat application in mouse flank tumors. This should be less of an issue in the clinic as the next generation hybrid magnetic resonance-guided high-intensity focused ultrasound now being used for tumor hyperthermia therapy allows a highly focused heating of the region with real-time temperature mapping and energy deposition [99].

As heat shows great chemo- and radiosensitizing qualities, hyperthermia has high potential as an adjuvant in multimodal treatment approaches, especially for sarcoma, melanoma, breast, or colon cancer [99]. The therapeutic effects of chemo- or radiotherapy can be enhanced by the administration of hyperthermia. Mild hyperthermia, at temperatures in the range of 39 to 44 °C, is able to disturb the *de novo* synthesis of DNA by denaturation of synthetases and polymerases resulting in arrest of the cell cycle. It can furthermore induce apoptosis or necrosis, and interfere in a number of DNA repair mechanisms [98, 100]. Recently, there is also great interest in hyperthermia in the context of oncological immunotherapy, especially in regards to the therapy of metastases. In particular, as hyperthermia can activate immune cells, initiate the release of exosomes and HSPs that present tumor antigens, enhance surface molecule expression on heated tumor cells, and thereby increase the immune sensitivity of tumors cells to the immune system. Lately, a phenomenon, called the abscopal effect, that was first discovered for local radiotherapy was now also detected for hyperthermia. It describes the findings that local tumor treatment is able to affect the growth of distant tumors and metastases and it is presumably mediated by the activation of the immune system [101].

In summary, our data demonstrate the potential of using a heat-inducible promoter (HSP70B) to drive NIS expression in MSCs, which allow an increased tumor-specific, temperature- and time-dependent NIS-mediated accumulation of radioiodide in heat-treated tumors. Application of ¹³¹I led to significantly reduced tumor growth and prolonged survival of animals receiving HSP70B-NIS-MSCs, ¹³¹I and hyperthermia. This proof-of-principle study has opened a new and exciting chapter on the way towards a future clinical application of genetically engineered MSCs in the context of *NIS* gene therapy with high translational relevance.

4.7 Abbreviations

ANOVA: analysis of variances; CCL5: CC-chemokine ligand 5; cDNA: complementary DNA; CMV: cytomegalovirus; cpm: counts per minute; DNA: deoxyribonucleic acid; FBS: fetal bovine serum; HCC: hepatocellular carcinoma; HIF1 α : hypoxia-inducible factor 1 α ; HSP: heat shock protein; HSV-TK: herpes simplex virus-thymidine kinase; ID: injected dose; i.p.: intraperitoneal; i.v.: intravenous; L-T4: L-thyroxine; MSCs: mesenchymal stem cells; mRNA: messenger ribonucleic acid; MTT: 3-(4,5-dimethylthiazol-2-yl)-2,5-diphenyltetrazolium bromide; NaCl: saline; NIS: sodium iodide symporter; PBS: phosphate-buffered saline; PET: positron-emission tomography; RANTES: regulated on activation, normal T cell expressed and secreted; RNA: ribonucleic acid; RT-PCR: real-time polymerase chain reaction; s.c.: subcutaneous; SEM: standard error of the mean; SG: salivary glands; TGFB1: transforming growth factor beta 1.

4.8 Acknowledgements

We are grateful to Dr Barbara von Ungern-Sternberg, Rosel Oos, and Dr Markus Strigl (Department of Nuclear Medicine, LMU Munich, Munich, Germany), and Jakob Allmann (Department of Nuclear Medicine, Klinikum rechts der Isar der Technischen Universität München, Munich, Germany) for their support with imaging and therapy studies. The authors thank Prof. Doris Mayr (Department of Pathology, LMU Munich, Munich, Germany) for preparation of paraffin-embedded slides. The authors owe special thanks to Prof. Julia Mayerle, Dr Ujjwal Mahajan and Dr Ivonne Regel (Department of Internal Medicine II, LMU Munich, Munich, Germany) for always allowing the use of their equipment and giving assistance.

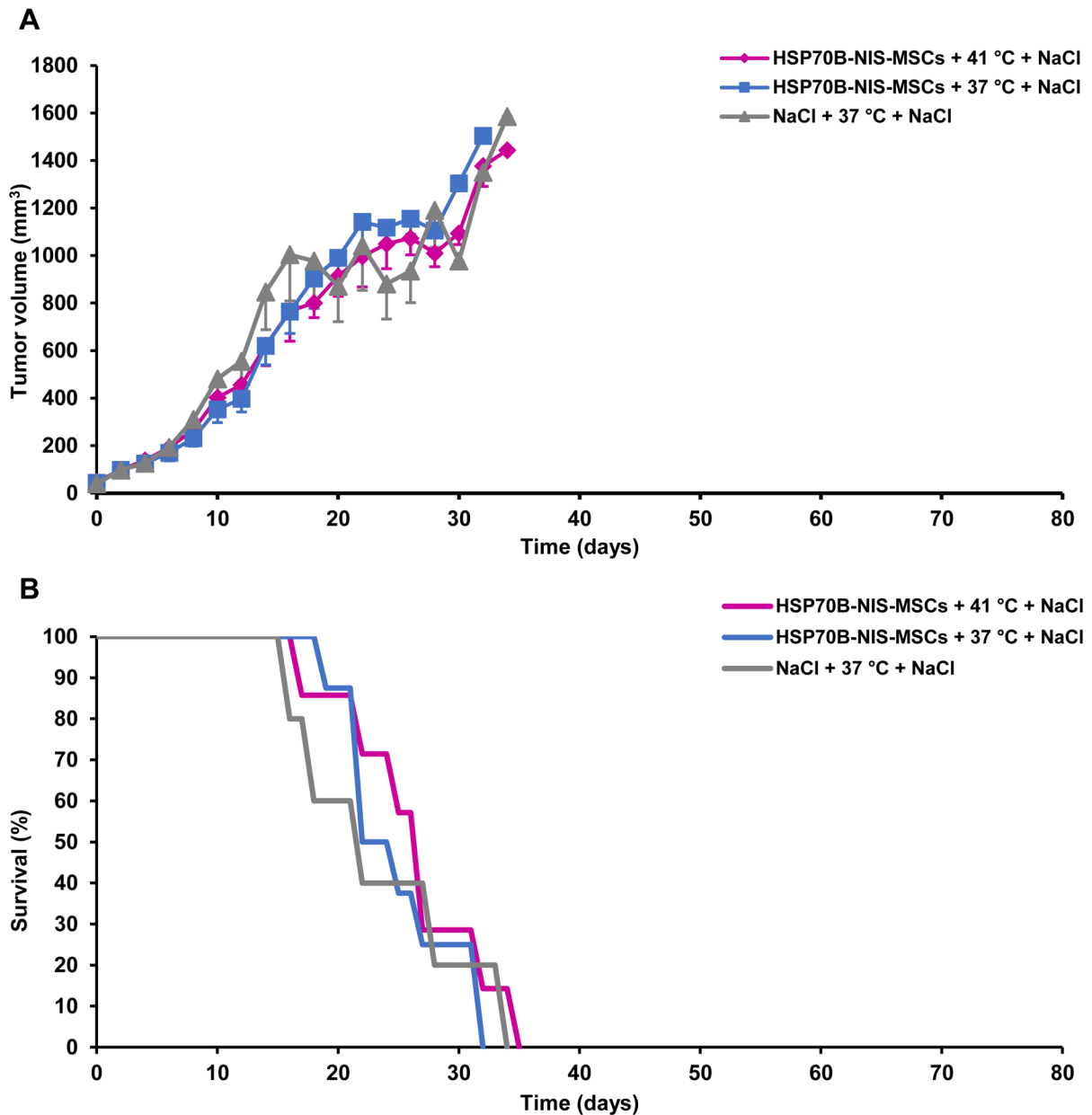
This work was supported by a grant from the Wilhelm Sander-Stiftung to C.S. and P.J.N. (2014.129.1), a grant from the Deutsche Forschungsgemeinschaft within the Collaborative Research Center SFB 824 to C.S. (project C8) as well as within the Priority Program SPP1629 to C.S. and P.J.N.

This work was performed as partial fulfillment of the doctoral thesis of M. Tutter at the Faculty for Chemistry and Pharmacy of the LMU Munich.

4.9 Competing Interests

The authors have declared that no competing interest exists.

4.10 Supplement



Supplementary Figure 1 Control groups for heat-induced MSC-mediated NIS gene therapy in vivo. Three days after systemic injections of HSP70B-NIS-MSCs, hyperthermia was administered to mice harboring HuH7 xenograft tumors. 12 to 18 h later, saline was applied instead of ¹³¹I as control. This treatment cycle was repeated for a total of three times. Tumor growth (A) and overall survival (B) were evaluated for the treatment with HSP70B-NIS-MSCs, hyperthermia, and NaCl (HSP-NIS-MSCs + 41 °C + NaCl; n = 7), compared to a normothermic control group (HSP70B-NIS-MSCs + 37 °C + NaCl; n = 8), and saline control group (NaCl + 37 °C + NaCl; n = 5). Results are expressed as mean ± SEM.

5. Summary

The sodium iodide symporter (NIS) is the only human transporter protein that facilitates iodide uptake from the blood into the thyroid, as the first step of thyroid hormone synthesis. The ability of NIS to transport various radioisotopes provides the advantage of a combined diagnostic imaging/therapy (theranostic) strategy. In its role as reporter gene *NIS* allows expanded non-invasive *in vivo* monitoring of MSC homing and engraftment at the tumor site in concert with molecular imaging of heat-inducible transgene expression by ^{123}I -scintigraphy and ^{124}I -, or ^{18}F -TFB-PET imaging. NIS has been used for almost 75 years for ^{131}I treatment of thyroid cancer in the clinical setting, based on its role as therapy gene. Delivery of the theranostic *NIS* gene into non-thyroidal tumors opens the exciting possibility of transferring the well-established clinical protocol of radioiodine imaging and therapy to extra-thyroidal tumors. Previous studies convincingly demonstrated the successful transfer of the *NIS* gene to various cancer entities using viruses, polymers or mesenchymal stem cells (MSCs) as delivery vehicles. The excellent tumor homing ability of MSCs has made them attractive candidates as gene therapy vehicles.

However, one of the major prerequisites for future clinical translation is the proof of a safe, tumor-selective, and effective transfer of the gene. With the aim to enhance the effectiveness and tumor-selectivity of MSC-mediated *NIS* gene therapy, in this thesis the combination with hyperthermia protocols was explored. While the intrinsic biologic effects of elevated temperature in cancer tissues is still not well understood, it has been well-demonstrated that increasing the temperature of the tumor (temperatures ranging from 39 °C to 42.5 °C) acts as an adjuvant, in multimodal cancer treatment schemes in clinical practice, such as radio- and chemotherapy as hyperthermia shows great chemo- and radiosensitizing qualities.

One proposed effect of hyperthermia is the induction of the secretion of inflammatory chemokines and cytokines that are considered attractants for MSCs. The first aim of this thesis therefore was to study the potential of regional hyperthermia to enhance recruitment of MSCs to the tumor stroma. As a first step, the impact of hyperthermia on the hepatocellular carcinoma (HCC) cell line HuH7 and its capability to secrete the MSC-attracting cytokines was tested. The upregulation of diverse factors involved in MSC migration in response to mild hyperthermia (1 hour at 41 °C) was demonstrated *in vitro* and confirmed *ex vivo* by RT-PCR. A subsequent 3D live cell migration assay confirmed the preferred movement of MSC towards supernatants derived from heat-treated HuH7 cancer cells as compared to unheated ones. This effect seen *in vitro* was further validated *in vivo* in an HCC xenograft tumor model. With the help of the *NIS* reporter gene system, the optimal time point and schedule of hyperthermia application for the highest stimulation of MSC migration after hyperthermia treatment was explored by ^{123}I -scintigraphy. Three days before the imaging, constitutively *NIS* expressing MSCs (CMV-*NIS*-MSCs) were injected and hyperthermia treatment was conducted 6 hours, 24 hours, and 48

hours before or 24 hours and 48 hours after the MSC administration. Tumoral iodide accumulation was significantly enhanced in tumors that were heat-treated 24 hours post MSC-injection compared to normothermic controls. The ^{123}I -scintigraphy-based *in vivo* NIS imaging series was followed by evaluation of the therapeutic effectivity of ^{131}I using the most effective hyperthermia/MSC/radioiodide application protocol evaluated in the previous imaging study. The optimal treatment scheme, hyperthermia 24 hours after MSC injection followed by ^{131}I administration two days later, results in a prolonged survival and decreased tumor growth of animals receiving hyperthermia (41 °C) in addition to MSCs. Taken together, it was shown here for the first time that hyperthermia has the power to significantly boost MSC recruitment to the tumor stroma.

The second aim of the thesis was to build on previous results with the potential of hyperthermia to maximize the efficacy of the MSC-mediated *NIS* gene therapy concept by adding a new dimension of precise control of *NIS* transgene expression. With the goal of gaining spatial and temporal control of NIS activation, MSCs were engineered to express the *NIS* gene under control of the heat-inducible HSP70B promoter. The ideal duration of hyperthermia application for maximal promoter activation and time point of maximal transgene expression after hyperthermia treatment was analyzed *in vitro* and *in vivo* utilizing the theranostic function of NIS, which permits the control of gene delivery efficiency by non-invasive imaging of functional tumoral NIS expression and therapeutic intervention by application of cytotoxic ^{131}I .

In vitro, HSP70B-NIS-MSCs were successfully characterized demonstrating low basal NIS activity with a high heat-induced functional *NIS* gene expression by iodide uptake assay, RT-PCR, Western blot, and NIS-specific immunofluorescence staining. Following systemic application of HSP70B-NIS-MSCs, regional heat-treatment of subcutaneous HCC (HuH7) xenograft tumors resulted in increased tumor-specific, temperature- and time-dependent accumulation of iodide analyzed by ^{123}I -scintigraphy that closely matched our *in vitro* results. The strongest iodine uptake *in vivo* was found 12 hours after hyperthermia treatment that was only slightly later than that seen in the cell culture studies (6 – 8 hours after promoter activation). Therapeutic ^{131}I -application plus hyperthermia treatment led to prolonged survival with strongly reduced tumor growth with reduced blood vessel density and proliferation index, demonstrating the long-term antiangiogenic therapeutic efficacy of ^{131}I as compared to all control groups. This translational study has opened a new and exciting chapter on the way towards a future clinical application of genetically engineered MSCs in the context of *NIS* gene therapy.

In conclusion, the work presented in this thesis highlights the potential of combining regional hyperthermia with MSC-mediated *NIS* gene therapy from two different perspectives. On the one hand, hyperthermia showed a significant stimulatory effect on the migration rate of MSCs,

on the other hand, regional hyperthermia was successfully used to induce tumor-specific transgene expression in a spatial and temporal manner. Both strategies support the use of regional hyperthermia to optimize the efficacy of MSC-based *NIS* gene cancer therapy with great potential for successful future clinical translation.

6. Publications

6.1 Original Papers

Tutter M, Schug C, Schmohl KA, Urnauer S, Schwenk N, Petrini M, Lokerse WJ, Zach C, Ziegler S, Bartenstein P, Weber WA, Multhoff G, Wagner E, Lindner LH, Nelson PJ, Spitzweg C. Regional hyperthermia enhances mesenchymal stem cell recruitment to tumor stroma: Implications for mesenchymal stem cell-based tumor therapy. [Submitted manuscript]

Tutter M, Schug C, Schmohl KA, Urnauer S, Schwenk N, Petrini M, Lokerse WJ, Zach C, Ziegler S, Bartenstein P, Weber WA, Wagner E, Lindner LH, Nelson PJ, Spitzweg C. Effective control of tumor growth through spatial and temporal control of theranostic-sodium iodide symporter (NIS) gene expression using a heat-inducible gene promoter in engineered mesenchymal stem cells. [This manuscript has been accepted for publication in Theranostics and assigned the DOI doi:10.7150/thno.41489]

Schmohl KA, Han Y, **Tutter M**, Schwenk N, Ziegler S, Bartenstein P, Nelson PJ, Spitzweg C. Thyroid status affects tumour growth mediated by integrin $\alpha\beta 3$. [Submitted manuscript]

Schug C, Kitzberger C, Sievert W, Spellerberg R, **Tutter M**, Schmohl KA, Schwenk N, Zach C, Schwaiger M, Multhoff G, Wagner E, Nelson PJ and Spitzweg C. Radiation-induced Amplification of TGFB1-induced Mesenchymal Stem Cell-mediated NIS Gene 131I Therapy. Clin Cancer Res. 2019 Oct 1;25(19):5997-6008

Urnauer S, Schmohl KA, **Tutter M**, Schug C, Schwenk N, Morys S, Ziegler S, Bartenstein P, Clevert DA, Wagner E, Spitzweg C. Dual-targeting strategy for improved nonviral gene transfer of the theranostic sodium iodide symporter. Gene Ther. 2019 Apr;26(3-4):93-108

Schug C, Urnauer S, Jaeckel C, Schmohl KA, **Tutter M**, Steiger K, Schwenk N, Schwaiger M, Wagner E, Nelson PJ and Spitzweg C, TGFB1-driven induction of tumor-selective NIS transgene expression using mesenchymal stem cell-mediated gene delivery. Endocr Relat Cancer. 2019 Jan 1;26(1):89-101

Urnauer S, Müller AM, Schug C, Schmohl KA, **Tutter M**, Schwenk N, Rödl W, Morys S, Ingrisich M, Bertram J, Bartenstein P, Clevert DA, Wagner E, Spitzweg C. EGFR-targeted nonviral NIS gene transfer for bioimaging and therapy of disseminated colon cancer metastases. *Oncotarget*. 2017 Sep 16;8(54):92195-92208

6.2 Oral Presentations

89th Annual Meeting of the American Thyroid Association, Chicago, IL, USA, October 2019. **Tutter M**, Schug C, Schmohl KA, Schwenk N, Lokerse WJ, Lindner LH, Nelson PJ, Spitzweg C. Heat-inducible mesenchymal stem cell (MSC)-mediated sodium iodide symporter (NIS) gene therapy. *Highlighted oral session*.

62th Annual Meeting of the German Society of Endocrinology, Göttingen, Germany, March 2018. **Tutter M**, Schug C, Schmohl KA, Schwenk N, Lokerse WJ, Lindner LH, Nelson PJ, Spitzweg C. Heat-inducible mesenchymal stem cell-mediated sodium iodide symporter (NIS) gene transfer.

18th Symposium Gentianum, Klausurtagung der Medizinischen Klinik und Poliklinik IV, Frauenchiemsee, Germany, Februar 2019. **Tutter M**, Schug C, Schmohl KA, Kitzberger C, Schwenk N, Lokerse WJ, Lindner LH, Nelson PJ, Spitzweg C. Challenges and chances of combination of hyperthermia with mesenchymal stem cell-mediated sodium iodide symporter gene therapy.

88th Annual Meeting of the American Thyroid Association, Washington, DC, USA, October 2018. **Tutter M**, Schug C, Schmohl KA, Schwenk N, Lokerse WJ, Lindner LH, Nelson PJ, Spitzweg C. Heat-inducible mesenchymal stem cell-mediated sodium iodide symporter (NIS) gene transfer.

40th Annual Meeting of the European Thyroid Association, Belgrade, Serbia, September 2017. **Tutter M**, Schug C, Schmohl KA, Schwenk N, Lokerse W, Lindner LH, Nelson PJ, Spitzweg C. Regional hyperthermia for optimization of efficacy and tumor selectivity of mesenchymal stem cell (MSC)-mediated sodium iodide symporter (NIS) gene therapy.

6.3 Poster Presentations

Endocrine Society's Annual Meeting (ENDO) 2020, San Francisco, CA, USA, March 2020. **Tutter M**, Schug C, Schmohl KA, Schwenk N, Petrini M, Lindner LH, Nelson PJ, Spitzweg C. Regional hyperthermia enhances selective mesenchymal stem cell migration towards the tumor stroma (presented by Spitzweg C).

41st Annual Meeting of the European Thyroid Association, Newcastle upon Tyne, UK, September 2018. **Tutter M**, Schug C, Schmohl KA, Schwenk N, Lokerse WJ, Lindner LH, Nelson PJ, Spitzweg C. Mild regional hyperthermia enhances selective mesenchymal stem cell migration towards the tumor stroma.

61th Annual Meeting of the German Society of Endocrinology, Bonn, Germany, March 2018. **Tutter M**, Schug C, Schmohl KA, Urnauer S, Schwenk N, Lokerse WJ, Lindner LH, Nelson PJ, Spitzweg C. Mild regional hyperthermia enhances selective mesenchymal stem cell migration towards the tumor stroma (presented by Schug C).

87th Annual Meeting of the American Thyroid Association, Victoria, Canada, October 2017. **Tutter M**, Schug C, Schmohl KA, Urnauer S, Schwenk N, Lokerse WJ, Lindner LH, Nelson PJ, Spitzweg C. Regional hyperthermia for optimization of efficacy and tumor selectivity of mesenchymal stem cell (MSC)-mediated sodium iodide symporter (NIS) gene therapy.

60th Annual Meeting of the German Society of Endocrinology, Würzburg, Germany, April 2017. **Tutter M**, Schug C, Schmohl KA, Urnauer S, Müller AM, Schwenk N, Lokerse WJ, Lindner LH, Nelson PJ, Spitzweg C. Regional hyperthermia for optimization of efficacy and tumor selectivity of mesenchymal stem cell (MSC)-mediated sodium iodide symporter (NIS) gene therapy.

6.4 Awards

2019 Women Advancing Thyroid Research (WATR) Award

89th Annual Meeting of the American Thyroid Association, Chicago, IL, USA, October 2019.

Tutter M.

The Max Pierre König Poster Award 2018 of the European Thyroid Association

41st Annual Meeting of the European Thyroid Association, Newcastle upon Tyne, UK, September 2018. **Tutter M**, Schug C, Schmohl KA, Schwenk N, Lokerse WJ, Lindner LH, Nelson PJ, Spitzweg C. Mild regional hyperthermia enhances selective mesenchymal stem cell migration towards the tumor stroma.

6.5 Grants

Travel grant, German Society of Endocrinology

89th Annual Meeting of the American Thyroid Association, Chicago, IL, USA, October 2019.

E. Chester Ridgway Trainee Grant

For the participation at the 89th Annual Meeting of the American Thyroid Association Trainee Grant Program, Chicago, IL, USA, October 2019.

E. Chester Ridgway Trainee Grant

For participation at the 88th Annual Meeting of the American Thyroid Association Trainee Grant Program, Washington, DC, USA, October 2018.

Travel grant, European Thyroid Association

41st Annual Meeting of the European Thyroid Association, Newcastle upon Tyne, UK, September 2018.

Travel grant, German Society of Endocrinology

87th Annual Meeting of the American Thyroid Association, Victoria, Canada, October 2017.

E. Chester Ridgway Trainee Grant

For the participation at the 87th Annual Meeting of the American Thyroid Association Trainee Grant Program, Victoria, Canada, October 2017.

Travel grant, German Society of Endocrinology

60th Annual Meeting of the German Society of Endocrinology, Würzburg, Germany, April 2017.

7. References

1. Bray, F., et al., *Global cancer statistics 2018: GLOBOCAN estimates of incidence and mortality worldwide for 36 cancers in 185 countries*. *CA Cancer J Clin*, 2018. **68**(6): p. 394-424.
2. Torre, L.A., et al., *Global Cancer Incidence and Mortality Rates and Trends--An Update*. *Cancer Epidemiol Biomarkers Prev*, 2016. **25**(1): p. 16-27.
3. Hanahan, D. and R.A. Weinberg, *The hallmarks of cancer*. *Cell*, 2000. **100**(1): p. 57-70.
4. Weinberg, R.A., *How cancer arises*. *Sci Am*, 1996. **275**(3): p. 62-70.
5. Hanahan, D. and R.A. Weinberg, *Hallmarks of cancer: the next generation*. *Cell*, 2011. **144**(5): p. 646-74.
6. Liberti, M.V. and J.W. Locasale, *The Warburg Effect: How Does it Benefit Cancer Cells?* *Trends Biochem Sci*, 2016. **41**(3): p. 211-218.
7. Balkwill, F.R., M. Capasso, and T. Hagemann, *The tumor microenvironment at a glance*. *J Cell Sci*, 2012. **125**(Pt 23): p. 5591-6.
8. Urruticoechea, A., et al., *Recent advances in cancer therapy: an overview*. *Curr Pharm Des*, 2010. **16**(1): p. 3-10.
9. Falzone, L., S. Salomone, and M. Libra, *Evolution of Cancer Pharmacological Treatments at the Turn of the Third Millennium*. *Front Pharmacol*, 2018. **9**: p. 1300.
10. Kumar, S.R., et al., *Clinical development of gene therapy: results and lessons from recent successes*. *Mol Ther Methods Clin Dev*, 2016. **3**: p. 16034.
11. Ginn, S.L., et al., *Gene therapy clinical trials worldwide to 2017: An update*. *J Gene Med*, 2018. **20**(5): p. e3015.
12. Burke, B., et al., *Macrophages in gene therapy: cellular delivery vehicles and in vivo targets*. *J Leukoc Biol*, 2002. **72**(3): p. 417-28.
13. Spitzweg, C., et al., *Advanced radioiodine-refractory differentiated thyroid cancer: the sodium iodide symporter and other emerging therapeutic targets*. *Lancet Diabetes Endocrinol*, 2014. **2**(10): p. 830-42.

14. Kogai, T., et al., *Regulation by thyroid-stimulating hormone of sodium/iodide symporter gene expression and protein levels in FRTL-5 cells*. *Endocrinology*, 1997. **138**(6): p. 2227-32.
15. Ahn, B.C., *Sodium iodide symporter for nuclear molecular imaging and gene therapy: from bedside to bench and back*. *Theranostics*, 2012. **2**(4): p. 392-402.
16. Hingorani, M., et al., *The biology of the sodium iodide symporter and its potential for targeted gene delivery*. *Curr Cancer Drug Targets*, 2010. **10**(2): p. 242-67.
17. Darrouzet, E., et al., *The sodium/iodide symporter: state of the art of its molecular characterization*. *Biochim Biophys Acta*, 2014. **1838**(1 Pt B): p. 244-53.
18. Eskandari, S., et al., *Thyroid Na⁺/I⁻ symporter. Mechanism, stoichiometry, and specificity*. *J Biol Chem*, 1997. **272**(43): p. 27230-8.
19. Dohan, O., et al., *The Na⁺/I⁻ symporter (NIS) mediates electroneutral active transport of the environmental pollutant perchlorate*. *Proc Natl Acad Sci U S A*, 2007. **104**(51): p. 20250-5.
20. Ravera, S., et al., *The Sodium/Iodide Symporter (NIS): Molecular Physiology and Preclinical and Clinical Applications*. *Annu Rev Physiol*, 2017. **79**: p. 261-289.
21. Spitzweg, C. and J.C. Morris, *The sodium iodide symporter: its pathophysiological and therapeutic implications*. *Clin Endocrinol (Oxf)*, 2002. **57**(5): p. 559-74.
22. Wyszomirska, A., *Iodine-131 for therapy of thyroid diseases. Physical and biological basis*. *Nucl Med Rev Cent East Eur*, 2012. **15**(2): p. 120-3.
23. Cooper, D.S., et al., *Management guidelines for patients with thyroid nodules and differentiated thyroid cancer*. *Thyroid*, 2006. **16**(2): p. 109-42.
24. Dai, G., O. Levy, and N. Carrasco, *Cloning and characterization of the thyroid iodide transporter*. *Nature*, 1996. **379**(6564): p. 458-60.
25. Spitzweg, C., et al., *Treatment of prostate cancer by radioiodine therapy after tissue-specific expression of the sodium iodide symporter*. *Cancer Res*, 2000. **60**(22): p. 6526-30.
26. Spitzweg, C., et al., *In vivo sodium iodide symporter gene therapy of prostate cancer*. *Gene Ther*, 2001. **8**(20): p. 1524-31.

27. Dingli, D., et al., *Image-guided radiovirotherapy for multiple myeloma using a recombinant measles virus expressing the thyroidal sodium iodide symporter*. Blood, 2004. **103**(5): p. 1641-6.
28. Klutz, K., et al., *Targeted radioiodine therapy of neuroblastoma tumors following systemic nonviral delivery of the sodium iodide symporter gene*. Clin Cancer Res, 2009. **15**(19): p. 6079-86.
29. Schmohl, K.A., et al., *Reintroducing the Sodium-Iodide Symporter to Anaplastic Thyroid Carcinoma*. Thyroid, 2017. **27**(12): p. 1534-1543.
30. Shi, S., et al., *Bone Marrow-Derived Mesenchymal Stem Cell-Mediated Dual-Gene Therapy for Glioblastoma*. Hum Gene Ther, 2019. **30**(1): p. 106-117.
31. Muller, A.M., et al., *Hypoxia-targeted ¹³¹I therapy of hepatocellular cancer after systemic mesenchymal stem cell-mediated sodium iodide symporter gene delivery*. Oncotarget, 2016. **7**(34): p. 54795-54810.
32. Knoop, K., et al., *Mesenchymal stem cell-mediated, tumor stroma-targeted radioiodine therapy of metastatic colon cancer using the sodium iodide symporter as theranostic gene*. J Nucl Med, 2015. **56**(4): p. 600-6.
33. Warner, S.G., et al., *A Novel Chimeric Poxvirus Encoding hNIS Is Tumor-Tropic, Imageable, and Synergistic with Radioiodine to Sustain Colon Cancer Regression*. Mol Ther Oncolytics, 2019. **13**: p. 82-92.
34. Dwyer, R.M., et al., *Mesenchymal Stem Cell-mediated delivery of the sodium iodide symporter supports radionuclide imaging and treatment of breast cancer*. Stem Cells, 2011. **29**(7): p. 1149-57.
35. Penheiter, A.R., et al., *Sodium iodide symporter (NIS)-mediated radiovirotherapy for pancreatic cancer*. AJR Am J Roentgenol, 2010. **195**(2): p. 341-9.
36. Schmohl, K.A., et al., *Imaging and targeted therapy of pancreatic ductal adenocarcinoma using the theranostic sodium iodide symporter (NIS) gene*. Oncotarget, 2017. **8**(20): p. 33393-33404.
37. Schug, C., et al., *A Novel Approach for Image-Guided (¹³¹I) Therapy of Pancreatic Ductal Adenocarcinoma Using Mesenchymal Stem Cell-Mediated NIS Gene Delivery*. Mol Cancer Res, 2019. **17**(1): p. 310-320.

38. Kakinuma, H., et al., *Probasin promoter (ARR(2)PB)-driven, prostate-specific expression of the human sodium iodide symporter (h-NIS) for targeted radioiodine therapy of prostate cancer*. *Cancer Res*, 2003. **63**(22): p. 7840-4.
39. Li, H., et al., *HSV-NIS, an oncolytic herpes simplex virus type 1 encoding human sodium iodide symporter for preclinical prostate cancer radiovirotherapy*. *Cancer Gene Ther*, 2013. **20**(8): p. 478-85.
40. Mansfield, D.C., et al., *Oncolytic vaccinia virus as a vector for therapeutic sodium iodide symporter gene therapy in prostate cancer*. *Gene Ther*, 2016. **23**(4): p. 357-68.
41. Trujillo, M.A., et al., *A steep radioiodine dose response scalable to humans in sodium-iodide symporter (NIS)-mediated radiovirotherapy for prostate cancer*. *Cancer Gene Ther*, 2012. **19**(12): p. 839-44.
42. Klutz, K., et al., *Sodium iodide symporter (NIS)-mediated radionuclide ((¹³¹I), (¹⁸⁸Re) therapy of liver cancer after transcriptionally targeted intratumoral in vivo NIS gene delivery*. *Hum Gene Ther*, 2011. **22**(11): p. 1403-12.
43. Grunwald, G.K., et al., *Sodium iodide symporter (NIS)-mediated radiovirotherapy of hepatocellular cancer using a conditionally replicating adenovirus*. *Gene Ther*, 2013. **20**(6): p. 625-33.
44. Grunwald, G.K., et al., *Systemic image-guided liver cancer radiovirotherapy using dendrimer-coated adenovirus encoding the sodium iodide symporter as theranostic gene*. *J Nucl Med*, 2013. **54**(8): p. 1450-7.
45. Grunwald, G.K., et al., *EGFR-Targeted Adenovirus Dendrimer Coating for Improved Systemic Delivery of the Theranostic NIS Gene*. *Mol Ther Nucleic Acids*, 2013. **2**: p. e131.
46. Pack, D.W., et al., *Design and development of polymers for gene delivery*. *Nat Rev Drug Discov*, 2005. **4**(7): p. 581-93.
47. Klutz, K., et al., *Image-guided tumor-selective radioiodine therapy of liver cancer after systemic nonviral delivery of the sodium iodide symporter gene*. *Hum Gene Ther*, 2011. **22**(12): p. 1563-74.
48. Klutz, K., et al., *Epidermal growth factor receptor-targeted (¹³¹I)-therapy of liver cancer following systemic delivery of the sodium iodide symporter gene*. *Mol Ther*, 2011. **19**(4): p. 676-85.

49. Urnauer, S., et al., *EGFR-targeted nonviral NIS gene transfer for bioimaging and therapy of disseminated colon cancer metastases*. *Oncotarget*, 2017. **8**(54): p. 92195-92208.
50. Urnauer, S., et al., *Systemic tumor-targeted sodium iodide symporter (NIS) gene therapy of hepatocellular carcinoma mediated by B6 peptide polyplexes*. *J Gene Med*, 2017. **19**(5): p. e2957.
51. Urnauer, S., et al., *Dual-targeted NIS polyplexes-a theranostic strategy toward tumors with heterogeneous receptor expression*. *Gene Ther*, 2019. **26**(3-4): p. 93-108.
52. Urnauer, S., et al., *Sequence-defined cMET/HGFR-targeted Polymers as Gene Delivery Vehicles for the Theranostic Sodium Iodide Symporter (NIS) Gene*. *Mol Ther*, 2016. **24**(8): p. 1395-404.
53. Caplan, A.I., *Mesenchymal stem cells*. *J Orthop Res*, 1991. **9**(5): p. 641-50.
54. Karp, J.M. and G.S. Leng Teo, *Mesenchymal stem cell homing: the devil is in the details*. *Cell Stem Cell*, 2009. **4**(3): p. 206-16.
55. Conget, P.A. and J.J. Minguell, *Phenotypical and functional properties of human bone marrow mesenchymal progenitor cells*. *J Cell Physiol*, 1999. **181**(1): p. 67-73.
56. Haynesworth, S.E., M.A. Baber, and A.I. Caplan, *Cell surface antigens on human marrow-derived mesenchymal cells are detected by monoclonal antibodies*. *Bone*, 1992. **13**(1): p. 69-80.
57. Chamberlain, G., et al., *Concise review: mesenchymal stem cells: their phenotype, differentiation capacity, immunological features, and potential for homing*. *Stem Cells*, 2007. **25**(11): p. 2739-49.
58. Dominici, M., et al., *Minimal criteria for defining multipotent mesenchymal stromal cells. The International Society for Cellular Therapy position statement*. *Cytotherapy*, 2006. **8**(4): p. 315-7.
59. Barbash, I.M., et al., *Systemic delivery of bone marrow-derived mesenchymal stem cells to the infarcted myocardium: feasibility, cell migration, and body distribution*. *Circulation*, 2003. **108**(7): p. 863-8.
60. George, J.C., *Stem cell therapy in acute myocardial infarction: a review of clinical trials*. *Transl Res*, 2010. **155**(1): p. 10-9.

61. Chen, J., et al., *Therapeutic benefit of intravenous administration of bone marrow stromal cells after cerebral ischemia in rats*. Stroke, 2001. **32**(4): p. 1005-11.
62. Ortiz, L.A., et al., *Mesenchymal stem cell engraftment in lung is enhanced in response to bleomycin exposure and ameliorates its fibrotic effects*. Proc Natl Acad Sci U S A, 2003. **100**(14): p. 8407-11.
63. Kidd, S., et al., *Direct evidence of mesenchymal stem cell tropism for tumor and wounding microenvironments using in vivo bioluminescent imaging*. Stem Cells, 2009. **27**(10): p. 2614-23.
64. Dvorak, H.F., *Tumors: wounds that do not heal. Similarities between tumor stroma generation and wound healing*. N Engl J Med, 1986. **315**(26): p. 1650-9.
65. Foster, D.S., et al., *The evolving relationship of wound healing and tumor stroma*. JCI Insight, 2018. **3**(18): p. e99911.
66. De Becker, A. and I.V. Riet, *Homing and migration of mesenchymal stromal cells: How to improve the efficacy of cell therapy?* World J Stem Cells, 2016. **8**(3): p. 73-87.
67. Hall, B., M. Andreeff, and F. Marini, *The participation of mesenchymal stem cells in tumor stroma formation and their application as targeted-gene delivery vehicles*. Handb Exp Pharmacol, 2007(180): p. 263-83.
68. Sun, Z., S. Wang, and R.C. Zhao, *The roles of mesenchymal stem cells in tumor inflammatory microenvironment*. J Hematol Oncol, 2014. **7**: p. 14.
69. Kalimuthu, S., et al., *Migration of mesenchymal stem cells to tumor xenograft models and in vitro drug delivery by doxorubicin*. Int J Med Sci, 2018. **15**(10): p. 1051-1061.
70. Nakamizo, A., et al., *Human bone marrow-derived mesenchymal stem cells in the treatment of gliomas*. Cancer Res, 2005. **65**(8): p. 3307-18.
71. Bayo, J., et al., *The therapeutic potential of bone marrow-derived mesenchymal stromal cells on hepatocellular carcinoma*. Liver Int, 2014. **34**(3): p. 330-42.
72. Knoop, K., et al., *Stromal targeting of sodium iodide symporter using mesenchymal stem cells allows enhanced imaging and therapy of hepatocellular carcinoma*. Hum Gene Ther, 2013. **24**(3): p. 306-16.
73. Nakamura, K., et al., *Antitumor effect of genetically engineered mesenchymal stem cells in a rat glioma model*. Gene Ther, 2004. **11**(14): p. 1155-64.

74. Studeny, M., et al., *Mesenchymal stem cells: potential precursors for tumor stroma and targeted-delivery vehicles for anticancer agents*. J Natl Cancer Inst, 2004. **96**(21): p. 1593-603.
75. Loebinger, M.R., et al., *Mesenchymal stem cell delivery of TRAIL can eliminate metastatic cancer*. Cancer Res, 2009. **69**(10): p. 4134-42.
76. Pessina, A., et al., *Mesenchymal stromal cells primed with Paclitaxel attract and kill leukaemia cells, inhibit angiogenesis and improve survival of leukaemia-bearing mice*. Br J Haematol, 2013. **160**(6): p. 766-78.
77. Komarova, S., et al., *Mesenchymal progenitor cells as cellular vehicles for delivery of oncolytic adenoviruses*. Mol Cancer Ther, 2006. **5**(3): p. 755-66.
78. Chulpanova, D.S., et al., *Application of Mesenchymal Stem Cells for Therapeutic Agent Delivery in Anti-tumor Treatment*. Front Pharmacol, 2018. **9**: p. 259.
79. Krueger, T.E.G., et al., *Concise Review: Mesenchymal Stem Cell-Based Drug Delivery: The Good, the Bad, the Ugly, and the Promise*. Stem Cells Transl Med, 2018. **7**(9): p. 651-663.
80. Conrad, C., et al., *Genetically engineered stem cells for therapeutic gene delivery*. Curr Gene Ther, 2007. **7**(4): p. 249-60.
81. de Melo, S.M., et al., *The Anti-Tumor Effects of Adipose Tissue Mesenchymal Stem Cell Transduced with HSV-Tk Gene on U-87-Driven Brain Tumor*. PLoS One, 2015. **10**(6): p. e0128922.
82. Niess, H., et al., *Selective targeting of genetically engineered mesenchymal stem cells to tumor stroma microenvironments using tissue-specific suicide gene expression suppresses growth of hepatocellular carcinoma*. Ann Surg, 2011. **254**(5): p. 767-74; discussion 774-5.
83. Zischek, C., et al., *Targeting tumor stroma using engineered mesenchymal stem cells reduces the growth of pancreatic carcinoma*. Ann Surg, 2009. **250**(5): p. 747-53.
84. Niess, H., et al., *Treatment of advanced gastrointestinal tumors with genetically modified autologous mesenchymal stromal cells (TREAT-ME1): study protocol of a phase I/II clinical trial*. BMC Cancer, 2015. **15**: p. 237.

85. von Einem, J.C., et al., *Treatment of advanced gastrointestinal cancer with genetically modified autologous mesenchymal stem cells: Results from the phase 1/2 TREAT-ME-1 trial*. *Int J Cancer*, 2019. **145**(6): p. 1538-1546.
86. Knoop, K., et al., *Image-guided, tumor stroma-targeted 131I therapy of hepatocellular cancer after systemic mesenchymal stem cell-mediated NIS gene delivery*. *Mol Ther*, 2011. **19**(9): p. 1704-13.
87. Schug, C., et al., *TGFB1-driven mesenchymal stem cell-mediated NIS gene transfer*. *Endocr Relat Cancer*, 2019. **26**(1): p. 89-101.
88. Schmohl, K.A., et al., *Integrin alphavbeta3-Mediated Effects of Thyroid Hormones on Mesenchymal Stem Cells in Tumor Angiogenesis*. *Thyroid*, 2019. **29**(12): p. 1843-1857.
89. Egea, V., et al., *TNF-alpha respecifies human mesenchymal stem cells to a neural fate and promotes migration toward experimental glioma*. *Cell Death Differ*, 2011. **18**(5): p. 853-63.
90. Rosova, I., et al., *Hypoxic preconditioning results in increased motility and improved therapeutic potential of human mesenchymal stem cells*. *Stem Cells*, 2008. **26**(8): p. 2173-82.
91. Cheng, Z., et al., *Targeted migration of mesenchymal stem cells modified with CXCR4 gene to infarcted myocardium improves cardiac performance*. *Mol Ther*, 2008. **16**(3): p. 571-9.
92. Kim, S.M., et al., *Irradiation enhances the tumor tropism and therapeutic potential of tumor necrosis factor-related apoptosis-inducing ligand-secreting human umbilical cord blood-derived mesenchymal stem cells in glioma therapy*. *Stem Cells*, 2010. **28**(12): p. 2217-28.
93. Klopp, A.H., et al., *Tumor irradiation increases the recruitment of circulating mesenchymal stem cells into the tumor microenvironment*. *Cancer Res*, 2007. **67**(24): p. 11687-95.
94. Schug, C., et al., *External Beam Radiation Therapy Enhances Mesenchymal Stem Cell-Mediated Sodium-Iodide Symporter Gene Delivery*. *Hum Gene Ther*, 2018. **29**(11): p. 1287-1300.

95. Schug, C., et al., *Radiation-Induced Amplification of TGF β 1-Induced Mesenchymal Stem Cell-Mediated Sodium Iodide Symporter (NIS) Gene (131I) Therapy*. Clin Cancer Res, 2019. **25**(19): p. 5997-6008.
96. Repasky, E.A., S.S. Evans, and M.W. Dewhirst, *Temperature matters! And why it should matter to tumor immunologists*. Cancer Immunol Res, 2013. **1**(4): p. 210-6.
97. Peer, A.J., et al., *Diverse immune mechanisms may contribute to the survival benefit seen in cancer patients receiving hyperthermia*. Immunol Res, 2010. **46**(1-3): p. 137-54.
98. Hildebrandt, B., et al., *The cellular and molecular basis of hyperthermia*. Crit Rev Oncol Hematol, 2002. **43**(1): p. 33-56.
99. Datta, N.R., et al., *Local hyperthermia combined with radiotherapy and/or chemotherapy: recent advances and promises for the future*. Cancer Treat Rev, 2015. **41**(9): p. 742-53.
100. Issels, R., et al., *Hallmarks of hyperthermia in driving the future of clinical hyperthermia as targeted therapy: translation into clinical application*. Int J Hyperthermia, 2016. **32**(1): p. 89-95.
101. Lee, S., et al., *Immunogenic Effect of Hyperthermia on Enhancing Radiotherapeutic Efficacy*. Int J Mol Sci, 2018. **19**(9): p. e2795.
102. Qin, W., et al., *Modulated electro-hyperthermia enhances dendritic cell therapy through an abscopal effect in mice*. Oncol Rep, 2014. **32**(6): p. 2373-9.
103. Rubner, Y., et al., *How does ionizing irradiation contribute to the induction of anti-tumor immunity?* Front Oncol, 2012. **2**: p. 75.
104. Toraya-Brown, S. and S. Fiering, *Local tumour hyperthermia as immunotherapy for metastatic cancer*. Int J Hyperthermia, 2014. **30**(8): p. 531-9.
105. Frey, B., et al., *Old and new facts about hyperthermia-induced modulations of the immune system*. Int J Hyperthermia, 2012. **28**(6): p. 528-42.
106. Evans, S.S., et al., *Fever-range hyperthermia dynamically regulates lymphocyte delivery to high endothelial venules*. Blood, 2001. **97**(9): p. 2727-2733.
107. Skitzki, J.J., E.A. Repasky, and S.S. Evans, *Hyperthermia as an immunotherapy strategy for cancer*. Curr Opin Investig Drugs, 2009. **10**(6): p. 550-558.

108. Vaupel, P.W. and D.K. Kelleher, *Pathophysiological and vascular characteristics of tumours and their importance for hyperthermia: heterogeneity is the key issue*. Int J Hyperthermia, 2010. **26**(3): p. 211-23.
109. Mantso, T., et al., *Effects of hyperthermia as a mitigation strategy in DNA damage-based cancer therapies*. Semin Cancer Biol, 2016. **37-38**: p. 96-105.
110. Limmer, S., et al., *Gemcitabine treatment of rat soft tissue sarcoma with phosphatidylglycerol-based thermosensitive liposomes*. Pharm Res, 2014. **31**(9): p. 2276-86.
111. Xu, S., et al., *Bone marrow-derived mesenchymal stromal cells are attracted by multiple myeloma cell-produced chemokine CCL25 and favor myeloma cell growth in vitro and in vivo*. Stem Cells, 2012. **30**(2): p. 266-79.
112. Spaeth, E., et al., *Inflammation and tumor microenvironments: defining the migratory itinerary of mesenchymal stem cells*. Gene Ther, 2008. **15**(10): p. 730-8.
113. Heled, Y., C. Fleischmann, and Y. Epstein, *Cytokines and their role in hyperthermia and heat stroke*. J Basic Clin Physiol Pharmacol, 2013. **24**(2): p. 85-96.
114. Baril, P., P. Martin-Duque, and G. Vassaux, *Visualization of gene expression in the live subject using the Na/I symporter as a reporter gene: applications in biotherapy*. Br J Pharmacol, 2010. **159**(4): p. 761-71.
115. Penheiter, A.R., S.J. Russell, and S.K. Carlson, *The sodium iodide symporter (NIS) as an imaging reporter for gene, viral, and cell-based therapies*. Curr Gene Ther, 2012. **12**(1): p. 33-47.
116. Spitzweg, C., et al., *Prostate-specific antigen (PSA) promoter-driven androgen-inducible expression of sodium iodide symporter in prostate cancer cell lines*. Cancer Res, 1999. **59**(9): p. 2136-41.
117. Spitzweg, C., et al., *Image-guided radioiodide therapy of medullary thyroid cancer after carcinoembryonic antigen promoter-targeted sodium iodide symporter gene expression*. Hum Gene Ther, 2007. **18**(10): p. 916-24.
118. Rao, W., Z.S. Deng, and J. Liu, *A review of hyperthermia combined with radiotherapy/chemotherapy on malignant tumors*. Crit Rev Biomed Eng, 2010. **38**(1): p. 101-16.

119. Dewhirst, M.W., C.T. Lee, and K.A. Ashcraft, *The future of biology in driving the field of hyperthermia*. Int J Hyperthermia, 2016. **32**(1): p. 4-13.
120. Hagenhoff, A., et al., *Harnessing mesenchymal stem cell homing as an anticancer therapy*. Expert Opin Biol Ther, 2016. **16**(9): p. 1079-92.
121. Fischer, U.M., et al., *Pulmonary passage is a major obstacle for intravenous stem cell delivery: the pulmonary first-pass effect*. Stem Cells Dev, 2009. **18**(5): p. 683-92.
122. Xie, C., et al., *Systemically Infused Mesenchymal Stem Cells Show Different Homing Profiles in Healthy and Tumor Mouse Models*. Stem Cells Transl Med, 2017. **6**(4): p. 1120-1131.
123. Thoren, F.B., H. Anderson, and O. Strannegard, *Late divergence of survival curves in cancer immunotherapy trials: interpretation and implications*. Cancer Immunol Immunother, 2013. **62**(10): p. 1547-51.
124. Issels, R.D., et al., *Effect of Neoadjuvant Chemotherapy Plus Regional Hyperthermia on Long-term Outcomes Among Patients With Localized High-Risk Soft Tissue Sarcoma: The EORTC 62961-ESHO 95 Randomized Clinical Trial*. JAMA Oncol, 2018. **4**(4): p. 483-492.
125. Issels, R.D., et al., *Neo-adjuvant chemotherapy alone or with regional hyperthermia for localised high-risk soft-tissue sarcoma: a randomised phase 3 multicentre study*. Lancet Oncol, 2010. **11**(6): p. 561-70.
126. Wendtner, C.M., et al., *Response to neoadjuvant chemotherapy combined with regional hyperthermia predicts long-term survival for adult patients with retroperitoneal and visceral high-risk soft tissue sarcomas*. J Clin Oncol, 2002. **20**(14): p. 3156-64.
127. Spitzweg, C., et al., *Clinical review 132: The sodium iodide symporter and its potential role in cancer therapy*. J Clin Endocrinol Metab, 2001. **86**(7): p. 3327-35.
128. Merron, A., et al., *Assessment of the Na/I symporter as a reporter gene to visualize oncolytic adenovirus propagation in peritoneal tumours*. Eur J Nucl Med Mol Imaging, 2010. **37**(7): p. 1377-85.
129. Miller, A. and S.J. Russell, *The use of the NIS reporter gene for optimizing oncolytic virotherapy*. Expert Opin Biol Ther, 2016. **16**(1): p. 15-32.

130. Riesco-Eizaguirre, G., et al., *Telomerase-driven expression of the sodium iodide symporter (NIS) for in vivo radioiodide treatment of cancer: a new broad-spectrum NIS-mediated antitumor approach*. J Clin Endocrinol Metab, 2011. **96**(9): p. E1435-43.
131. Shen, W., et al., *Immunovirotherapy with vesicular stomatitis virus and PD-L1 blockade enhances therapeutic outcome in murine acute myeloid leukemia*. Blood, 2016. **127**(11): p. 1449-58.
132. Chung, T., et al., *Dihydropyrimidine Dehydrogenase Is a Prognostic Marker for Mesenchymal Stem Cell-Mediated Cytosine Deaminase Gene and 5-Fluorocytosine Prodrug Therapy for the Treatment of Recurrent Gliomas*. Theranostics, 2016. **6**(10): p. 1477-90.
133. Droujinine, I.A., M.A. Eckert, and W. Zhao, *To grab the stroma by the horns: from biology to cancer therapy with mesenchymal stem cells*. Oncotarget, 2013. **4**(5): p. 651-64.
134. Rossignoli, F., et al., *MSC-Delivered Soluble TRAIL and Paclitaxel as Novel Combinatory Treatment for Pancreatic Adenocarcinoma*. Theranostics, 2019. **9**(2): p. 436-448.
135. Rosenzweig, R., et al., *The Hsp70 chaperone network*. Nat Rev Mol Cell Biol, 2019. **20**(11): p. 665-680.
136. Calderwood, S.K., et al., *Signal Transduction Pathways Leading to Heat Shock Transcription*. Sign Transduct Insights, 2010. **2**: p. 13-24.
137. Rome, C., F. Couillaud, and C.T. Moonen, *Spatial and temporal control of expression of therapeutic genes using heat shock protein promoters*. Methods, 2005. **35**(2): p. 188-98.
138. Gong, M., et al., *Immortalized mesenchymal stem cells: an alternative to primary mesenchymal stem cells in neuronal differentiation and neuroregeneration associated studies*. J Biomed Sci, 2011. **18**: p. 87.
139. Weiss, S.J., N.J. Philp, and E.F. Grollman, *Iodide transport in a continuous line of cultured cells from rat thyroid*. Endocrinology, 1984. **114**(4): p. 1090-8.
140. Jiang, H. and T.R. DeGrado, *[(18)F]Tetrafluoroborate ([18)F]TFB) and its analogs for PET imaging of the sodium/iodide symporter*. Theranostics, 2018. **8**(14): p. 3918-3931.

141. Barton, K.N., et al., *Phase I study of noninvasive imaging of adenovirus-mediated gene expression in the human prostate*. Mol Ther, 2008. **16**(10): p. 1761-9.
142. Dispenzieri, A., et al., *Phase I trial of systemic administration of Edmonston strain of measles virus genetically engineered to express the sodium iodide symporter in patients with recurrent or refractory multiple myeloma*. Leukemia, 2017. **31**(12): p. 2791-2798.
143. Galanis, E., et al., *Oncolytic measles virus expressing the sodium iodide symporter to treat drug-resistant ovarian cancer*. Cancer Res, 2015. **75**(1): p. 22-30.
144. Russell, S.J., et al., *Remission of disseminated cancer after systemic oncolytic virotherapy*. Mayo Clin Proc, 2014. **89**(7): p. 926-33.
145. Maxson, S., et al., *Concise review: role of mesenchymal stem cells in wound repair*. Stem Cells Transl Med, 2012. **1**(2): p. 142-9.
146. Niess, H., et al., *Genetic engineering of mesenchymal stromal cells for cancer therapy: turning partners in crime into Trojan horses*. Innov Surg Sci, 2016. **1**(1): p. 19-32.
147. Ponte, A.L., et al., *The in vitro migration capacity of human bone marrow mesenchymal stem cells: comparison of chemokine and growth factor chemotactic activities*. Stem Cells, 2007. **25**(7): p. 1737-45.
148. Dwyer, R.M., et al., *Advances in mesenchymal stem cell-mediated gene therapy for cancer*. Stem Cell Res Ther, 2010. **1**(3): p. 25.
149. Voellmy, R., et al., *Isolation and functional analysis of a human 70,000-dalton heat shock protein gene segment*. Proc Natl Acad Sci U S A, 1985. **82**(15): p. 4949-53.
150. Leung, T.K., et al., *The human heat-shock genes HSPA6 and HSPA7 are both expressed and localize to chromosome 1*. Genomics, 1992. **12**(1): p. 74-9.
151. Parsian, A.J., et al., *The human Hsp70B gene at the HSPA7 locus of chromosome 1 is transcribed but non-functional*. Biochim Biophys Acta, 2000. **1494**(1-2): p. 201-5.
152. Brade, A.M., et al., *Heat-directed gene targeting of adenoviral vectors to tumor cells*. Cancer Gene Ther, 2000. **7**(12): p. 1566-74.
153. Braiden, V., et al., *Eradication of breast cancer xenografts by hyperthermic suicide gene therapy under the control of the heat shock protein promoter*. Hum Gene Ther, 2000. **11**(18): p. 2453-63.

-
154. Liu, Y., et al., *High intensity focused ultrasound-induced gene activation in solid tumors*. J Acoust Soc Am, 2006. **120**(1): p. 492-501.
 155. Smith, R.C., et al., *Spatial and temporal control of transgene expression through ultrasound-mediated induction of the heat shock protein 70B promoter in vivo*. Hum Gene Ther, 2002. **13**(6): p. 697-706.
 156. Balogi, Z., et al., *Hsp70 interactions with membrane lipids regulate cellular functions in health and disease*. Prog Lipid Res, 2019. **74**: p. 18-30.
 157. Siddiqui, F., et al., *Induction of the human heat shock promoter HSP70B by nutritional stress: implications for cancer gene therapy*. Cancer Invest, 2008. **26**(6): p. 553-61.
 158. Multhoff, G., et al., *A stress-inducible 72-kDa heat-shock protein (HSP72) is expressed on the surface of human tumor cells, but not on normal cells*. Int J Cancer, 1995. **61**(2): p. 272-9.
 159. Stangl, S., et al., *Preclinical Evaluation of the Hsp70 Peptide Tracer TPP-PEG24-DFO[(89)Zr] for Tumor-Specific PET/CT Imaging*. Cancer Res, 2018. **78**(21): p. 6268-6281.
 160. Schmohl, K.A., et al., *Establishment of an Effective Radioiodide Thyroid Ablation Protocol in Mice*. Eur Thyroid J, 2015. **4**(Suppl 1): p. 74-80.

8. Acknowledgements

First, I would like to express my thankfulness to my supervisor Prof. Dr. Christine Spitzweg for providing me with this very special and exciting project. I am very grateful that I had the chance to work on my thesis in her laboratory and be part of her great research group. Thank you, Christine, for your continuous scientific support, for encouraging me to surpass myself at various levels, and for letting me travel to scientific meetings all around Europa, to my all-time favorite city Vancouver and to the US. Special thanks for the little things to create a pleasant working atmosphere, like hiding Easter bunnies or good luck pigs at our desks, for inviting us to an annual Christmas celebration, and especially for the unforgettable ETA dinner in Belgrade.

Furthermore, I would like to thank Prof. Dr. Ernst Wagner for introducing me to science already during my studies of pharmacy, for his scientific input, and for accepting me as an external doctoral student at the faculty of Pharmacy.

I am very grateful to Prof. Dr. Peter Nelson for always having an open ear, for helpful advice, and for always being really enthusiastic and making everything sound fast and easy, especially a doctoral thesis.

Thank you to Prof. Dr. Lars Lindner and his team, especially Matteo, for the great collaboration and for always being extremely friendly and helpful.

My warm appreciation goes to all current and former members of the AG Spitzweg, who created the greatest working atmosphere imaginable. I really loved our shared lunch/coffee breaks, endless discussions about every possible subject, and of course, especially our congress trips. Thank you Katy for not nicking my blanket too often, always poring over my problems with me and especially trying to make the best out of my scrawl. Chrissi, thanks for shouldering the “Imaging-queen” crown with me and for always pampering “die Kleine”. Sarah, thank you for making me a fan of “to-do lists” and for all the fun time we had together day and night. Special thanks to Nathalie for keeping the lab running and for always encouraging me. Caro and Rebekka, thank you for taking over as the newbies, for sharing the “Schlauch”-room with me and for all the laughs we had together. Additionally, I would like to thank Yang for his ability to deal with the girl-power in our lab and for introducing me to the Chinese kitchen. Furthermore, many thanks to Andrea, Viktoria, and Elke who contributed greatly to the best atmosphere in the lab and to our neighboring lab partners, Ralf, Renate, Ujjwal, Ivonne, and Simon for continuous support and always allowing me to use their equipment.

Special thanks to the people of the Department of Nuclear Medicine at Klinikum Großhadern, especially Rosel, Karin, and Barbara and at Klinikum Rechts der Isar, in particular Steffi and the team of the “Strahlenschutz”, for always doing their best to support me with my imaging and long-lasting therapy studies.

Special appreciations goes to the Wilhelm Sander-Stiftung for funding my work and to the SFB 824 and SPP 1629 for generous financial support.

I would like to thank my friends who always believed in me and cheered me up, especially Viola (2020, “our year”). Finally, sincere thanks to my family who always supported and encouraged me. In particular, thank you Fredi, especially for always hearing me and for not being too angry with me for not being able to make any plan in advance.